

EUROPEAN ORGANISATION FOR NUCLEAR RESEARCH (CERN)



Submitted to: JHEP



CERN-EP-2025-127
25th June 2025

Probing the Higgs boson CP properties in vector-boson fusion production in the $H \rightarrow \tau^+\tau^-$ channel with the ATLAS detector

The ATLAS Collaboration

The CP properties of the Higgs boson are studied in the vector-boson fusion production mode. The analysis exploits the decay mode of the Higgs boson into two τ -leptons using 140 fb^{-1} of proton–proton collision data at $\sqrt{s} = 13\text{ TeV}$ collected by the ATLAS experiment at the Large Hadron Collider. Results are obtained using the Optimal Observable method. CP-violating interactions between the Higgs boson and electroweak gauge bosons are considered in the effective field theory framework, with the interaction strength described in the HISZ basis by \tilde{d} , and in the Warsaw basis by $c_{H\tilde{W}}$, $c_{H\tilde{B}}$, and $c_{H\tilde{W}B}$. No deviations relative to the Standard Model are observed, and limits are obtained on the strength parameters. The \tilde{d} parameter is constrained to the interval $[-0.012, 0.044]$ at the 95% confidence level while $c_{H\tilde{W}}$ is constrained to $[-0.24, 0.83]$, when considering both linear and quadratic effects of physics beyond the Standard Model.

Contents

1	Introduction	2
2	CP-odd observables and methodology	4
3	ATLAS detector	6
4	Data and simulated event samples	7
5	Event selection	10
6	Background estimation	13
7	Systematic uncertainties	17
8	Fitting procedure	18
9	Results	19
10	Conclusion	24

1 Introduction

The origin of the observed baryon asymmetry in the universe is one of the fundamental open questions in our current understanding of particle physics. In 1967 Sakharov proposed three necessary conditions [1] to explain the generation of the baryon asymmetry. One of these conditions includes the violation in fundamental interactions of the invariance under combined charge (C) and parity (P) conjugation. In the Standard Model (SM) of particle physics, CP-violating contributions arise from a complex phase in the quark mixing matrix. However, the magnitude of these effects is not enough to explain the observed value of the baryon asymmetry in the universe [2–6].

The discovery of the Higgs boson at the Large Hadron Collider (LHC) [7] by the ATLAS and CMS collaborations [8, 9] has opened a new sector in which possible CP-violating interactions can be investigated. In the SM, the Higgs boson is CP-even (scalar) in the interaction with other SM particles, both in production and decay. Any deviation from the SM predictions would be a sign of physics beyond the SM (BSM). In particular, a promising avenue for testing CP invariance is in the interaction between the Higgs boson (H) and electroweak gauge bosons, namely the HVV vertex (where $V = W^\pm, Z$ vector bosons) [10]. The current results from the ATLAS and CMS Collaborations strongly support the scalar nature of the Higgs boson, consistent with SM expectation [11–14]. In order to search for a clear sign of physics beyond the SM, the results are interpreted in the effective field theory (EFT) framework, and limits are set on the Wilson coefficients describing the strength of the CP-violating interactions terms with the Higgs boson. The BSM contributions to the SM tensor structure are parameterised with additional higher dimensional operators $O_i^{(d)}$ of dimension d and combine the SM Lagrangian \mathcal{L}_{SM} to form an EFT Lagrangian:

$$\mathcal{L}_{\text{EFT}} = \mathcal{L}_{\text{SM}} + \sum_i \frac{c_i^{(d)}}{\Lambda^{(d-4)}} O_i^{(d)}$$

with dimension $d > 4$, Λ the scale of the new physics, and $c_i^{(d)}$ the Wilson coefficients describing the strength of the new interactions. In this paper only operators of dimension six are considered. Operators with odd dimension imply lepton and baryon number violation, and are therefore ignored. Higher dimension operators such as dimension-8 are also not considered, since they are suppressed by an additional factor Λ^2 . From this formulation of the effective Lagrangian it is possible to obtain a complete set of independent operators. There is no unique way to form such a set of operators, and one of the most used is the HISZ basis [15, 16]. In this formulation, after electroweak symmetry breaking, the Lagrangian coefficients, corresponding to the CP-violating terms in the HVV vertex can be described as a function of two dimensionless parameters \tilde{d} and \tilde{d}_B [16, 17],

$$\begin{aligned}\tilde{c}_{H\gamma\gamma} &= \frac{g}{2m_W}(\tilde{d} \sin^2 \theta_W + \tilde{d}_B \cos^2 \theta_W) & \tilde{c}_{H\gamma Z} &= \frac{g}{2m_W} \sin 2\theta_W (\tilde{d} - \tilde{d}_B) \\ \tilde{c}_{HZZ} &= \frac{g}{2m_W}(\tilde{d} \cos^2 \theta_W + \tilde{d}_B \sin^2 \theta_W) & \tilde{c}_{HWW} &= \frac{g}{m_W} \tilde{d},\end{aligned}$$

where θ_W is the Weinberg angle, and g is the SU(2) coupling constant. Assuming the arbitrary condition $\tilde{d} = \tilde{d}_B$, the CP-violating effect can then be parameterised by a single parameter \tilde{d} . Another widely used EFT parameterisation is the Warsaw basis [18], adopted by both ATLAS [12, 19] and CMS [20] in the SMEFT [21] formalism. In this basis, three CP-odd terms contribute to the HVV vertex. These CP-odd operators with their corresponding Wilson coefficients are:

$$\frac{c_{H\tilde{W}}}{\Lambda^2} H^\dagger H \tilde{W}_{\mu\nu}^I W^{\mu\nu I}, \frac{c_{H\tilde{B}}}{\Lambda^2} H^\dagger H \tilde{B}_{\mu\nu} B^{\mu\nu}, \frac{c_{H\tilde{W}B}}{\Lambda^2} H^\dagger H \sigma^I \tilde{W}_{\mu\nu}^I B^{\mu\nu},$$

where the Higgs doublet and its complex conjugate are defined by H and H^\dagger , $W_{\mu\nu}^I$ and $B_{\mu\nu}$ are the field strength tensor for the W^I ($I = 1, 2, 3$) and B gauge fields, and $\tilde{W}_{\mu\nu}^I = \epsilon^{\mu\nu\rho\sigma} W_{\rho\sigma}^I$ ($\tilde{B}_{\mu\nu} = \epsilon^{\mu\nu\rho\sigma} B_{\rho\sigma}$) are their dual, and σ^I are the Pauli matrices. The two representations are not independent, and it is possible to transform one into the other. If it is assumed that $c_{H\tilde{W}} = c_{H\tilde{B}}$ and $c_{H\tilde{W}B} = 0$, it is possible to show that $\tilde{d} = \frac{v^2}{\Lambda^2} c_{H\tilde{W}} = \frac{v^2}{\Lambda^2} c_{H\tilde{B}}$, where v is the Higgs vacuum expectation value. The changes in the cross-section due to BSM effects can be parameterised with an interference term that depends linearly on the Wilson coefficient, and is responsible for the CP-odd effects, and a quadratic term that is purely from BSM physics, but CP-even. In this analysis, the interpretations use both the linear and quadratic terms, but the case where only the linear term is included in the BSM parameterisation is also considered. The Wilson coefficients in both parameterisations have been constrained by different analyses from LEP experiments [22–24], and ATLAS and CMS, in both Run 1 and Run 2, and in different channels. These include measurements of CP-odd observables in $H \rightarrow \gamma\gamma$ in the vector-boson fusion (VBF) production channel [12]. Another analysis based on CP-odd observables investigated the channel $H \rightarrow ZZ^* \rightarrow 4\ell$ [11, 25], where the HVV coupling enters in both the production and decay for VBF production, and only in the decay for gluon–gluon fusion (ggF) production. A similar analysis was also performed in the channel $H \rightarrow WW^* \rightarrow \ell\nu\ell\nu$ [13]. The $H \rightarrow \tau^+\tau^-$ channel¹ has also been used by ATLAS to constrain the Wilson coefficients in the HISZ basis in both Run 1 [26] and in a 36 fb^{-1} partial Run 2 dataset [27]. A differential measurement of the $H \rightarrow \tau\tau$ channel was done by ATLAS using the full Run 2 dataset [28], where the CP-sensitive azimuthal angle between the two VBF jets, $\Delta\phi_{jj}^{\text{sign}}$ (defined in Section 2), was unfolded and provided constraints on different EFT parameters. To date, no hints of CP violations have been observed and the best constraints on \tilde{d} have been set in Ref. [11], with limits $[-0.017, 0.014]$ at 68% confidence level (CL) including both linear and quadratic terms in the parameterisation of the BSM effects. For $c_{H\tilde{W}}$, $c_{H\tilde{B}}$, and $c_{H\tilde{W}B}$, limits at the 68% CL are set at $[-0.07, 1.09]$, $[-0.42, 0.31]$, and $[-0.56, 0.53]$, respectively, assuming a scale of

¹ For simplicity a pair of $\tau^+\tau^-$ are referred to as $\tau\tau$ in the rest of the paper.

new physics of $\Lambda = 1$ TeV and considering only the linear term in the BSM effects. For both bases, the limits obtained considering the linear only and both linear and quadratic terms in the parameterisation of the BSM effects are found to be in agreement.

In this analysis, a search for CP violation in the VBF production vertex of the Higgs boson is performed, using the $H \rightarrow \tau\tau$ decay mode. With a comparatively high branching ratio of 6% [29], this channel provides a phase space with a high signal-to-background ratio and a high efficiency for Higgs boson candidate reconstruction. The analysis is performed using a dataset of 140 fb^{-1} of proton–proton (pp) collisions recorded by the ATLAS experiment during the Run 2 of the LHC between 2015 and 2018. The analysis is based on the Optimal Observable method [30–32]. This observable combines the full information of the multidimensional production phase space, independent of the decay mode, providing a full description of the production process. Other CP-odd observables are also used in the analysis for comparison.

The analysis presented in this paper follows closely the publication in Ref. [27], but with several improvements: new background estimates were performed and novel machine learning techniques were implemented to increase the signal-to-background ratio. The results are interpreted in the context of the HISZ and Warsaw bases.

The paper is structured as follows: Section 2 describes the CP-odd observables used in the analysis. Section 3 describes the ATLAS detector and Section 4 the Monte Carlo (MC) simulations and data samples used in the analysis. Section 5 describes the event selection and the implementation of the new machine learning techniques, while Sections 6 and 7 describe the background estimation and the main sources of systematic uncertainties. Section 8 describes the fit setup and in Section 9 the results are shown.

2 CP-odd observables and methodology

Tests of CP-invariance can be performed in a model independent way by measuring the mean value of a CP-odd observable $\langle O_{\text{CP}} \rangle$. If CP-invariance holds, the mean value vanishes: $\langle O_{\text{CP}} \rangle = 0$. An observation of a non-vanishing mean value is then a clear sign of CP-violation. The production kinematics consisting of the reconstructed Higgs boson four-momentum and the two jets from the VBF production (tagging jets) can, under the assumption of a fixed Higgs mass and massless jets, be characterised by a seven-dimensional phase space. The Optimal Observable method combines the information of these seven phase space variables into a single observable, which is shown to have the highest sensitivity to small values of the CP-violating strength parameter. It is defined by the ratio of the interference term in the matrix element (ME) to the SM contribution:

$$OO = \frac{2\Re(\mathcal{M}_{\text{SM}}^* \mathcal{M}_{\text{CP-odd}})}{|\mathcal{M}_{\text{SM}}|^2}.$$

The mean value of the Optimal Observable can be experimentally measured, and if no CP violation is present $\langle OO \rangle = 0$, as the observable is a CP-odd (and \hat{T} -odd²) variable. This assumes that any effects from rescattering (i.e., new particles being on mass shell in the loop corrections to the HVV vertex) are negligible [10], since the initial-state of VBF production of the Higgs boson is not a CP-symmetric process. Figure 1(a) shows the distribution of the OO for SM VBF Higgs production and for two example

² \hat{T} denotes the time reversal according to Ref. [10], which inverts the directions of momenta and spins.

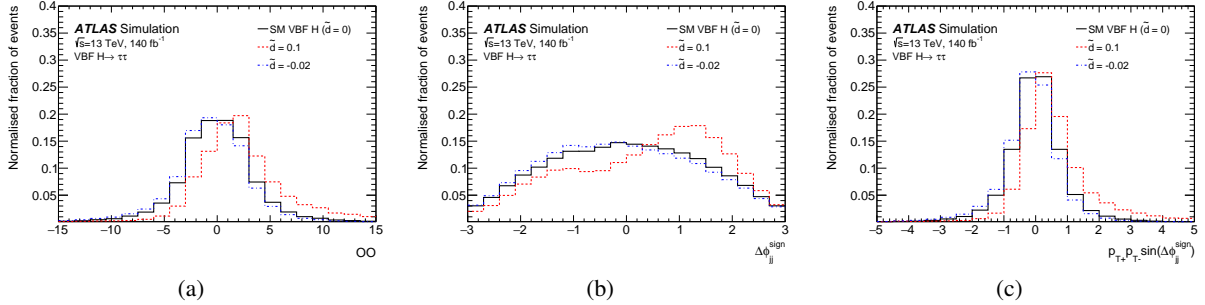


Figure 1: Distributions for SM VBF Higgs boson production and two VBF Higgs boson samples with $\tilde{d} \neq 0$, for (a) the Optimal Observable, OO , (b) $\Delta\phi_{jj}^{\text{sign}}$, and (c) $p_{T+}p_{T-} \sin(\Delta\phi_{jj}^{\text{sign}})$, shown for final states where one τ -lepton decays hadronically, and the other one, leptonically. The MC simulations used are those described in Section 4.

distributions where $\tilde{d} \neq 0$, on simulated samples after the selections described in Section 5. This Figure shows how the mean of the OO is shifted to higher or lower values, depending on the sign of the \tilde{d} parameter.

The values of the leading-order matrix elements needed for the calculation of the Optimal Observable are extracted from HAWK [33–35], using the HISZ basis with condition $\tilde{d} = \tilde{d}_B$. The evaluation requires the four vectors of the Higgs boson and the two tagging jets. The Bjorken x values of the incoming partons in positive (x_1) and negative (x_2) z -direction can be derived exploiting energy-momentum conservation from the Higgs boson and tagging jet four-momenta as

$$x_{1/2}^{\text{reco}} = \frac{m_{Hjj}}{\sqrt{s}} e^{\pm y_{Hjj}},$$

where m_{Hjj} (y_{Hjj}) is the mass (rapidity) of the vectorial sum of the tagging jets and the Higgs boson four-momentum, the latter estimated by using the missing mass calculator (MMC) [36]. As the flavour of the incoming and outgoing partons cannot be determined experimentally, the sum over all possible flavour configurations $ij \rightarrow klH$ weighted by the parton distribution functions is calculated separately for the matrix elements in numerator and denominator:

$$\begin{aligned} 2\Re(\mathcal{M}_{\text{SM}}^* \mathcal{M}_{\text{CP-odd}}) &= \sum_{i,j,k,l} f_i(x_1) f_j(x_2) 2\Re(\mathcal{M}_{\text{SM}}^* \mathcal{M}_{\text{CP-odd}})(ij \rightarrow klH) \\ |\mathcal{M}_{\text{SM}}|^2 &= \sum_{i,j,k,l} f_i(x_1) f_j(x_2) |\mathcal{M}_{\text{SM}}|^2(ij \rightarrow klH). \end{aligned}$$

Another simple CP-odd observable suggested in Ref. [37] is defined based on the “signed” azimuthal angular difference between the two tagging VBF jets:

$$\epsilon_{\mu\nu\rho\sigma} b_+^\mu p_+^\nu b_-^\rho p_-^\sigma = 2p_{T+}p_{T-} \sin(\phi_+ - \phi_-) = 2p_{T+}p_{T-} \sin(\Delta\phi_{jj}^{\text{sign}}),$$

where b_{+-}^μ denotes the normalised four-momenta of the two incoming protons, $p_{+-}^\mu(\phi_{+-})$ denote the four-momenta (azimuthal angles) of the two outgoing VBF tagging jets, and where p_{+-} points into the same detector hemisphere as b_{+-}^μ . In the literature, $\Delta\phi_{jj}^{\text{sign}}$ is also a commonly proposed CP-odd observable; however, the combined term $p_{T+}p_{T-} \sin(\Delta\phi_{jj}^{\text{sign}})$ is usually more sensitive than $\Delta\phi_{jj}^{\text{sign}}$, due to

the additional information of the momentum of the tagging jets. In this analysis $p_{\mathrm{T}+} p_{\mathrm{T}-} \sin(\Delta\phi_{jj}^{\mathrm{sign}})$ is also considered for comparison to the Optimal Observable. Figures 1(b) and 1(c) show the distributions of $\Delta\phi_{jj}^{\mathrm{sign}}$ and $p_{\mathrm{T}+} p_{\mathrm{T}-} \sin(\Delta\phi_{jj}^{\mathrm{sign}})$, respectively.

3 ATLAS detector

The ATLAS detector [38] at the LHC covers nearly the entire solid angle around the collision point.³ It consists of an inner tracking detector surrounded by a thin superconducting solenoid, electromagnetic and hadronic calorimeters, and a muon spectrometer incorporating three large superconducting air-core toroidal magnets.

The inner-detector system (ID) is immersed in a 2 T axial magnetic field and provides charged-particle tracking in the range $|\eta| < 2.5$. The high-granularity silicon pixel detector covers the vertex region and typically provides four measurements per track, the first hit generally being in the insertable B-layer (IBL) installed before Run 2 [39, 40]. It is followed by the SemiConductor Tracker (SCT), which usually provides eight measurements per track. These silicon detectors are complemented by the transition radiation tracker (TRT), which enables radially extended track reconstruction up to $|\eta| = 2.0$. The TRT also provides electron identification information based on the fraction of hits (typically 30 in total) above a higher energy-deposit threshold corresponding to transition radiation.

The calorimeter system covers the pseudorapidity range $|\eta| < 4.9$. Within the region $|\eta| < 3.2$, electromagnetic calorimetry is provided by barrel and endcap high-granularity lead/liquid-argon (LAr) calorimeters, with an additional thin LAr presampler covering $|\eta| < 1.8$ to correct for energy loss in material upstream of the calorimeters. Hadronic calorimetry is provided by the steel/scintillator-tile calorimeter, segmented into three barrel structures within $|\eta| < 1.7$, and two copper/LAr hadronic endcap calorimeters. The solid angle coverage is completed with forward copper/LAr and tungsten/LAr calorimeter modules optimised for electromagnetic and hadronic energy measurements, respectively.

The muon spectrometer (MS) comprises separate trigger and high-precision tracking chambers measuring the deflection of muons in a magnetic field generated by the superconducting air-core toroidal magnets. The field integral of the toroids ranges between 2.0 and 6.0 T m across most of the detector. Three layers of precision chambers, each consisting of layers of monitored drift tubes, cover the region $|\eta| < 2.7$, complemented by cathode-strip chambers in the forward region, where the background is highest. The muon trigger system covers the range $|\eta| < 2.4$ with resistive-plate chambers in the barrel, and thin-gap chambers in the endcap regions.

The luminosity is measured mainly by the LUCID–2 [41] detector that records Cherenkov light produced in the quartz windows of photomultipliers located close to the beampipe.

Events were selected by the first-level trigger system implemented in custom hardware, followed by selections made by algorithms implemented in software in the high-level trigger [42]. The first-level trigger

³ ATLAS uses a right-handed coordinate system with its origin at the nominal interaction point (IP) in the centre of the detector and the z -axis along the beam pipe. The x -axis points from the IP to the centre of the LHC ring, and the y -axis points upwards. Polar coordinates (r, ϕ) are used in the transverse plane, ϕ being the azimuthal angle around the z -axis. The pseudorapidity is defined in terms of the polar angle θ as $\eta = -\ln \tan(\theta/2)$ and is equal to the rapidity $y = \frac{1}{2} \ln \left(\frac{E+p_z}{E-p_z} \right)$ in the relativistic limit. Angular distance is measured in units of $\Delta R \equiv \sqrt{(\Delta y)^2 + (\Delta\phi)^2}$.

Table 1: Summary of nominal samples used including the information about the matrix element (ME) generators, the parton shower (PS), parton distribution function (PDF) sets used to compute the ME and the PS, the set of tuned parameters (Tune), and the order of the cross-section calculation used for normalisation of the samples (Order). Further details are given in the text.

Process	Generator		PDF set		Tune	Order (QCD / EWK)
	ME	PS	ME	PS		
Higgs						
ggF	POWHEG BOX v2	PYTHIA 8.2	PDF4LHC15NNLO	CTEQ6L1	AZNLO	N ³ LO / NLO
VBF	POWHEG BOX v2	PYTHIA 8.2	PDF4LHC15NLO	CTEQ6L1	AZNLO	NNLO / NLO
VH	POWHEG BOX v2	PYTHIA 8.2	PDF4LHC15NLO	CTEQ6L1	AZNLO	(N)NLO / NLO
t <bar>t}H</bar>	POWHEG BOX v2	PYTHIA 8.2	NNPDF3.0NLO	NNPDF2.3LO	A14	NNLO / NLO
tHq	MG5_AMC@NLO 2.6.0	PYTHIA 8.2	NNPDF3.0NLO	NNPDF2.3LO	A14	NLO / NLO
Non-Higgs						
t <bar>t}/ single top</bar>	POWHEG BOX v2	PYTHIA 8.2	NNPDF3.0NLO	NNPDF2.3LO	A14	NNLL / NNLO
V+jets	SHERPA 2.2.1	SHERPA 2.2.1	NNPDF3.0NNLO	NNPDF3.0NNLO	SHERPA	NNLO
EWK V+jets	SHERPA 2.2.1	SHERPA 2.2.1	NNPDF3.0NNLO	NNPDF3.0NNLO	SHERPA	LO
Diboson	SHERPA 2.2.2/2.2.1	SHERPA 2.2.2/2.2.1	NNPDF3.0NNLO	NNPDF3.0NNLO	SHERPA	NLO

accepted events from the 40 MHz bunch crossings at a rate close to 100 kHz, which the high-level trigger further reduced in order to record complete events to disk at about 1.25 kHz.

A software suite [43] is used in data simulation, in the reconstruction and analysis of real and simulated data, in detector operations, and in the trigger and data acquisition systems of the experiment.

4 Data and simulated event samples

This analysis uses the full dataset collected by the ATLAS detector during Run 2 (2015–2018) of the LHC, consisting of events produced from pp collisions at a centre-of-mass energy of $\sqrt{s} = 13$ TeV. Events are selected only if they are recorded under stable beam conditions where all relevant detector subsystems are in good operating condition [44], and satisfy data-quality requirements. The dataset corresponds to a total integrated luminosity of 140 fb^{-1} [45].

Monte Carlo simulated event samples are used to model the $H \rightarrow \tau\tau$ signal and most of the backgrounds from SM processes, including $Z(\rightarrow \tau\tau) + \text{jets}$, top-quark processes and multi-boson production. A summary of the generators used for the simulation is shown in Table 1. Backgrounds arising from misidentified objects are estimated with a data-driven method described in Section 6. The same event generators as in Ref. [27] are used, with the exception of the generator used for the parton shower (PS) of the $t\bar{t}$ and single top simulations. The normalisation of all Higgs boson samples accounts for the decay branching ratio calculated with HDECAY [46–48] and PROPHECY4F [49–51]. For all samples, excluding those simulated using SHERPA, the decays of bottom and charm hadrons were performed by EvtGEN [52].

Higgs boson production via gluon–gluon fusion was simulated at next-to-next-to-leading-order (NNLO) accuracy in QCD using Powheg Box v2 [53–56], with the PDF4LHC15NNLO parton distribution function (PDF) set [57]. The simulation achieves NNLO accuracy for arbitrary inclusive $gg \rightarrow H$ observables by reweighting the Higgs boson rapidity spectrum in HJ-MiNLO [58–60] to that of HNNLO [61]. For PS, the CTEQ6L1 [62] PDF and the set of tuned parameters (tune) AZNLO [63] of PYTHIA 8.2 [64] were used.

The gluon–gluon fusion prediction from the MC samples was normalised to the next-to-next-to-next-to-leading-order (N^3LO) cross-section in QCD plus electroweak corrections at next-to-leading-order (NLO) [65–75].

Higgs boson production via vector-boson fusion was simulated with PowHEG Box v2 and interfaced with PYTHIA 8.2 for PS and non-perturbative effects, with parameters set according to the AZNLO tune. The PowHEG Box prediction is accurate at NLO and uses the PDF4LHC15NLO PDF set. It was normalised to an approximate-NNLO QCD cross-section with NLO electroweak corrections [33, 34, 76].

Higgs boson production in association with a vector boson was simulated using PowHEG Box v2 and interfaced with PYTHIA 8.2 for PS and non-perturbative effects. The PowHEG Box prediction is accurate at NLO for VH boson plus one-jet production. The loop-induced $gg \rightarrow ZH$ process was generated separately at leading order. The PDF4LHC15NLO PDF set and the AZNLO tune of PYTHIA 8.2 were used. The MC prediction was normalised to cross-sections calculated at NNLO in QCD with NLO electroweak corrections for $q\bar{q}/qg \rightarrow VH$ and at NLO and next-to-leading-logarithm accuracy in QCD for $gg \rightarrow ZH$ [35, 77–82].

The production of $t\bar{t}H$ events was modelled using the PowHEG Box v2 generator at NLO with the NNPDF3.0NLO PDF set. The events were interfaced to PYTHIA 8.2 using the A14 tune [83] and the NNPDF2.3LO [84] PDF set.

The production of tHq events was modelled using the MADGRAPH5_AMC@NLO 2.6.0 [85] generator at NLO with the NNPDF3.0NLO PDF. The events were interfaced with PYTHIA 8.2 using the A14 tune and the NNPDF2.3LO PDF set.

The production of V +jets was simulated with the SHERPA 2.2.1 [86] generator using NLO ME for up to two partons, and leading-order (LO) ME for up to four partons calculated with the Comix [87] and OPENLOOPS [88–90] libraries. They were matched with the SHERPA PS [91] using the MEPS@NLO prescription [92–95] using the set of tuned parameters developed by the SHERPA authors. The NNPDF3.0NNLO set of PDFs was used and the samples were normalised to an NNLO prediction [96].

Electroweak production of $\ell\ell jj$, $\ell\nu jj$ and $vv jj$ final states (EW V +jets) was simulated with SHERPA 2.2.1 using leading-order ME with up to one additional parton emission. The ME were merged with the SHERPA PS following the prescription described above. The NNPDF3.0NNLO set of PDFs was employed. The samples were produced using the VBF approximation, which avoids overlap with semileptonic diboson topologies by requiring a t -channel colour-singlet exchange.

The production of $t\bar{t}$ events was modelled using the PowHEG Box v2 generator at NLO with the NNPDF3.0NLO PDF set and the h_{damp} parameter⁴ set to $1.5 m_{\text{top}}$ [97]. The events were interfaced to PYTHIA 8.2 to model the PS, hadronisation, and underlying event, with parameters set according to the A14 tune and using the NNPDF2.3LO set of PDFs. The $t\bar{t}$ sample was normalised to the cross-section prediction at NNLO in QCD including the resummation of next-to-next-to-leading logarithmic (NNLL) soft-gluon terms calculated using Top++ 2.0 [98–104].

Single-top t -channel production was modelled using the PowHEG Box v2 generator at NLO in QCD using the four-flavour scheme and the corresponding NNPDF3.0NLO set of PDFs. The events were interfaced with PYTHIA 8.2 using the A14 tune and the NNPDF2.3LO set of PDFs. The inclusive cross-section was

⁴ The h_{damp} parameter is a resummation damping factor and one of the parameters that controls the matching of PowHEG ME to the PS and thus effectively regulates the high-transverse momentum (p_T) radiation against which the $t\bar{t}$ system recoils.

corrected to the theory prediction calculated at NLO in QCD with NNLL soft-gluon corrections [105, 106].

The associated production of top quarks with W bosons (tW) was modelled by the Powheg Box v2 generator at NLO in QCD using the five-flavour scheme and the NNPDF3.0NLO set of PDFs. The diagram removal scheme [107] was used to remove interference and overlap with $t\bar{t}$ production. The related uncertainty was estimated by comparison with an alternative sample generated using the diagram subtraction scheme [97, 107]. The events were interfaced to Pythia 8.2 using the A14 tune and the NNPDF2.3LO set of PDFs.

Samples of diboson final states (VV) were simulated with the Sherpa 2.2.1 or 2.2.2 generator depending on the process, including off-shell effects and Higgs boson contributions, where appropriate. Fully leptonic final states and semileptonic final states, where one boson decays leptonically and the other hadronically, were generated using ME at NLO accuracy in QCD for up to one additional parton and at LO accuracy for up to three additional parton emissions. Samples for the loop-induced processes $gg \rightarrow VV$ were generated using LO-accurate ME for up to one additional parton emission for both the cases of fully leptonic and semileptonic final states. The ME calculations were matched and merged with the Sherpa PS based on Catani–Seymour dipole factorisation [87, 91] using the MEPS@NLO prescription [92–95]. The virtual QCD corrections were provided by the OPENLOOPS library [88–90]. The NNPDF3.0NNLO set of PDFs was used, along with the dedicated set of tuned PS parameters developed by the Sherpa authors.

The effect of multiple interactions in the same and neighbouring bunch crossings (pile-up) was modelled by overlaying the simulated hard-scattering event with inelastic proton–proton events generated with Pythia 8.1 [108] using the NNPDF2.3LO set of PDFs and the A3 set of tuned parameters [109]. All samples were processed through an ATLAS detector simulation [110] based on GEANT4 [111].

In this analysis, only Higgs boson production via VBF is considered as signal. This includes the decay into $H \rightarrow \tau\tau$ and the decay $H \rightarrow WW^* \rightarrow \ell\nu\ell\nu$. The analysis is not sensitive to the CP violating effects in the $H \rightarrow WW^*$ decay vertex, since the Optimal Observable contains only production kinematics information, and it is the same for both decay channels. All other Higgs boson production mechanisms are considered as backgrounds, with all other couplings set to the SM values. Non-VBF Higgs boson production, along with $Z \rightarrow \ell\ell$ and $W \rightarrow \tau\nu + \text{jets}$, are for the remainder of the text grouped together and denoted “other backgrounds”.

The production of the signal samples with non-vanishing values of CP violation in the HVV vertex is obtained with a reweighting procedure, based on the EFT interpretation considered. For the HISZ basis, an event-based weight is obtained from the ratio of the squared ME value of the VBF process associated with a specific amount of CP mixing (given in terms of \tilde{d}) to that obtained from the SM. These weights are obtained from HAWK, considering the $2 \rightarrow 2 + H$ and $2 \rightarrow 3 + H$ processes separately. The MEs are evaluated using the parton-level information of the four momentum and flavour of the initial and final state partons and the Higgs boson.

For the Warsaw basis, a procedure similar to the one described in Ref. [12] is used, where an event-weight is obtained based on the $\mathcal{O}\mathcal{O}$ distribution at different values of the Warsaw basis operator considered. The weights are obtained as

$$\frac{d\sigma}{d\mathcal{O}\mathcal{O}} = \left(\frac{d\sigma}{d\mathcal{O}\mathcal{O}} \right)^{\text{NLO}} \times \left(\frac{d\sigma}{d\mathcal{O}\mathcal{O}} \right)_{c_i}^{\text{MG5}} \Bigg/ \left(\frac{d\sigma}{d\mathcal{O}\mathcal{O}} \right)_{c_i=0}^{\text{MG5}},$$

where the term with “NLO” is the SM VBF signal prediction, while those with “MG5” describe the predictions obtained with MadGraph [85, 112] for a given value of the CP-violating coupling constant

considered (c_i). The **MADGRAPH** samples for $c_i \neq 0$ are obtained by setting the scale of the new physics to $\Lambda = 1$ TeV, and fixing all the other Wilson coefficient to zero. The **MADGRAPH** samples are generated at LO and effects of higher-order QCD and electroweak corrections are assumed to factor out in the ratio. The procedure is done separately for each Wilson coefficient considered.

5 Event selection

This analysis targets final states with at least two jets and a $H \rightarrow \tau\tau$ decay candidate. Three combinations of τ -lepton decays are considered: fully hadronic ($\tau_{\text{had}}\tau_{\text{had}}$), where both τ -leptons decay to hadrons (with $\tau_{\text{had-vis}}$ being the visible part) and a ν ; semileptonic ($\tau_{\text{lep}}\tau_{\text{had}}$), where one decays hadronically and the other to $\ell\nu\bar{\nu}$, $\ell = e, \mu$; and leptonic ($\tau_{\text{lep}}\tau_{\text{lep}}$), where one decays to $e\nu\bar{\nu}$ and the other to $\mu\nu\bar{\nu}$. Same-flavour leptonic decays are rejected due to the large contribution from $Z \rightarrow ee$ and $Z \rightarrow \mu\mu$ backgrounds.

The definition of the reconstructed objects follows what is described in more detail in Ref. [28]. The full description of the requirements in each channel is given in Table 2.

Events were collected with the lowest unprescaled single-lepton, dilepton, or di-hadronic τ -lepton triggers [113–116]. Each trigger chain has a different online requirement on the p_T of the reconstructed leptons, depending on the year. The offline requirements are set tighter to ensure that the analysis is on the trigger efficiency plateau, and follow the selection used in Ref. [28]. All channels require exactly two identified and isolated τ -lepton decay candidates, and events with an additional τ -lepton candidate are rejected. The two τ -candidates are required to have opposite sign electric charge. All channels are required to have a missing transverse energy of $E_T^{\text{miss}} > 20$ GeV, to improve the resolution of the MMC. In the $\tau_{\text{lep}}\tau_{\text{lep}}$ channel an additional lower limit on the collinear mass [117] of the two- τ -lepton system is required, $m_{\tau\tau}^{\text{coll}} > (m_Z - 25)$ GeV (where m_Z is the Z boson mass), to ensure orthogonality with the $H \rightarrow WW^*$ analysis [118]. The effect on signal acceptance is negligible. Moreover, it is also required that the dilepton invariant mass lies in the range of $30 \text{ GeV} < m_{e\mu} < 100 \text{ GeV}$ to enhance the fraction of Higgs events and reduce the number of $Z \rightarrow \tau\tau$ events. In the $\tau_{\text{lep}}\tau_{\text{had}}$ channel a requirement on the transverse mass between the lepton and the missing transverse energy of $m_T < 70$ GeV is instead imposed to reduce the contribution from leptonic W decays.

In all channels, the contribution from events containing a top-quark is reduced by vetoing events with b -tagged jets; the $\tau_{\text{lep}}\tau_{\text{lep}}$ and $\tau_{\text{lep}}\tau_{\text{had}}$ channels use an 85% working point (WP) of the DL1r b -tagging algorithm, while in the $\tau_{\text{had}}\tau_{\text{had}}$ channel a 70% WP [119] is used, to ensure similar performance in all the channels. The $\tau_{\text{lep}}\tau_{\text{lep}}$ and $\tau_{\text{lep}}\tau_{\text{had}}$ channels require the leading jet to have a transverse momentum of $p_T^{j_1} > 40$ GeV, to enhance the VBF contribution. In the $\tau_{\text{had}}\tau_{\text{had}}$ channel, the requirement is raised to $p_T^{j_1} > 70$ GeV, and it is also required that the leading jet be within the pseudorapidity range of $|\eta| < 3.2$. This is done to ensure candidate events are on the di-hadronic τ -lepton triggers efficiency plateau. Requirements on the angular distance between the reconstructed decays of the two τ -candidates are applied in all channels, to reject non-resonant background events. Additional requirements are applied on the momentum fraction, x_1/x_2 , of each τ -lepton carried by its visible decay products in the collinear approximation to enhance the sensitivity to the Higgs signal and reduce background contributions.

A set of requirements to define the VBF topology is applied. Each event is required to have at least two jets, where in addition to the leading jet requirements above, the sub-leading jet must have a transverse momentum $p_T^{j_2}$ greater than 30 GeV, the invariant mass of the two leading jets m_{jj} must be greater than 350 GeV, and the pseudorapidity separation $|\Delta\eta_{jj}|$ between the two jets must be greater than 3.0, with

Table 2: Summary of the event selection for all sub-channels of the analysis. For electrons and muons, the lowest p_T requirement depends on the trigger used, which changes with the year of data taking. The p_T requirements per year are listed in Ref. [28].

Criteria	$\tau_e \tau_\mu$		$\tau_{\text{lep}} \tau_{\text{had}}$	
	$\tau_e \tau_{\text{had}}$	$\tau_\mu \tau_{\text{had}}$	$\tau_{\text{had}} \tau_{\text{had}}$	
Preselection				
$N(e)$	1	1	0	0
$N(\mu)$	1	0	1	0
$N(\tau_{\text{had-vis}})$	0	1	1	2
$N(b\text{-jets})$	0 (85% WP)	0 (85% WP)	0 (85% WP)	0 (70% WP)
p_T [GeV]	e/μ : $p_T > 10$ to 27.3 $\tau_{\text{had-vis}}$: $p_T > 30$	e/μ : $p_T > 10$ to 27.3, $\tau_{\text{had-vis}}$: $p_T > 40$, 30		
Identification	e/μ : Medium	e/μ : Medium, $\tau_{\text{had-vis}}$: RNN Medium	$\tau_{\text{had-vis}}$: RNN Medium	
Isolation	e : Loose, μ : Tight	e : Loose	μ : Tight	
Electric charge	Opposite charge			
E_T^{miss} [GeV]	> 20			
Kinematics	$m_{\tau\tau}^{\text{coll}} > (m_Z - 25)$ GeV 30 GeV $< m_{e\mu} <$ 100 GeV	$m_T < 70$ GeV		
Leading jet	$p_T > 40$ GeV		$p_T > 70$ GeV, $ \eta < 3.2$	
Angular	$\Delta R_{e\mu} < 2.5$ $ \Delta\eta_{e\mu} < 1.5$	$\Delta R_{\ell\tau_{\text{had-vis}}} < 2.5$ $ \Delta\eta_{\ell\tau_{\text{had-vis}}} < 1.5$	$0.6 < \Delta R_{\tau_{\text{had-vis}}\tau_{\text{had-vis}}} < 2.5$ $ \Delta\eta_{\tau_{\text{had-vis}}\tau_{\text{had-vis}}} < 1.5$	
Coll. app. x_1/x_2	0.1 $< x_1 <$ 1.0 0.1 $< x_2 <$ 1.0	0.1 $< x_1 <$ 1.4 0.1 $< x_2 <$ 1.2	0.1 $< x_1 <$ 1.4 0.1 $< x_2 <$ 1.4	
VBF inclusive	sub-leading jet $p_T > 30$ GeV $m_{jj} > 350$ GeV, $ \Delta\eta_{jj} > 3$ $\eta(j_1) \times \eta(j_2) < 0$ lepton centrality: all visible decay products of the two τ -leptons lie between the two jets in η			

each jet in a separate hemisphere of the detector. Additionally, all visible decay products of the τ -leptons must lie in η between the two leading jets.

To construct an enriched signal region (SR), a multivariate classifier based on neural network (NN) is used. The network is implemented in KERAS [120] using TENSORFLOW [121] as backend. For each channel, a separate NN is optimised to best exploit the different compositions and features of the channels. All three channels have similar features in architecture and training procedure: the ADAM optimizer algorithm [122] is used, with ReLU activation functions [123], and L2 regularisation [124] and k -fold (with $k = 5$) to prevent overfitting. A binary classifier is built for the $\tau_{\text{lep}}\tau_{\text{had}}$ and $\tau_{\text{had}}\tau_{\text{had}}$ channel, while in the $\tau_{\text{lep}}\tau_{\text{lep}}$ channel a multi-class classifier is optimised, with the categories being: signal, $Z \rightarrow \tau\tau$, misidentified τ -lepton decays, and other backgrounds. This is done to better describe the background coming from misidentified τ -lepton decays. The training is performed assuming the SM predictions, therefore no CP-odd component is added, only the VBF Higgs SM sample is used. The NN is then tested for different CP-violating hypotheses, and is found to be consistent with the SM case, indicating the NN is not inducing any biases in the choice of events based on the CP hypothesis considered. Each channel uses as input a different set of observables, optimised to achieve the best separation between signal and background. The list of input variables used in the training is shown in Table 3. The different input variables can be categorised as follows:

- Four-vectors of the two τ -decay products, and of the two leading VBF tagging jets.
- Missing transverse energy vector and its ratio to the transverse momentum of other objects. Additionally, the $E_{\text{T}}^{\text{miss}}$ centrality⁵ and missing transverse energy constructed using only the hard-scatter particles, $E_{\text{T},\text{HPTO}}^{\text{miss}}$, are considered in the training. The transverse masses using the $E_{\text{T}}^{\text{miss}}$ and both τ -decay products are also considered.
- Properties of the resonant di- τ system are used, such as the invariant mass of the τ -decay products (using both the missing mass calculator, $m_{\tau\tau}^{\text{MMC}}$ [36], and using only the visible part of the τ -decay products $m_{\tau\tau}^{\text{vis}}$), and the angular distances, $\Delta R_{\tau_1\tau_2}$, $\Delta\eta_{\tau_1\tau_2}$, and $\Delta\phi_{\tau_1\tau_2}$. In addition, the scalar sum, $p_{\text{T}}(\tau_1) + p_{\text{T}}(\tau_2)$, and the ratio, $p_{\text{T}}(\tau_1)/p_{\text{T}}(\tau_2)$, of the transverse momenta of the two τ -decay products are considered. The ratio of the difference and the sum of transverse momenta of the di- τ decay products, $[p_{\text{T}}(\tau_1) - p_{\text{T}}(\tau_2)]/[p_{\text{T}}(\tau_1) + p_{\text{T}}(\tau_2)]$, is also used.
- Properties of the VBF topology: invariant mass of the dijet system, m_{jj} , the product and the difference of the pseudorapidity of the two leading jets and the transverse momentum of their vectorial sum, η -centrality of the τ -decay products, $C_{jj}(\tau_1)$, $C_{jj}(\tau_2)$ ⁶, with respect to the pseudorapidity of the two tagging jets. Furthermore, the training also uses momenta of different systems composed of the objects considered in the VBF topology definition (di- τ -decay products, two leading jets, and $E_{\text{T}}^{\text{miss}}$). The azimuthal separation and the invariant mass between the di- τ -system and the leading jet is also considered.

The most important input features in the training are the reconstructed masses $m_{\tau\tau}^{\text{MMC}}$, $m_{\tau\tau}^{\text{vis}}$, m_{jj} , and the transverse momentum of the system composed of the τ -decay products, jets and $E_{\text{T}}^{\text{miss}}$, $p_{\text{T}}(\tau_1, \tau_2, j_1, j_2, E_{\text{T}}^{\text{miss}})$.

⁵ The $E_{\text{T}}^{\text{miss}} - \phi$ -centrality quantifies the angular direction of the missing transverse momentum relative to the visible τ -decay products in the transverse plane, and is constructed as: $E_{\text{T}}^{\text{miss}} - \phi\text{-centrality}/\sqrt{2} = \frac{r+s}{\sqrt{r^2+s^2}}$, where $r = \sin(\phi(E_{\text{T}}^{\text{miss}}) - \phi(\tau_1))/\sin(\phi(\tau_2) - \phi(\tau_1))$ and $s = \sin(\phi(\tau_2) - \phi(E_{\text{T}}^{\text{miss}}))/\sin(\phi(\tau_2) - \phi(\tau_1))$.

⁶ $C_{jj}(\tau) = \exp\left[\frac{-4}{(\eta_{j_1} - \eta_{j_2})^2}\left(\eta_{\tau} - \frac{\eta_{j_1} + \eta_{j_2}}{2}\right)^2\right]$, where η_{τ} , $\eta_{j_{1/2}}$ are the pseudorapidities of the τ -decay products and the two leading jets, respectively. This variable has a value of unity when the object is halfway in η between the two jets, $1/e$ when the object is aligned with one of the jets, and $< 1/e$ when the object is not between the jets in η .

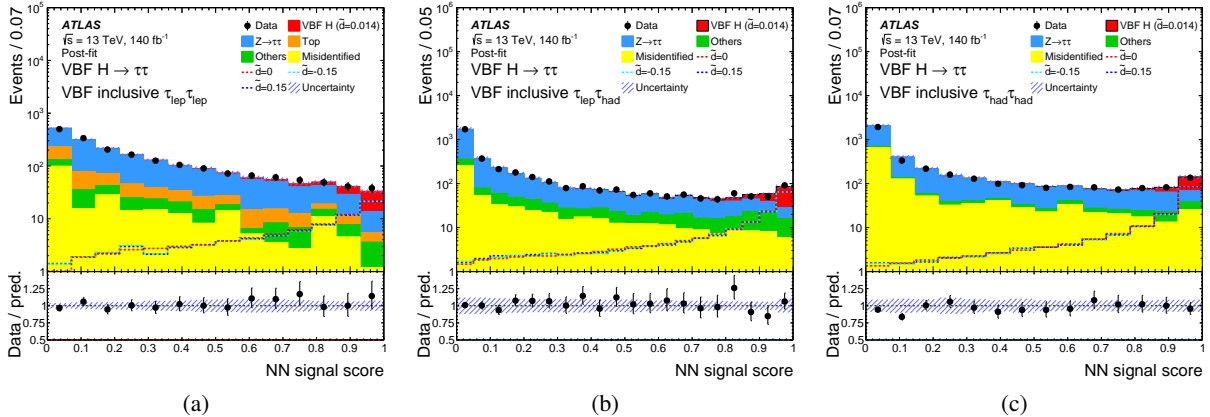


Figure 2: Post-fit distribution of the neural network signal score for the three channels, (a) $\tau_{\text{lep}}\tau_{\text{lep}}$, (b) $\tau_{\text{lep}}\tau_{\text{had}}$, and (c) $\tau_{\text{had}}\tau_{\text{had}}$. The ratio of the SM predictions to the observed data is shown in the bottom panel. The “Other bkg” includes diboson, $Z \rightarrow \ell\ell$, and $W \rightarrow \tau\nu + \text{jets}$, and other non-VBF-Higgs processes. The hatched area represents the impact of the experimental, theoretical and statistical uncertainties in the Standard Model predictions. The dashed lines represent examples of signal samples, for different values of \tilde{d} .

Figure 2 shows the distribution of the NN signal score for the three channels considered, after the fit described in Section 8. All systematic uncertainties described in Section 7 are included in the hatched area. This figure shows the ability of the NN to select a region with a high signal-to-background ratio (s/b). The MC predictions are in good agreement with the observed data in all channels. Figure 2 also shows the NN score distributions for signal samples with different \tilde{d} hypotheses. These BSM samples are all in agreement showing how the NN is insensitive to the value of the CP-violating strength parameter. Two orthogonal signal regions are defined for each channel, based on the values of the NN signal score. The high NN score SR ($\text{SR}^{\text{HighNN}}$) is defined by all the events with NN signal score greater than a threshold value. The optimal threshold value, along with the optimal OO binning, is found by choosing the value that gives the most stringent expected 68% CL \tilde{d} interval. A second SR, called low NN score SR (SR^{LowNN}), is then defined by selecting the events with an NN signal score between the $\text{SR}^{\text{HighNN}}$ optimal cut and the NN signal score below which the ratio s/b is less than 5%. Despite having a lower signal-to-background ratio than $\text{SR}^{\text{HighNN}}$, SR^{LowNN} still contributes to the sensitivity, and also helps to better constrain the impact of the systematic uncertainties. The region with an NN signal score lower than the SR^{LowNN} threshold is used as a validation region, VR^{LowNN} . Table 4 shows the definition of the SRs and VRs used, and the corresponding ratio $s/\sqrt{s+b}$.

6 Background estimation

The major backgrounds that contribute to the total yields in the SRs of this analysis are $Z(\rightarrow \tau\tau) + \text{jets}$, misidentified τ candidates (*fakes*), top-quark processes, and multi-boson production. These backgrounds are estimated with different techniques based on MC simulations and data-driven methods.

The main background for each channel comes from $Z(\rightarrow \tau\tau) + \text{jets}$. These events have the same signature as the Higgs signal, and similar kinematics. For these reasons, designing a signal-free control region (CR) where to constrain $Z(\rightarrow \tau\tau) + \text{jets}$ at high NN value is extremely challenging. Instead this background

Table 3: Summary of the set of input variables used in the different channels. The order does not reflect the importance of each variable.

	Variable	$\tau_{\text{lep}} \tau_{\text{lep}}$	$\tau_{\text{lep}} \tau_{\text{had}}$	$\tau_{\text{had}} \tau_{\text{had}}$
τ -lepton properties	$\eta(\tau_1), \eta(\tau_2)$		•	
	$p_T(\tau_1), p_T(\tau_2)$		•	
	$\phi(\tau_1), \phi(\tau_2)$		•	
	$E(\tau_1), E(\tau_2)$		•	
	$C_{jj}(\tau_1)$	•	•	•
	$C_{jj}(\tau_2)$	•	•	•
Mass	$m_{\tau\tau}^{\text{MMC}}$	•	•	•
	$m_{\tau\tau}^{\text{vis}}$	•	•	•
	m_{jj}	•	•	•
	$m_T(\tau_1, E_T^{\text{miss}})$	•	•	•
	$m_T(\tau_2, E_T^{\text{miss}})$	•	•	•
	$m(\tau_1, \tau_2, j_1)$	•	•	•
Angular distances	$\eta^{j_1} \times \eta^{j_2}$	•	•	•
	$\Delta R_{\tau_1 \tau_2}$	•	•	•
	$\Delta \eta_{\tau_1 \tau_2}$	•	•	•
	$\Delta \phi_{\tau_1 \tau_2}$	•	•	•
	$\Delta \eta_{jj}$	•	•	•
	$\Delta \phi_{H, j_1}$	•	•	•
Jet properties	$p_T(\tau_1, \tau_2, j_1, j_2)$		•	
	$p_T(j_1, j_2)$	•	•	•
	$p_T(\tau_1, \tau_2, j_1, j_2, E_T^{\text{miss}})$	•	•	•
	$p_T(j_2), p_T(j_3)$	•		•
	$\eta(j_1), \eta(j_2)$		•	
	$\phi(j_1), \phi(j_2)$		•	
	$E(j_1), E(j_2)$		•	
	$p_T(\tau_1) + p_T(\tau_2)$	•		•
	$p_T(\tau_1, \tau_2)$	•	•	•
	$p_T(\tau_1, \tau_2, E_T^{\text{miss}})$	•	•	•
	$p_T(\tau_1, \tau_2, j_1, E_T^{\text{miss}})$	•	•	•
	$p_T(\tau_1)/p_T(\tau_2)$	•		•
Missing transverse energy	$\Delta p_T(\tau_1, \tau_2)/(p_T(\tau_1) + p_T(\tau_2))$	•		•
	E_T^{miss}		•	
	$E_T^{\text{miss}} \phi$		•	
	$E_T^{\text{miss}}/p_T(\tau_1)$	•	•	•
	$E_T^{\text{miss}}/p_T(\tau_2)$	•	•	•
	$E_T^{\text{miss}} - \phi\text{-centrality}/\sqrt{2}$	•	•	•
	$E_{T,\text{HPTO}}^{\text{miss}}$	•		•

is estimated following a procedure called *embedding* [125], where the $Z(\rightarrow \tau\tau) + \text{jets}$ yields in the SR predicted by the MC simulations are normalised by a scale factor that is obtained in a dedicated control region, following closely the procedure in Ref. [28], called *object-level embedding*.

The embedding method relies on the assumption that, at Born level, $Z \rightarrow \ell\ell$ (where ℓ is only e or μ) and $Z \rightarrow \tau\tau$ are kinematically identical processes. This means that by substituting the leptons (e or μ) in $Z \rightarrow \ell\ell$ data events with τ -lepton decays from simulation, and then recomputing all the necessary variables in the event, it is possible to get a template of the $Z \rightarrow \tau\tau$ background directly from data. These templates are obtained starting from data and MC events in an enriched $Z(\rightarrow \ell\ell) + \text{jets}$ region, where the momentum of the reconstructed leptons are scaled using a parameterisation that accounts for the differences in efficiency of triggers, the reconstruction procedure and kinematics between the prompt leptons and the τ -lepton decays. After this procedure, all the kinematic variables are recomputed to account for the rescaled lepton momentum, including the E_T^{miss} from the additional neutrinos of the τ -leptons decays. For each SR a dedicated $Z(\rightarrow \tau\tau) + \text{jets}$ CR is defined with the same selections but using the template samples, $Z\tau\tau\text{CR}^{\text{HighNN}}$ for the high NN score SR and $Z\tau\tau\text{CR}^{\text{LowNN}}$ for the low NN score SR. These CRs are then included in the fit to constrain the $Z(\rightarrow \tau\tau) + \text{jets}$ in the SR.

Dedicated systematic uncertainties are added to account for the modelling differences between the embedded $Z(\rightarrow \tau\tau) + \text{jets}$ MC and the nominal $Z \rightarrow \tau\tau$ in the SR. The VR^{LowNN} is then used to check the modelling of the $Z(\rightarrow \tau\tau) + \text{jets}$ after the normalisation with the embedding procedure. Figure 3 shows the OO distribution in each VR, after a background-only fit.

The second largest background component comes from events where one or two τ -leptons are incorrectly categorised. In these events, jets are misidentified as electrons, muons, or as τ_{had} . These backgrounds account for 4% to 30% of the total SM background, depending on the channel and region. Background events with misidentified τ candidates are estimated by using a data driven method, with different methodologies depending on the channel.

In the $\tau_{\text{lep}}\tau_{\text{lep}}$ channel, the matrix method [126] is used to estimate the background from misidentified e or μ . In this channel, events are selected from two control regions ($\text{CR}_{\ell\ell}^{\text{real}}$ and $\text{CR}_{\ell\ell}^{\text{fake}}$) similar to the SR, but without the requirements on the isolation and loosened identification criteria of the leptons (Loose ID WP for e and Medium ID WP for μ). The number of misidentified leptons in the SR is then related to the number of leptons passing the loose and tight isolation and identification criteria, based on the

Table 4: Summary of NN signal score values used for defining the SRs and the VR for each channel, and their corresponding ratio $s/\sqrt{s+b}$.

Channel	Region	NN signal score	$s/\sqrt{s+b}$
$\tau_{\text{lep}}\tau_{\text{lep}}$	$\text{SR}^{\text{HighNN}}$	> 0.91	3.50
	SR^{LowNN}	$0.67 - 0.91$	1.98
	VR^{LowNN}	< 0.67	0.51
$\tau_{\text{lep}}\tau_{\text{had}}$	$\text{SR}^{\text{HighNN}}$	> 0.91	6.93
	SR^{LowNN}	$0.63 - 0.91$	2.69
	VR^{LowNN}	< 0.63	0.30
$\tau_{\text{had}}\tau_{\text{had}}$	$\text{SR}^{\text{HighNN}}$	> 0.93	6.86
	SR^{LowNN}	$0.60 - 0.93$	2.42
	VR^{LowNN}	< 0.60	0.34

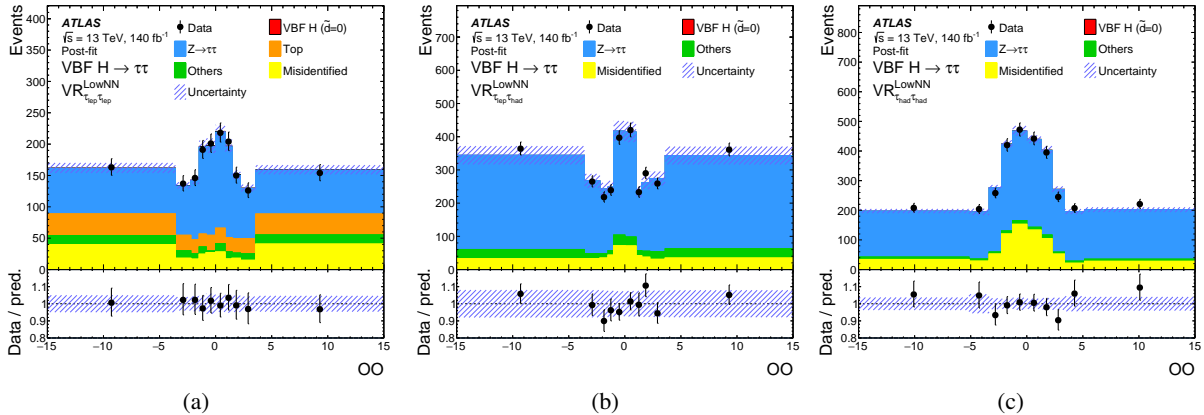


Figure 3: Distributions of the OO in the VR for the three channels: (a) $\tau_{\text{lep}}\tau_{\text{lep}}$, (b) $\tau_{\text{lep}}\tau_{\text{had}}$, (c) $\tau_{\text{had}}\tau_{\text{had}}$, after a background-only fit. The value of the parameter of interest, the signal strength, the normalisation of backgrounds, and the systematic uncertainties are set to the value from the best fit result. In the bottom panel, the hatched area represent the total post-fit systematic uncertainty in the final SM prediction.

efficiencies for real and fake leptons. The real efficiencies are obtained from MC simulations, while the fake-lepton efficiencies are measured from data in a region with two leptons with the same sign. The method is validated in a region with the same selection criteria as the SR but with same-sign leptons. Any difference in this region is added as a systematic uncertainty. Additional uncertainties are assigned to this background taking into account the statistical uncertainties in the fake and real efficiencies, the uncertainty in the background subtraction when computing the efficiencies, and the different flavour composition between the SR and the loosened $\text{CR}_{\ell\ell}^{\text{fake}}$.

In the $\tau_{\text{lep}}\tau_{\text{had}}$ and $\tau_{\text{had}}\tau_{\text{had}}$ channels, misidentified τ candidates are estimated by using the fake-factor method [126]. Events are selected from a control region ($\text{CR}^{\text{anti}-\tau}$) with the same selection as the SR, but with a loosened requirement on the τ_{had} identification criterion, and failing to meet the nominal identification requirement from Table 2. Contributions from real τ_{had} in this region are estimated with MC simulations and subtracted. The final number of misidentified τ candidates in the SR is then obtained by multiplying the background-subtracted events in the $\text{CR}^{\text{anti}-\tau}$ by a *fake-factor*, \mathcal{F} . This factor is the ratio of the number of τ candidates passing the identification criterion in Table 2 to the number of those failing the same criterion. These factors are obtained in separate dedicated CRs. Misidentified τ candidates originate mainly from $W+\text{jets}$ and dijet events, and the ratio of passing to failing identification criteria can be different for the two processes, in different kinematic regions. For this reason, one fake-factor is computed for each process, in a different CR. The final fake-factor is then a weighted mean of the two based on the relative composition in the SR. Additionally, the fake-factors are estimated separately for 1-prong and 3-prong τ candidates. The final estimate is validated in a region with the same selection as the SR, but with same-sign τ candidates. The non-closure is taken as an uncertainty as a function of the Optimal Observable. Additional uncertainties are added taking into account the statistical uncertainty in the computation of \mathcal{F} and the relative composition in the SR, and the uncertainty in the background subtraction in the $\text{CR}^{\text{anti}-\tau}$ and in the \mathcal{F} computation.

Other sources of backgrounds from misidentified objects are estimated directly from simulations.

In the $\tau_{\text{lep}}\tau_{\text{lep}}$ channel, processes including a top quark have a sizeable contribution. This background is estimated directly from the MC simulations, but it is normalised to the data in a dedicated CR (TopCR)

obtained with the same selection as the SR but inverting the veto on the number of b -jet in the events. In the $\tau_{\text{lep}}\tau_{\text{had}}$ and $\tau_{\text{had}}\tau_{\text{had}}$ channels the contributions from top-quark processes are estimated directly from MC.

In all three channels, other smaller prompt contributions are estimated directly from MC.

7 Systematic uncertainties

Systematic uncertainties affecting both the shape of the Optimal Observable and the event yields in the signal and control regions are considered. These can be grouped in three main categories: experimental uncertainties, uncertainties in data-driven modelling, and theoretical uncertainties.

Experimental systematic uncertainties include those related to the trigger, reconstruction, and identification of objects in the final state. These sources include electron and muon energy or momentum scale and resolution [127, 128], $\tau_{\text{had-vis}}$ energy scale and resolution [129], b -tagging efficiency [130, 131], $E_{\text{T}}^{\text{miss}}$ reconstruction [132], jet energy scale and resolution [133], pile-up modelling [134], and the luminosity measurement [45]. Jet and $E_{\text{T}}^{\text{miss}}$ reconstruction and theory uncertainties constitute the dominant sources of systematic uncertainty, at 20% and 15%, respectively.

Uncertainties in the data-driven background modelling affect the three channels differently. For $\tau_{\text{lep}}\tau_{\text{lep}}$, the uncertainties in the matrix method estimates are related to the limited statistical precision in the computation of the real and fake-lepton efficiencies, the MC background subtraction, and the flavour composition difference between the signal region and the fake control region. For $\tau_{\text{lep}}\tau_{\text{had}}$ and $\tau_{\text{had}}\tau_{\text{had}}$, statistical uncertainties in the individual fake factors, and uncertainties due to differences in composition between the SR and the regions where the fake factors are computed, are considered. Uncertainties affecting the $Z \rightarrow \tau\tau$ embedded MC sample are evaluated by propagating all experimental uncertainties listed above. In addition the effects of trigger efficiencies, muon and $\tau_{\text{had-vis}}$ reconstruction and isolation efficiencies, and e/μ energy scale and resolution are considered.

Theory uncertainties in the signal and background cross-sections are evaluated by varying the PDF sets and the renormalisation and factorisation scales, as well as the value of the strong coupling constant α_s , used in MC generation.

For $Z(\rightarrow \tau\tau) + \text{jets}$ production, 100 PDF variations are considered, taking the standard deviation as the uncertainty. The PDF sets are evaluated for up- and down-variations of α_s , and a combined uncertainty is derived by adding the uncertainties in PDF and α_s variations in quadrature. Uncertainties in renormalisation and factorisation scales are determined based on the maximum absolute difference when independently varying their values up or down by a factor of two, resulting in a seven-point variation. In addition, uncertainties in the jet-to-parton matching scheme (CKKW) and resummation scale are evaluated using parameterisations as function of the jet multiplicity and Z transverse momentum.

For top processes, uncertainties related to the choice of matrix element and parton shower generators are assessed by comparing to alternative generators, while uncertainties in initial- and final-state radiation are evaluated by varying the scale of emission, as described in Ref. [135]. The PDF uncertainty is evaluated by varying the PDF sets for both the production and the parton shower, and the two are treated as separate uncertainties.

Uncertainties in signal processes are similarly evaluated by PDF and α_s variations, and uncertainties in the matrix element and parton shower are assessed through alternative generators. The effect of

Table 5: Summary of the different sources of systematic uncertainty and their impact on the final fit results, expressed as a percentage of the fitted \tilde{d} 68% CL interval. Experimental systematic uncertainties in the reconstruction of the objects include the reconstruction efficiency, energy scale and resolution, and trigger efficiencies. "Sample size" includes the per-bin statistical uncertainties in the simulated MC samples, and the data-driven backgrounds of misidentified τ -leptons.

Systematic source	Uncertainty [%]
Jet/ E_T^{miss} reconstruction	± 20
Signal theory	± 15
Background theory	± 11
Normalisation factors	$+6.0$ -5.5
Misidentified τ -leptons	± 4.8
τ -leptons reconstruction	± 4.0
Sample size	± 3.0
Leptons reconstruction	± 2.4
Luminosity	± 0.4
Flavour tagging	± 0.3
Embedding	± 0.2
Total systematic uncertainty	± 30
Total statistical uncertainty	± 95

choosing a different matrix element generator is assessed by comparing the nominal signal sample with an alternative sample using `MADGRAPH5_AMC@NLO` [85], but keeping the same parton shower model. Instead, the parton shower uncertainty is obtained through the comparison with an alternative sample using `HERWIG 7` [136] instead of `PYTHIA 8`.

For VBF, VH and $t\bar{t}H$ production, QCD scale uncertainties from missing higher-order corrections are evaluated through the seven-point variation of renormalisation and factorisation scales. For ggF Higgs production, additional uncertainties related to the ggF kinematics are considered, following the approach described in Ref. [137]. These include effects from the Higgs p_T shape, VBF topology selection, and top-quark-mass dependence.

Table 5 shows the impact as a percentage of the main systematic uncertainties in the final \tilde{d} 68% CL interval obtained after the fit described in Section 8. The impact of a given systematic uncertainty in the fitted parameter \tilde{d} is estimated from the covariance matrix as described in Ref. [138]. The main limitation on the sensitivity comes from the statistical uncertainties in the actual observed data, while all the other sources only account for a small fraction.

8 Fitting procedure

The statistical analysis is performed using a binned maximum-likelihood fit, where the likelihood function is defined as the product of Poisson distributions for each bin of each fit region (SRs and CRs), and Gaussian terms for the systematic uncertainties. The probability distributions $\mathcal{L}(\mathbf{x}; \mu, \boldsymbol{\theta})$ depends on the actual data \mathbf{x} , the parameter of interest μ , and further nuisance parameters $\boldsymbol{\theta}$, corresponding to the systematic uncertainties. The sensitivity to the CP-odd coupling (either in the HISZ or the Warsaw basis), is estimated

by doing a negative log-likelihood scan (NLL). The NLL is computed for different hypotheses of the parameter of interest, using signal template samples constructed by reweighting the SM VBF Higgs signal as described in Section 4. The best-fit value is the minimum of the NLL curve with respect to the SM NLL (ΔNLL), with a confidence interval of $[\mu - \sigma_\mu, \mu + \sigma_\mu]$. The 68% and 95% CL intervals are obtained by reading where the ΔNLL curves intersect the points at 0.5 and 1.92 respectively.

Each of the SRs defined in Table 4, $\text{SR}^{\text{HighNN}}$ and SR^{LowNN} , are binned in $\mathcal{O}\mathcal{O}$. The binning of the signal regions in the three channels is optimised to have an equal number of expected SM signal events in each bin. All three channels have a total of 10 bins. The bin boundaries are then fixed to be symmetric around zero.

For each SR, one CR ($Z\tau\tau\text{CR}^{\text{HighNN}}$ and $Z\tau\tau\text{CR}^{\text{LowNN}}$) is defined to constrain the $Z \rightarrow \tau\tau$ background. These regions have the same kinematic cuts as the nominal corresponding SR, including the NN score, but using embedded results, as described in Section 6. These CRs each consist of only one bin. A single common normalisation factor is applied to scale the $Z \rightarrow \ell\ell$ MC in the $Z \rightarrow \tau\tau$ CR as well as the $Z \rightarrow \tau\tau$ MC in the corresponding SRs. One common normalisation factor is used for each channel. Table 6 shows the embedding normalisation factors (NF) obtained for the three channels. In the $\tau_{\text{lep}}\tau_{\text{lep}}$ channel, the TopCR is used to constrain the top backgrounds ($t\bar{t}$ and single top) with one nuisance parameter, with a value of $NF^{\text{top}} = 0.95^{+0.08}_{-0.07}$. In total six SRs and seven CRs are used in the fit.

The normalisation of the signal sample (NF^{VBFH}) is added as a common free floating normalisation factor. In this way, the analysis is not sensitive to overall changes in the total cross-section that might be due to additional CP-even terms, but only considers differences in shapes of $\mathcal{O}\mathcal{O}$, and is therefore only sensitive to the interference term of the EFT model. All the other Higgs production modes are assumed as background and their normalisation is set to the SM prediction. The observed value for the signal normalisation factor is found to be $NF^{\text{VBFH}} = 0.87^{+0.14}_{-0.13}$, which is consistent with the SM prediction.

Two fit setups are considered, one where the three channels ($\tau_{\text{had}}\tau_{\text{had}}$, $\tau_{\text{lep}}\tau_{\text{had}}$, $\tau_{\text{lep}}\tau_{\text{lep}}$) are separately fitted, and one where they are fitted at the same time. In both fits, the experimental and theory systematic uncertainties are considered 100% correlated between channels, while the systematic uncertainties in the modelling of misidentified τ candidates are uncorrelated. All results are shown using the combined fit to the three channels, while the separate channels fit is used to provide the single channel ΔNLL curves.

9 Results

The combined fit procedure described in Section 8 is performed, and the post-fit Optimal Observable distributions in the SRs are shown in Figure 4. The value of the parameter of interest, systematic uncertainties, and background and signal normalisations are adjusted within their allowed constraints to

Table 6: Normalisation factors for the $Z \rightarrow \tau\tau$ MC background obtained with the embedding procedure.

Channel	$Z \rightarrow \tau\tau$ NF
$\tau_{\text{lep}}\tau_{\text{lep}}$	$1.03^{+0.10}_{-0.09}$
$\tau_{\text{lep}}\tau_{\text{had}}$	$0.95^{+0.18}_{-0.15}$
$\tau_{\text{had}}\tau_{\text{had}}$	$0.93^{+0.07}_{-0.07}$

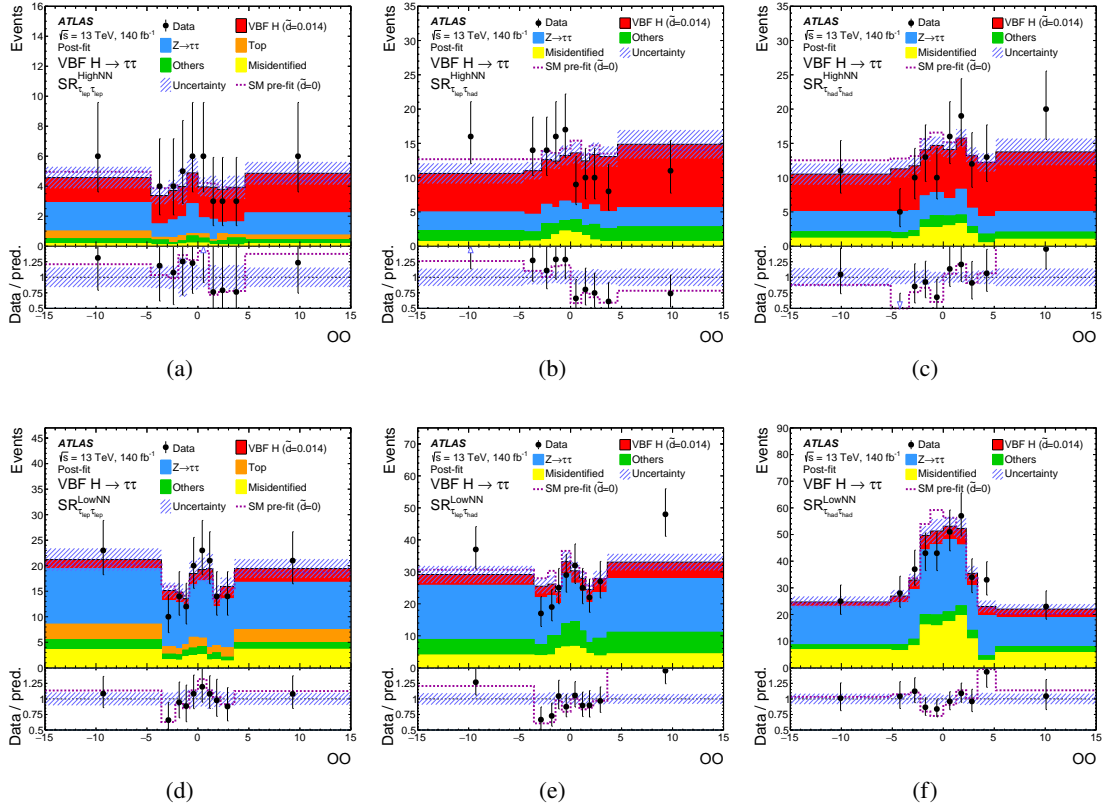


Figure 4: Post-fit distributions of the OO in the (a,b,c) SR^{HighNN} , (d,e,f) SR^{LowNN} and for the three channels: (a,d) $\tau_{lep}\tau_{lep}$, (b,e) $\tau_{lep}\tau_{had}$, (c,f) $\tau_{had}\tau_{had}$. The value of the parameter of interest, the signal strength, the normalisation of backgrounds and the systematic uncertainties are set to the value from the best fit result. The dashed line in the bottom panel shows the total pre-fit SM predictions (with $\tilde{d} = 0$). The dashed area represent the total post-fit systematic uncertainty in the final SM prediction.

minimize the ΔNLL . Tables 7 and 8 show the signal and background predicted yields and the observed data events in the SRs and CRs. Overall, good agreement is observed between SM predictions and data within the systematic uncertainties. In the SR^{HighNN} , the $\tau_{had}\tau_{had}$ channel shows a small excess in the highest bin of the OO , and an overprediction for negative OO , while in the $\tau_{lep}\tau_{had}$ channel, the lowest bins show a slight underprediction. In the SR^{LowNN} the agreement is also good within systematic uncertainties, with just one bin in the $\tau_{lep}\tau_{had}$ channel where the prediction is lower than the observed data, a trend in OO opposite to that seen in the SR^{HighNN} . In the $\tau_{lep}\tau_{lep}$ channel, the SM predictions are in good agreement with the observations in both SRs.

The best estimator of the CP-violating strength parameters in the different EFT bases are extracted from the fit procedure, together with the 68% and 95% CL intervals. Table 9 shows the summary of the best fit results of the strength parameters, and their corresponding 68% and 95% CL intervals for \tilde{d} and $c_{H\tilde{W}}$. The other Warsaw basis parameters are not considered, since their sensitivity is between 10 and 20 times worse than $c_{H\tilde{W}}$. Figure 5 shows a comparison of the expected and observed ΔNLL curves for each interpretation. The observed ΔNLL curves for the single-channel fits are also shown with dashed lines. The agreement between the combined fit and the single-channel fits is found to be at 2.8σ , due to the statistical fluctuations in the first and last bins as seen in Figure 4.

Table 7: Post-fit event yields in the SRs and the Top CR for the three channels in the analysis. The “Other bkg” includes diboson, $Z \rightarrow \ell\ell$, and $W \rightarrow \tau\nu + \text{jets}$, and other non-VBF-Higgs processes. The uncertainties in the MC predictions include theory, experimental and statistical uncertainties.

	$\tau_{\text{lep}}\tau_{\text{lep}}$			$\tau_{\text{lep}}\tau_{\text{had}}$			$\tau_{\text{had}}\tau_{\text{had}}$	
	SR		CR Top	SR		SR	SR	
	High NN	Low NN		High NN	Low NN		High NN	Low NN
$Z \rightarrow \tau\tau$	12.7 ± 3.0	97 ± 11	246 ± 29	26 ± 5	138 ± 18	30 ± 5	192 ± 24	
Other bkg	3.1 ± 0.7	12.8 ± 2.1	28.5 ± 1.4	18 ± 5	55 ± 12	12 ± 4	29 ± 7	
Misid. τ -leptons	1.27 ± 0.35	22 ± 6	155.7 ± 1.6	11.9 ± 2.5	49 ± 10	18 ± 5	109 ± 18	
Top	2.9 ± 1.1	18 ± 4	2130 ± 60	0 ± 0	0 ± 0	0 ± 0	0 ± 0	
VBF H	21.1 ± 3.1	22.3 ± 3.5	7.8 ± 0.5	71 ± 10	40 ± 7	71 ± 10	41 ± 7	
Total	41 ± 4	172 ± 10	2570 ± 50	127 ± 9	282 ± 15	131 ± 9	371 ± 18	
Data	46	172	2571	125	281	129	374	

The fit is repeated on a simulated dataset but using the $p_{T+}p_{T-} \sin(\Delta\phi_{jj}^{\text{sign}})$ and $\Delta\phi_{jj}^{\text{sign}}$ observables and expected 95% CL limits are obtained. The expected limits obtained with the Optimal Observable are

Table 8: Post-fit event yields in the embedding CRs for the three channels in the analysis. The uncertainties in the MC predictions include theory, experimental and statistical uncertainties.

	$\tau_{\text{lep}}\tau_{\text{lep}}$		$\tau_{\text{lep}}\tau_{\text{had}}$		$\tau_{\text{had}}\tau_{\text{had}}$	
	$Z\tau\tau\text{CR}_{\tau_{\text{lep}}\tau_{\text{lep}}}^{\text{HighNN}}$	$Z\tau\tau\text{CR}_{\tau_{\text{lep}}\tau_{\text{lep}}}^{\text{LowNN}}$	$Z\tau\tau\text{CR}_{\tau_{\text{lep}}\tau_{\text{had}}}^{\text{HighNN}}$	$Z\tau\tau\text{CR}_{\tau_{\text{lep}}\tau_{\text{had}}}^{\text{LowNN}}$	$Z\tau\tau\text{CR}_{\tau_{\text{had}}\tau_{\text{had}}}^{\text{HighNN}}$	$Z\tau\tau\text{CR}_{\tau_{\text{had}}\tau_{\text{had}}}^{\text{LowNN}}$
	$Z \rightarrow \ell\ell$ (emb)	15.4 ± 2.4	86 ± 8	44 ± 6	158 ± 12	34.6 ± 3.2
Emb. bkg	0.16 ± 0.01	1.13 ± 0.03	1.04 ± 0.06	2.67 ± 0.09	1.00 ± 0.05	5.07 ± 0.13
Total	15.6 ± 2.4	87 ± 8	45 ± 6	161 ± 12	35.6 ± 3.2	198 ± 13
Data	16	84	44	162	40	192

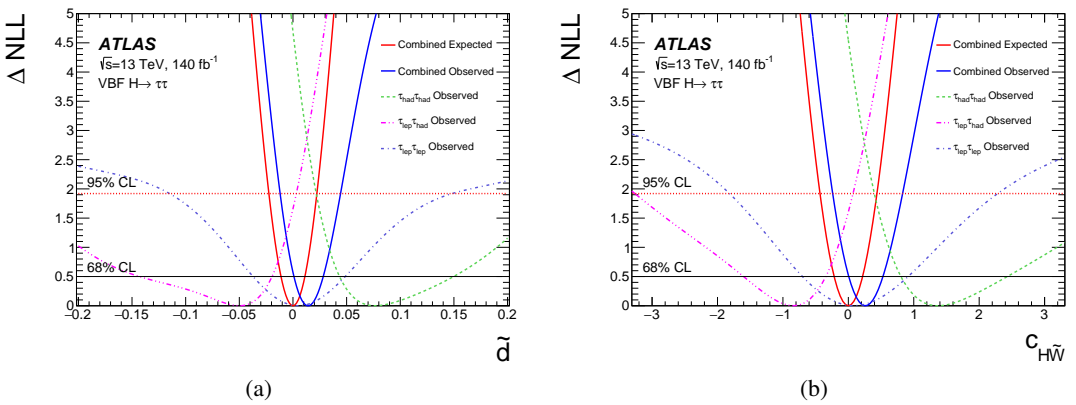


Figure 5: Expected and observed ΔNLL distributions for the combined fit as a function of the CP-violating strength parameters (a) \tilde{d} , and (b) $c_{H\bar{W}}$. The dashed lines show the observed ΔNLL curves for the fit to the single channels. The expected curve is obtained assuming the SM predictions. The horizontal lines correspond to the ΔNLL values used to determine the 68% and 95% confidence intervals.

Table 9: Expected and observed 68% and 95% CL intervals on the CP-violating parameters obtained from the combined fit of the Optimal Observable. For the $c_{H\bar{W}}$ results a new-physics scale at $\Lambda = 1$ TeV is assumed.

Parameter	Observed best value	68% CL (Exp.)	95% CL (Exp.)	68% CL (Obs.)	95% CL (Obs.)
\tilde{d} (lin.+quad.)	0.014	[−0.011, 0.011]	[−0.022, 0.022]	[0.001, 0.028]	[−0.012, 0.044]
\tilde{d} (lin. only)	0.011	[−0.011, 0.011]	[−0.021, 0.022]	[0.000, 0.023]	[−0.012, 0.034]
$c_{H\bar{W}}$ (lin.+quad.)	0.26	[−0.22, 0.22]	[−0.43, 0.44]	[0.01, 0.53]	[−0.24, 0.83]
$c_{H\bar{W}}$ (lin. only)	0.21	[−0.21, 0.22]	[−0.41, 0.44]	[−0.02, 0.45]	[−0.23, 0.70]

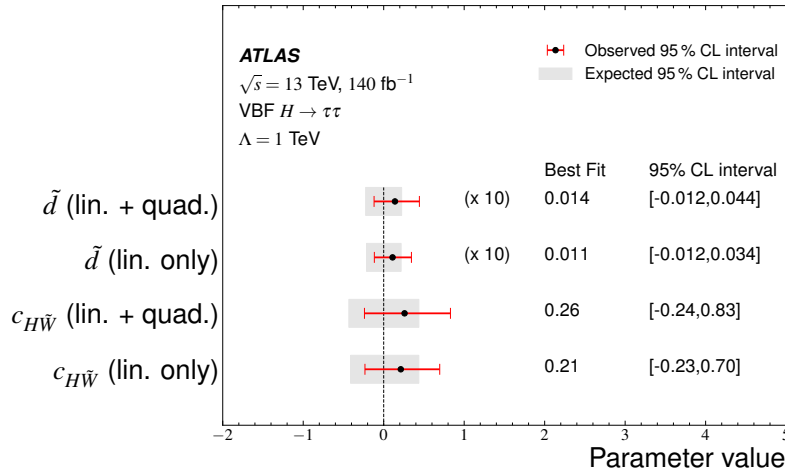


Figure 6: Expected and observed best fit values and 95% CL intervals for all the CP-violating strength parameters considered in the analysis. The \tilde{d} values are scaled by a factor ten for illustrative purposes. For the $c_{H\bar{W}}$ results a new-physics scale at $\Lambda = 1$ TeV is assumed.

5% stronger than the expected limits obtained using the $p_{T+}p_{T-} \sin(\Delta\phi_{jj}^{\text{sign}})$, and 30% stronger than those obtained with $\Delta\phi_{jj}^{\text{sign}}$.

Figure 6 shows a comparison of the expected and observed best fit values, using in the reweighting processes both the linear and quadratic terms or the linear term only. For all the interpretations, the difference of adding the quadratic term is small, relaxing the limits by about 10%. In all cases, the CP-violating strength parameters are compatible with zero. The expected confidence interval on \tilde{d} represents a large improvement relative to what was set in Ref [27], and improves also the limits relative to the analysis based on $\Delta\phi_{jj}^{\text{sign}}$ [28].

Figure 7 shows a comparison of the expected and observed best fit values between different ATLAS analyses. The results are compared with the $H \rightarrow ZZ \rightarrow 4\ell$ analysis [11] and the $H \rightarrow \gamma\gamma$ VBF measurements [12] for \tilde{d} and $c_{H\bar{W}}$. The results for $c_{H\bar{W}}$ are also compared with the $H \rightarrow \tau\tau$ differential cross-section measurement based on $\Delta\phi_{jj}^{\text{sign}}$ [28] and the $H \rightarrow WW^* \rightarrow \ell\nu\ell\nu$ analysis [13]. This analysis, the $H \rightarrow ZZ \rightarrow 4\ell$ analysis, and the $H \rightarrow \gamma\gamma$ VBF measurements use datasets with no overlap. However, the $H \rightarrow \tau\tau$ $\Delta\phi_{jj}$ differential measurement uses similar final states in the same dataset as this analysis. In the $c_{H\bar{W}}$ results for all the analyses a new-physics scale at $\Lambda = 1$ TeV is assumed, and $c_{H\bar{W}}$ is fitted while the other CP-odd operators are assumed to be zero, except in the $H \rightarrow WW^* \rightarrow \ell\nu\ell\nu$ analysis where all the Warsaw basis CP-odd and CP-even coefficients are fitted simultaneously, with a correlation between the

coupling measurements of less than 5%. For both $c_{H\tilde{W}}$ and \tilde{d} the EFT parameterisation includes both the linear and quadratic terms, except for the $H \rightarrow WW^* \rightarrow \ell\nu\ell\nu$ analysis, where only the linear term is considered.

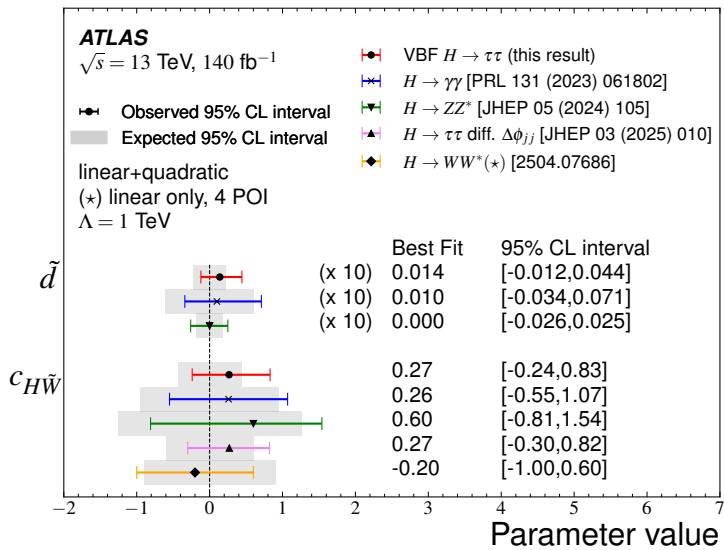


Figure 7: Comparison of results of the analysis presented with the ATLAS $H \rightarrow ZZ^* \rightarrow 4\ell$ analysis [11] and the ATLAS $H \rightarrow \gamma\gamma$ VBF measurements [12] for \tilde{d} and $c_{H\tilde{W}}$. The results for $c_{H\tilde{W}}$ are also compared with the ATLAS $H \rightarrow \tau\tau$ differential cross-section measurement based on $\Delta\phi_{jj}^{\text{sign}}$ [28] and the ATLAS $H \rightarrow WW^* \rightarrow \ell\nu\ell\nu$ analysis [13], based on pure shape information. The data points show the observed results, and the uncertainty bands correspond to the 95 % CL interval including statistical and systematic uncertainties. The \tilde{d} values are scaled by a factor ten for illustrative purposes. For the $c_{H\tilde{W}}$ results a new-physics scale at $\Lambda = 1$ TeV is assumed. The EFT parameterisation includes both the linear and quadratic terms, and $c_{H\tilde{W}}$ is fitted while the other CP-odd operators are assumed to be zero, except for the ATLAS $H \rightarrow WW^* \rightarrow \ell\nu\ell\nu$ analysis, where only the linear term is considered and all the Warsaw basis CP-odd and CP-even coefficients are fitted simultaneously (and therefore labelled as 4 POI), with a correlation between the coupling measurements of less than 5%.

10 Conclusion

A test of the CP invariance of the Higgs boson in the vertex with vector bosons was presented, in the final state with the Higgs boson decaying into pairs of τ -leptons, using the full LHC Run 2 proton–proton collision dataset of 140 fb^{-1} collected by the ATLAS experiment at $\sqrt{s} = 13\text{ TeV}$. The Optimal Observable is used to probe the CP properties of the Higgs boson.

No statistically significant deviation relative to the Standard Model prediction of a CP-even coupling between the Higgs boson and vector bosons is observed. The results are interpreted using two different EFT bases, in particular the HISZ and the Warsaw bases, with sensitivity mainly on \tilde{d} and $c_{H\tilde{W}}$. The HISZ parameter \tilde{d} is constrained to a 95% CL interval of $[-0.012, +0.044]$, while the Warsaw basis parameter $c_{H\tilde{W}}$ is constrained to $[-0.24, +0.83]$ for $\Lambda = 1\text{ TeV}$, in both cases considering the linear and quadratic terms in the reweighting procedure. The expected 95% CL interval based on the Standard Model predictions for the two operators are $\tilde{d} \in [-0.022, +0.022]$ and $c_{H\tilde{W}} \in [-0.43, +0.44]$, also considering both the linear and quadratic terms in the parameterisation. The observed limits on these operators are among the most stringent so far, and greatly improve on the previous ATLAS analysis that was based on a partial Run 2 dataset using 36 fb^{-1} by being able to also set constraints at the 95% CL on the observed parameters. Additionally, new interpretations are added, which can be used for future combination with other analyses.

Acknowledgements

We thank CERN for the very successful operation of the LHC and its injectors, as well as the support staff at CERN and at our institutions worldwide without whom ATLAS could not be operated efficiently.

The crucial computing support from all WLCG partners is acknowledged gratefully, in particular from CERN, the ATLAS Tier-1 facilities at TRIUMF/SFU (Canada), NDGF (Denmark, Norway, Sweden), CC-IN2P3 (France), KIT/GridKA (Germany), INFN-CNAF (Italy), NL-T1 (Netherlands), PIC (Spain), RAL (UK) and BNL (USA), the Tier-2 facilities worldwide and large non-WLCG resource providers. Major contributors of computing resources are listed in Ref. [139].

We gratefully acknowledge the support of ANPCyT, Argentina; YerPhI, Armenia; ARC, Australia; BMWFW and FWF, Austria; ANAS, Azerbaijan; CNPq and FAPESP, Brazil; NSERC, NRC and CFI, Canada; CERN; ANID, Chile; CAS, MOST and NSFC, China; Minciencias, Colombia; MEYS CR, Czech Republic; DNRF and DNSRC, Denmark; IN2P3-CNRS and CEA-DRF/IRFU, France; SRNSFG, Georgia; BMBF, HGF and MPG, Germany; GSRI, Greece; RGC and Hong Kong SAR, China; ICHEP and Academy of Sciences and Humanities, Israel; INFN, Italy; MEXT and JSPS, Japan; CNRST, Morocco; NWO, Netherlands; RCN, Norway; MNiSW, Poland; FCT, Portugal; MNE/IFA, Romania; MSTDI, Serbia; MSSR, Slovakia; ARIS and MVZI, Slovenia; DSI/NRF, South Africa; MICIU/AEI, Spain; SRC and Wallenberg Foundation, Sweden; SERI, SNSF and Cantons of Bern and Geneva, Switzerland; NSTC, Taipei; TENMAK, Türkiye; STFC/UKRI, United Kingdom; DOE and NSF, United States of America.

Individual groups and members have received support from BCKDF, CANARIE, CRC and DRAC, Canada; CERN-CZ, FORTE and PRIMUS, Czech Republic; COST, ERC, ERDF, Horizon 2020, ICSC-NextGenerationEU and Marie Skłodowska-Curie Actions, European Union; Investissements d’Avenir Labex, Investissements d’Avenir Idex and ANR, France; DFG and AvH Foundation, Germany; Herakleitos, Thales and Aristeia programmes co-financed by EU-ESF and the Greek NSRF, Greece; BSF-NSF and MINERVA,

Israel; NCN and NAWA, Poland; La Caixa Banking Foundation, CERCA Programme Generalitat de Catalunya and PROMETEO and GenT Programmes Generalitat Valenciana, Spain; Göran Gustafssons Stiftelse, Sweden; The Royal Society and Leverhulme Trust, United Kingdom.

In addition, individual members wish to acknowledge support from CERN: European Organization for Nuclear Research (CERN DOCT); Chile: Agencia Nacional de Investigación y Desarrollo (FONDECYT 1230812, FONDECYT 1240864); China: Chinese Ministry of Science and Technology (MOST-2023YFA1605700, MOST-2023YFA1609300), National Natural Science Foundation of China (NSFC - 12175119, NSFC 12275265); Czech Republic: Czech Science Foundation (GACR - 24-11373S), Ministry of Education Youth and Sports (ERC-CZ-LL2327, FORTE CZ.02.01.01/00/22_008/0004632), PRIMUS Research Programme (PRIMUS/21/SCI/017); EU: H2020 European Research Council (ERC - 101002463); European Union: European Research Council (BARD No. 101116429, ERC - 948254, ERC 101089007), European Regional Development Fund (SMASH COFUND 101081355, SLO ERDF), Horizon 2020 Framework Programme (MUCCA - CHIST-ERA-19-XAI-00), European Union, Future Artificial Intelligence Research (FAIR-NextGenerationEU PE00000013), Italian Center for High Performance Computing, Big Data and Quantum Computing (ICSC, NextGenerationEU); France: Agence Nationale de la Recherche (ANR-21-CE31-0022, ANR-22-EDIR-0002); Germany: Baden-Württemberg Stiftung (BW Stiftung-Postdoc Elite-programme), Deutsche Forschungsgemeinschaft (DFG - 469666862, DFG - CR 312/5-2); China: Research Grants Council (GRF); Italy: Istituto Nazionale di Fisica Nucleare (ICSC, NextGenerationEU), Ministero dell'Università e della Ricerca (NextGenEU I53D23000820006 M4C2.1.1, SOE2024_0000023); Japan: Japan Society for the Promotion of Science (JSPS KAKENHI JP22H01227, JSPS KAKENHI JP22H04944, JSPS KAKENHI JP22KK0227, JSPS KAKENHI JP24K23939, JSPS KAKENHI JP25H00650, JSPS KAKENHI JP25H01291, JSPS KAKENHI JP25K01023); Norway: Research Council of Norway (RCN-314472); Poland: Ministry of Science and Higher Education (IDUB AGH, POB8, D4 no 9722), Polish National Science Centre (NCN 2021/42/E/ST2/00350, NCN OPUS 2023/51/B/ST2/02507, NCN OPUS nr 2022/47/B/ST2/03059, NCN UMO-2019/34/E/ST2/00393, UMO-2022/47/O/ST2/00148, UMO-2023/49/B/ST2/04085, UMO-2023/51/B/ST2/00920, UMO-2024/53/N/ST2/00869); Portugal: Foundation for Science and Technology (FCT); Spain: Ministry of Science and Innovation (MCIN & NextGenEU PCI2022-135018-2, MICIN & FEDER PID2021-125273NB, RYC2019-028510-I, RYC2020-030254-I, RYC2021-031273-I, RYC2022-038164-I); Sweden: Carl Trygger Foundation (Carl Trygger Foundation CTS 22:2312), Swedish Research Council (Swedish Research Council 2023-04654, VR 2021-03651, VR 2022-03845, VR 2022-04683, VR 2023-03403, VR 2024-05451), Knut and Alice Wallenberg Foundation (KAW 2018.0458, KAW 2022.0358, KAW 2023.0366); Switzerland: Swiss National Science Foundation (SNSF - PCEFP2_194658); United Kingdom: Leverhulme Trust (Leverhulme Trust RPG-2020-004), Royal Society (NIF-R1-231091); United States of America: U.S. Department of Energy (ECA DE-AC02-76SF00515), Neubauer Family Foundation.

References

- [1] A. D. Sakharov, *Violation of CP invariance, C asymmetry, and baryon asymmetry of the universe*, *Pisma Zh. Eksp. Teor. Fiz.* **5** (1967) 32.
- [2] P. Huet and E. Sather, *Electroweak baryogenesis and standard model CP violation*, *Phys. Rev. D* **51** (1995) 379, arXiv: [hep-ph/9404302](#).
- [3] M. B. Gavela, P. Hernández, J. Orloff and O. Pène, *Standard Model CP-violation and Baryon asymmetry*, *Mod. Phys. Lett. A* **9** (1994) 795, arXiv: [hep-ph/9312215](#).
- [4] A. G. Cohen, D. B. Kaplan and A. E. Nelson, *Progress in Electroweak Baryogenesis*, *Ann. Rev. Nucl. Part. Sci.* **43** (1993) 27, arXiv: [hep-ph/9302210](#).
- [5] A. Riotto and M. Trodden, *Recent Progress in Baryogenesis*, *Ann. Rev. Nucl. Part. Sci.* **49** (1999) 35, arXiv: [hep-ph/9901362](#).
- [6] W.-S. Hou, *Source of CP Violation for Baryon Asymmetry of the Universe*, *Chin. J. Phys.* **47** (2009) 134, arXiv: [0803.1234](#).
- [7] L. Evans and P. Bryant, *LHC Machine*, *JINST* **3** (2008) S08001.
- [8] ATLAS Collaboration, *Observation of a new particle in the search for the Standard Model Higgs boson with the ATLAS detector at the LHC*, *Phys. Lett. B* **716** (2012) 1, arXiv: [1207.7214 \[hep-ex\]](#).
- [9] CMS Collaboration, *Observation of a new boson at a mass of 125 GeV with the CMS experiment at the LHC*, *Phys. Lett. B* **716** (2012) 30, arXiv: [1207.7235 \[hep-ex\]](#).
- [10] J. Brehmer, F. Kling, T. Plehn and T. M. P. Tait, *Better Higgs-CP tests through information geometry*, *Phys. Rev. D* **97** (2018) 095017, arXiv: [1712.02350 \[hep-ph\]](#).
- [11] ATLAS Collaboration, *Test of CP-invariance of the Higgs boson in vector-boson fusion production and in its decay into four leptons*, *JHEP* **05** (2024) 105, arXiv: [2304.09612 \[hep-ex\]](#).
- [12] ATLAS Collaboration, *Test of CP Invariance in Higgs Boson Vector-Boson-Fusion Production Using the $H \rightarrow \gamma\gamma$ Channel with the ATLAS Detector*, *Phys. Rev. Lett.* **131** (2023) 061802, arXiv: [2208.02338 \[hep-ex\]](#).
- [13] ATLAS Collaboration, *Measurements of Higgs boson production via gluon-gluon fusion and vector-boson fusion using $H \rightarrow WW^* \rightarrow \ell\nu\ell\nu$ decays in pp collisions with the ATLAS detector and their effective field theory interpretations*, (2025), arXiv: [2504.07686 \[hep-ex\]](#).
- [14] CMS Collaboration, *Constraints on anomalous Higgs boson couplings to vector bosons and fermions from the production of Higgs bosons using the $\tau\tau$ final state*, *Phys. Rev. D* **108** (2023) 032013, arXiv: [2205.05120 \[hep-ex\]](#).
- [15] K. Hagiwara, S. Ishihara, R. Szalapski and D. Zeppenfeld, *Low energy effects of new interactions in the electroweak boson sector*, *Phys. Rev. D* **48** (1993) 2182.
- [16] V. Hankele, G. Klämke, D. Zeppenfeld and T. Figy, *Anomalous Higgs boson couplings in vector boson fusion at the CERN LHC*, *Phys. Rev. D* **74** (2006) 095001, arXiv: [hep-ph/0609075](#).

- [17] W. Buchmüller and D. Wyler,
Effective lagrangian analysis of new interactions and flavour conservation,
Nucl. Phys. B **268** (1986) 621.
- [18] B. Grzadkowski, M. Iskrzyński, M. Misiak and J. Rosiek,
Dimension-Six Terms in the Standard Model Lagrangian, *JHEP* **10** (2010) 085,
arXiv: [1008.4884 \[hep-ph\]](#).
- [19] ATLAS Collaboration, *Measurement of the properties of Higgs boson production at $\sqrt{s} = 13 \text{ TeV}$ in the $H \rightarrow \gamma\gamma$ channel using 139 fb^{-1} of pp collision data with the ATLAS experiment*,
JHEP **07** (2023) 088, arXiv: [2207.00348 \[hep-ex\]](#).
- [20] CMS Collaboration,
Constraints on standard model effective field theory for a Higgs boson produced in association with W or Z bosons in the $H \rightarrow b\bar{b}$ decay channel in proton–proton collisions at $\sqrt{s} = 13 \text{ TeV}$,
JHEP **03** (2025) 114, arXiv: [2411.16907 \[hep-ex\]](#).
- [21] I. Brivio, *SMEFTsim 3.0 - a practical guide*, *JHEP* **04** (2021) 073, arXiv: [2012.11343 \[hep-ph\]](#).
- [22] J. Abdallah et al., *Study of W -boson polarisations and triple gauge boson couplings in the reaction $e+e^- \rightarrow W+W-$ at LEP 2*, *Eur. Phys. J. C* **54** (2008) 345, arXiv: [0801.1235 \[hep-ex\]](#).
- [23] OPAL Collaboration, *Measurement of W boson polarisations and CP-violating triple gauge couplings from W^+W^- production at LEP*, *Eur. Phys. J. C* **19** (2001) 229,
arXiv: [hep-ex/0009021](#).
- [24] ALEPH Collaboration,
Improved measurement of the triple gauge-boson couplings γWW and ZWW in e^+e^- collisions,
Phys. Lett. B **614** (2005) 7.
- [25] CMS Collaboration, *Constraints on anomalous Higgs boson couplings to vector bosons and fermions in its production and decay using the four-lepton final state*,
Phys. Rev. D **104** (2021) 052004, arXiv: [2104.12152 \[hep-ex\]](#).
- [26] ATLAS Collaboration, *Test of CP invariance in vector-boson fusion production of the Higgs boson using the Optimal Observable method in the ditau decay channel with the ATLAS detector*,
Eur. Phys. J. C **76** (2016) 658, arXiv: [1602.04516 \[hep-ex\]](#).
- [27] ATLAS Collaboration, *Test of CP invariance in vector-boson fusion production of the Higgs boson in the $H \rightarrow \tau\tau$ channel in proton–proton collisions at $\sqrt{s} = 13 \text{ TeV}$ with the ATLAS detector*,
Phys. Lett. B **805** (2020) 135426, arXiv: [2002.05315 \[hep-ex\]](#).
- [28] ATLAS Collaboration, *Differential cross-section measurements of Higgs boson production in the $H \rightarrow \tau^+\tau^-$ decay channel in pp collisions at $\sqrt{s} = 13 \text{ TeV}$ with the ATLAS detector*,
JHEP **03** (2025) 010, arXiv: [2407.16320 \[hep-ex\]](#).
- [29] Particle Data Group, *Review of Particle Physics*, *PTEP* **2020** (2020) 083C01.
- [30] D. Atwood and A. Soni, *Analysis for magnetic moment and electric dipole moment form factors of the top quark via $e^+e^- \rightarrow t\bar{t}$* , *Phys. Rev. D* **45** (1992) 2405.
- [31] M. Davier, L. Duflot, F. Le Diberder and A. Rougé,
The optimal method for the measurement of tau polarization, *Phys. Lett. B* **306** (1993) 411.
- [32] M. Diehl and O. Nachtmann,
Optimal observables for the measurement of three gauge boson couplings in $e^+e^- \rightarrow W^+W^-$,
Z. Phys. C **62** (1994) 397.

- [33] M. Ciccolini, A. Denner and S. Dittmaier, *Strong and Electroweak Corrections to the Production of a Higgs Boson + 2 Jets via Weak Interactions at the Large Hadron Collider*, *Phys. Rev. Lett.* **99** (2007) 161803, arXiv: [0707.0381 \[hep-ph\]](#).
- [34] M. Ciccolini, A. Denner and S. Dittmaier, *Electroweak and QCD corrections to Higgs production via vector-boson fusion at the CERN LHC*, *Phys. Rev. D* **77** (2008) 013002, arXiv: [0710.4749 \[hep-ph\]](#).
- [35] A. Denner, S. Dittmaier, S. Kallweit and A. Mück, *HAWK 2.0: A Monte Carlo program for Higgs production in vector-boson fusion and Higgs strahlung at hadron colliders*, *Comput. Phys. Commun.* **195** (2015) 161, arXiv: [1412.5390 \[hep-ph\]](#).
- [36] A. Elagin, P. Murat, A. Pranko and A. Safonov, *A new mass reconstruction technique for resonances decaying to $\tau\tau$* , *Nucl. Instrum. Meth. A* **654** (2011) 481, arXiv: [1012.4686 \[hep-ex\]](#).
- [37] V. Hankele, G. Klämke, D. Zeppenfeld and T. Figy, *Anomalous Higgs boson couplings in vector boson fusion at the CERN LHC*, *Phys. Rev. D* **74** (2006) 095001.
- [38] ATLAS Collaboration, *The ATLAS Experiment at the CERN Large Hadron Collider*, *JINST* **3** (2008) S08003.
- [39] ATLAS Collaboration, *ATLAS Insertable B-Layer: Technical Design Report*, ATLAS-TDR-19; CERN-LHCC-2010-013, 2010, URL: <https://cds.cern.ch/record/1291633>, Addendum: ATLAS-TDR-19-ADD-1; CERN-LHCC-2012-009, 2012, URL: <https://cds.cern.ch/record/1451888>.
- [40] B. Abbott et al., *Production and integration of the ATLAS Insertable B-Layer*, *JINST* **13** (2018) T05008, arXiv: [1803.00844 \[physics.ins-det\]](#).
- [41] G. Avoni et al., *The new LUCID-2 detector for luminosity measurement and monitoring in ATLAS*, *JINST* **13** (2018) P07017.
- [42] ATLAS Collaboration, *Performance of the ATLAS trigger system in 2015*, *Eur. Phys. J. C* **77** (2017) 317, arXiv: [1611.09661 \[hep-ex\]](#).
- [43] ATLAS Collaboration, *Software and computing for Run 3 of the ATLAS experiment at the LHC*, *Eur. Phys. J. C* **85** (2025) 234, arXiv: [2404.06335 \[hep-ex\]](#).
- [44] ATLAS Collaboration, *ATLAS data quality operations and performance for 2015–2018 data-taking*, *JINST* **15** (2020) P04003, arXiv: [1911.04632 \[physics.ins-det\]](#).
- [45] ATLAS Collaboration, *Luminosity determination in pp collisions at $\sqrt{s} = 13$ TeV using the ATLAS detector at the LHC*, *Eur. Phys. J. C* **83** (2023) 982, arXiv: [2212.09379 \[hep-ex\]](#).
- [46] A. Djouadi, J. Kalinowski and M. Spira, *HDECAY: a program for Higgs boson decays in the Standard Model and its supersymmetric extension*, *Comput. Phys. Commun.* **108** (1998) 56, arXiv: [hep-ph/9704448](#).
- [47] M. Spira, *QCD Effects in Higgs Physics*, *Fortsch. Phys.* **46** (1998) 203, arXiv: [hep-ph/9705337](#).
- [48] A. Djouadi, M. M. Mühlleitner and M. Spira, *Decays of Supersymmetric Particles: the Program SUSY-HIT (SUspect-SdecaY-Hdecay-Interface)*, *Acta Phys. Polon. B* **38** (2006) 635, arXiv: [hep-ph/0609292](#).

- [49] A. Bredenstein, A. Denner, S. Dittmaier and M. M. Weber, *Radiative corrections to the semileptonic and hadronic Higgs-boson decays $H \rightarrow WW/ZZ \rightarrow 4 \text{ fermions}$* , *JHEP* **02** (2007) 080, arXiv: [hep-ph/0611234](#).
- [50] A. Bredenstein, A. Denner, S. Dittmaier and M. M. Weber, *Precise predictions for the Higgs-boson decay $H \rightarrow WW/ZZ \rightarrow 4 \text{ leptons}$* , *Phys. Rev. D* **74** (2006) 013004, arXiv: [hep-ph/0604011 \[hep-ph\]](#).
- [51] A. Bredenstein, A. Denner, S. Dittmaier and M. M. Weber, *Precision calculations for the Higgs decays $H \rightarrow ZZ/WW \rightarrow 4 \text{ leptons}$* , *Nucl. Phys. B Proc. Suppl.* **160** (2006) 131, arXiv: [hep-ph/0607060 \[hep-ph\]](#).
- [52] D. J. Lange, *The EvtGen particle decay simulation package*, *Nucl. Instrum. Meth. A* **462** (2001) 152.
- [53] P. Nason and C. Oleari, *NLO Higgs boson production via vector-boson fusion matched with shower in POWHEG*, *JHEP* **02** (2010) 037, arXiv: [0911.5299 \[hep-ph\]](#).
- [54] S. Alioli, P. Nason, C. Oleari and E. Re, *A general framework for implementing NLO calculations in shower Monte Carlo programs: the POWHEG BOX*, *JHEP* **06** (2010) 043, arXiv: [1002.2581 \[hep-ph\]](#).
- [55] P. Nason, *A new method for combining NLO QCD with shower Monte Carlo algorithms*, *JHEP* **11** (2004) 040, arXiv: [hep-ph/0409146](#).
- [56] S. Frixione, P. Nason and C. Oleari, *Matching NLO QCD computations with parton shower simulations: the POWHEG method*, *JHEP* **11** (2007) 070, arXiv: [0709.2092 \[hep-ph\]](#).
- [57] J. Butterworth et al., *PDF4LHC recommendations for LHC Run II*, *J. Phys. G* **43** (2016) 023001, arXiv: [1510.03865 \[hep-ph\]](#).
- [58] K. Hamilton, P. Nason and G. Zanderighi, *MINLO: multi-scale improved NLO*, *JHEP* **10** (2012) 155, arXiv: [1206.3572 \[hep-ph\]](#).
- [59] J. M. Campbell et al., *NLO Higgs boson production plus one and two jets using the POWHEG BOX, MadGraph4 and MCFM*, *JHEP* **07** (2012) 092, arXiv: [1202.5475 \[hep-ph\]](#).
- [60] K. Hamilton, P. Nason, C. Oleari and G. Zanderighi, *Merging $H/W/Z + 0$ and 1 jet at NLO with no merging scale: a path to parton shower + NNLO matching*, *JHEP* **05** (2013) 082, arXiv: [1212.4504 \[hep-ph\]](#).
- [61] S. Catani and M. Grazzini, *Next-to-Next-to-Leading-Order Subtraction Formalism in Hadron Collisions and its Application to Higgs-Boson Production at the Large Hadron Collider*, *Phys. Rev. Lett.* **98** (2007) 222002, arXiv: [hep-ph/0703012](#).
- [62] J. Pumplin et al., *New Generation of Parton Distributions with Uncertainties from Global QCD Analysis*, *JHEP* **07** (2002) 012, arXiv: [hep-ph/0201195](#).
- [63] ATLAS Collaboration, *Measurement of the Z/γ^* boson transverse momentum distribution in pp collisions at $\sqrt{s} = 7 \text{ TeV}$ with the ATLAS detector*, *JHEP* **09** (2014) 145, arXiv: [1406.3660 \[hep-ex\]](#).
- [64] T. Sjöstrand et al., *An introduction to PYTHIA 8.2*, *Comput. Phys. Commun.* **191** (2015) 159, arXiv: [1410.3012 \[hep-ph\]](#).

- [65] D. de Florian et al.,
Handbook of LHC Higgs Cross Sections: 4. Deciphering the Nature of the Higgs Sector, (2017), arXiv: [1610.07922 \[hep-ph\]](#).
- [66] C. Anastasiou et al.,
High precision determination of the gluon fusion Higgs boson cross-section at the LHC, *JHEP* **05** (2016) 058, arXiv: [1602.00695 \[hep-ph\]](#).
- [67] C. Anastasiou, C. Duhr, F. Dulat, F. Herzog and B. Mistlberger,
Higgs Boson Gluon-Fusion Production in QCD at Three Loops, *Phys. Rev. Lett.* **114** (2015) 212001, arXiv: [1503.06056 \[hep-ph\]](#).
- [68] F. Dulat, A. Lazopoulos and B. Mistlberger, *iHixs 2 – Inclusive Higgs cross sections*, *Comput. Phys. Commun.* **233** (2018) 243, arXiv: [1802.00827 \[hep-ph\]](#).
- [69] R. V. Harlander and K. J. Ozeren,
Finite top mass effects for hadronic Higgs production at next-to-next-to-leading order, *JHEP* **11** (2009) 088, arXiv: [0909.3420 \[hep-ph\]](#).
- [70] R. V. Harlander and K. J. Ozeren,
Top mass effects in Higgs production at next-to-next-to-leading order QCD: Virtual corrections, *Phys. Lett. B* **679** (2009) 467, arXiv: [0907.2997 \[hep-ph\]](#).
- [71] R. V. Harlander, H. Mantler, S. Marzani and K. J. Ozeren,
Higgs production in gluon fusion at next-to-next-to-leading order QCD for finite top mass, *Eur. Phys. J. C* **66** (2010) 359, arXiv: [0912.2104 \[hep-ph\]](#).
- [72] A. Pak, M. Rogal and M. Steinhauser,
Finite top quark mass effects in NNLO Higgs boson production at LHC, *JHEP* **02** (2010) 025, arXiv: [0911.4662 \[hep-ph\]](#).
- [73] S. Actis, G. Passarino, C. Sturm and S. Uccirati,
NLO electroweak corrections to Higgs boson production at hadron colliders, *Phys. Lett. B* **670** (2008) 12, arXiv: [0809.1301 \[hep-ph\]](#).
- [74] S. Actis, G. Passarino, C. Sturm and S. Uccirati,
NNLO computational techniques: The cases $H \rightarrow \gamma\gamma$ and $H \rightarrow gg$, *Nucl. Phys. B* **811** (2009) 182, arXiv: [0809.3667 \[hep-ph\]](#).
- [75] M. Bonetti, K. Melnikov and L. Tancredi, *Higher order corrections to mixed QCD-EW contributions to Higgs boson production in gluon fusion*, *Phys. Rev. D* **97** (2018) 056017, arXiv: [1801.10403 \[hep-ph\]](#), Erratum: *Phys. Rev. D* **97** (2018) 099906(E).
- [76] P. Bolzoni, F. Maltoni, S.-O. Moch and M. Zaro,
Higgs Boson Production via Vector-Boson Fusion at Next-to-Next-to-Leading Order in QCD, *Phys. Rev. Lett.* **105** (2010) 011801, arXiv: [1003.4451 \[hep-ph\]](#).
- [77] M. L. Ciccolini, S. Dittmaier and M. Krämer,
Electroweak radiative corrections to associated WH and ZH production at hadron colliders, *Phys. Rev. D* **68** (2003) 073003, arXiv: [hep-ph/0306234](#).
- [78] O. Brein, A. Djouadi and R. Harlander,
NNLO QCD corrections to the Higgs-strahlung processes at hadron colliders, *Phys. Lett. B* **579** (2004) 149, arXiv: [hep-ph/0307206](#).

- [79] O. Brein, R. V. Harlander, M. Wiesemann and T. Zirke,
Top-quark mediated effects in hadronic Higgs-Strahlung, *Eur. Phys. J. C* **72** (2012) 1868,
arXiv: [1111.0761 \[hep-ph\]](#).
- [80] L. Altenkamp, S. Dittmaier, R. V. Harlander, H. Rzehak and T. J. E. Zirke,
Gluon-induced Higgs-strahlung at next-to-leading order QCD, *JHEP* **02** (2013) 078,
arXiv: [1211.5015 \[hep-ph\]](#).
- [81] O. Brein, R. V. Harlander and T. J. E. Zirke, *vh@nnlo – Higgs Strahlung at hadron colliders*,
Comput. Phys. Commun. **184** (2013) 998, arXiv: [1210.5347 \[hep-ph\]](#).
- [82] R. V. Harlander, A. Kulesza, V. Theeuwes and T. Zirke,
Soft gluon resummation for gluon-induced Higgs Strahlung, *JHEP* **11** (2014) 082,
arXiv: [1410.0217 \[hep-ph\]](#).
- [83] ATLAS Collaboration, *ATLAS Pythia 8 tunes to 7 TeV data*, ATL-PHYS-PUB-2014-021, 2014,
URL: <https://cds.cern.ch/record/1966419>.
- [84] NNPDF Collaboration, *Parton distributions with LHC data*, *Nucl. Phys. B* **867** (2013) 244,
arXiv: [1207.1303 \[hep-ph\]](#).
- [85] J. Alwall et al., *The automated computation of tree-level and next-to-leading order differential cross sections, and their matching to parton shower simulations*, *JHEP* **07** (2014) 079,
arXiv: [1405.0301 \[hep-ph\]](#).
- [86] E. Bothmann et al., *Event generation with Sherpa 2.2*, *SciPost Phys.* **7** (2019) 034,
arXiv: [1905.09127 \[hep-ph\]](#).
- [87] T. Gleisberg and S. Höche, *Comix, a new matrix element generator*, *JHEP* **12** (2008) 039,
arXiv: [0808.3674 \[hep-ph\]](#).
- [88] F. Buccioni et al., *OpenLoops 2*, *Eur. Phys. J. C* **79** (2019) 866, arXiv: [1907.13071 \[hep-ph\]](#).
- [89] F. Cascioli, P. Maierhöfer and S. Pozzorini, *Scattering Amplitudes with Open Loops*,
Phys. Rev. Lett. **108** (2012) 111601, arXiv: [1111.5206 \[hep-ph\]](#).
- [90] A. Denner, S. Dittmaier and L. Hofer,
COLLIER: A fortran-based complex one-loop library in extended regularizations,
Comput. Phys. Commun. **212** (2017) 220, arXiv: [1604.06792 \[hep-ph\]](#).
- [91] S. Schumann and F. Krauss,
A parton shower algorithm based on Catani–Seymour dipole factorisation, *JHEP* **03** (2008) 038,
arXiv: [0709.1027 \[hep-ph\]](#).
- [92] S. Höche, F. Krauss, M. Schönherr and F. Siegert,
A critical appraisal of NLO+PS matching methods, *JHEP* **09** (2012) 049,
arXiv: [1111.1220 \[hep-ph\]](#).
- [93] S. Höche, F. Krauss, M. Schönherr and F. Siegert,
QCD matrix elements + parton showers. The NLO case, *JHEP* **04** (2013) 027,
arXiv: [1207.5030 \[hep-ph\]](#).
- [94] S. Catani, F. Krauss, B. R. Webber and R. Kuhn, *QCD Matrix Elements + Parton Showers*,
JHEP **11** (2001) 063, arXiv: [hep-ph/0109231](#).
- [95] S. Höche, F. Krauss, S. Schumann and F. Siegert, *QCD matrix elements and truncated showers*,
JHEP **05** (2009) 053, arXiv: [0903.1219 \[hep-ph\]](#).

- [96] C. Anastasiou, L. Dixon, K. Melnikov and F. Petriello, *High-precision QCD at hadron colliders: Electroweak gauge boson rapidity distributions at next-to-next-to leading order*, *Phys. Rev. D* **69** (2004) 094008, arXiv: [hep-ph/0312266](#).
- [97] ATLAS Collaboration, *Studies on top-quark Monte Carlo modelling for Top2016*, ATL-PHYS-PUB-2016-020, 2016, URL: <https://cds.cern.ch/record/2216168>.
- [98] M. Beneke, P. Falgari, S. Klein and C. Schwinn, *Hadronic top-quark pair production with NNLL threshold resummation*, *Nucl. Phys. B* **855** (2012) 695, arXiv: [1109.1536 \[hep-ph\]](#).
- [99] M. Cacciari, M. Czakon, M. Mangano, A. Mitov and P. Nason, *Top-pair production at hadron colliders with next-to-next-to-leading logarithmic soft-gluon resummation*, *Phys. Lett. B* **710** (2012) 612, arXiv: [1111.5869 \[hep-ph\]](#).
- [100] P. Bärnreuther, M. Czakon and A. Mitov, *Percent-Level-Precision Physics at the Tevatron: Next-to-Next-to-Leading Order QCD Corrections to $q\bar{q} \rightarrow t\bar{t} + X$* , *Phys. Rev. Lett.* **109** (2012) 132001, arXiv: [1204.5201 \[hep-ph\]](#).
- [101] M. Czakon and A. Mitov, *NNLO corrections to top-pair production at hadron colliders: the all-fermionic scattering channels*, *JHEP* **12** (2012) 054, arXiv: [1207.0236 \[hep-ph\]](#).
- [102] M. Czakon and A. Mitov, *NNLO corrections to top pair production at hadron colliders: the quark-gluon reaction*, *JHEP* **01** (2013) 080, arXiv: [1210.6832 \[hep-ph\]](#).
- [103] M. Czakon, P. Fiedler and A. Mitov, *Total Top-Quark Pair-Production Cross Section at Hadron Colliders Through $O(\alpha_S^4)$* , *Phys. Rev. Lett.* **110** (2013) 252004, arXiv: [1303.6254 \[hep-ph\]](#).
- [104] M. Czakon and A. Mitov, *Top++: A program for the calculation of the top-pair cross-section at hadron colliders*, *Comput. Phys. Commun.* **185** (2014) 2930, arXiv: [1112.5675 \[hep-ph\]](#).
- [105] N. Kidonakis, *Two-loop soft anomalous dimensions for single top quark associated production with a W^- or H^-* , *Phys. Rev. D* **82** (2010) 054018, arXiv: [1005.4451 \[hep-ph\]](#).
- [106] N. Kidonakis, ‘Top Quark Production’, *Proceedings, Helmholtz International Summer School on Physics of Heavy Quarks and Hadrons (HQ2013)* (JINR, Dubna, Russia, 15th–28th July 2013) 139, arXiv: [1311.0283 \[hep-ph\]](#).
- [107] S. Frixione, E. Laenen, P. Motylinski, C. White and B. R. Webber, *Single-top hadroproduction in association with a W boson*, *JHEP* **07** (2008) 029, arXiv: [0805.3067 \[hep-ph\]](#).
- [108] T. Sjöstrand, S. Mrenna and P. Skands, *A brief introduction to PYTHIA 8.1*, *Comput. Phys. Commun.* **178** (2008) 852, arXiv: [0710.3820 \[hep-ph\]](#).
- [109] ATLAS Collaboration, *The Pythia 8 A3 tune description of ATLAS minimum bias and inelastic measurements incorporating the Donnachie–Landshoff diffractive model*, ATL-PHYS-PUB-2016-017, 2016, URL: <https://cds.cern.ch/record/2206965>.
- [110] ATLAS Collaboration, *The ATLAS Simulation Infrastructure*, *Eur. Phys. J. C* **70** (2010) 823, arXiv: [1005.4568 \[physics.ins-det\]](#).
- [111] S. Agostinelli et al., *GEANT4 – a simulation toolkit*, *Nucl. Instrum. Meth. A* **506** (2003) 250.

- [112] R. Frederix and S. Frixione, *Merging meets matching in MC@NLO*, *JHEP* **12** (2012) 061, arXiv: [1209.6215 \[hep-ph\]](#).
- [113] ATLAS Collaboration, *Performance of electron and photon triggers in ATLAS during LHC Run 2*, *Eur. Phys. J. C* **80** (2020) 47, arXiv: [1909.00761 \[hep-ex\]](#).
- [114] ATLAS Collaboration, *Performance of the ATLAS muon triggers in Run 2*, *JINST* **15** (2020) P09015, arXiv: [2004.13447 \[physics.ins-det\]](#).
- [115] ATLAS Collaboration, *The ATLAS inner detector trigger performance in pp collisions at 13 TeV during LHC Run 2*, *Eur. Phys. J. C* **82** (2022) 206, arXiv: [2107.02485 \[hep-ex\]](#).
- [116] ATLAS Collaboration, *Performance of the ATLAS Level-1 topological trigger in Run 2*, *Eur. Phys. J. C* **82** (2022) 7, arXiv: [2105.01416 \[hep-ex\]](#).
- [117] R. K. Ellis, I. Hinchliffe, M. Soldate and J. J. van der Bij, *Higgs Decay to $\tau^+\tau^-$ A Possible Signature of Intermediate Mass Higgs Bosons at high energy hadron colliders*, *Nucl. Phys. B* **297** (1988) 221.
- [118] ATLAS Collaboration, *Measurements of Higgs boson production by gluon–gluon fusion and vector-boson fusion using $H \rightarrow WW^* \rightarrow e\nu\mu\nu$ decays in pp collisions at $\sqrt{s} = 13$ TeV with the ATLAS detector*, *Phys. Rev. D* **108** (2023) 032005, arXiv: [2207.00338 \[hep-ex\]](#).
- [119] ATLAS Collaboration, *ATLAS flavour-tagging algorithms for the LHC Run 2 pp collision dataset*, *Eur. Phys. J. C* **83** (2023) 681, arXiv: [2211.16345 \[physics.data-an\]](#).
- [120] F. Chollet et al., *Keras*, 2015, URL: <https://keras.io>.
- [121] TensorFlow Developers, *TensorFlow*, version v2.15.0, 2023, URL: <https://doi.org/10.5281/zenodo.10126399>.
- [122] D. P. Kingma and J. Ba, *Adam: A Method for Stochastic Optimization*, 2017, arXiv: [1412.6980 \[cs.LG\]](#).
- [123] P. Mehta et al., *A high-bias, low-variance introduction to Machine Learning for physicists*, *Phys. Rept.* **810** (2019) 1, arXiv: [1803.08823](#).
- [124] C. Cortes, M. Mohri and A. Rostamizadeh, *L2 Regularization for Learning Kernels*, 2012, arXiv: [1205.2653 \[cs.LG\]](#).
- [125] ATLAS Collaboration, *Modelling $Z \rightarrow \tau\tau$ processes in ATLAS with τ -embedded $Z \rightarrow \mu\mu$ data*, *JINST* **10** (2015) P09018, arXiv: [1506.05623 \[hep-ex\]](#).
- [126] ATLAS Collaboration, *Tools for estimating fake/non-prompt lepton backgrounds with the ATLAS detector at the LHC*, *JINST* **18** (2023) T11004, arXiv: [2211.16178 \[hep-ex\]](#).
- [127] ATLAS Collaboration, *Electron and photon efficiencies in LHC Run 2 with the ATLAS experiment*, *JHEP* **05** (2024) 162, arXiv: [2308.13362 \[hep-ex\]](#).
- [128] ATLAS Collaboration, *Muon reconstruction and identification efficiency in ATLAS using the full Run 2 pp collision data set at $\sqrt{s} = 13$ TeV*, *Eur. Phys. J. C* **81** (2021) 578, arXiv: [2012.00578 \[hep-ex\]](#).
- [129] ATLAS Collaboration, *Identification of hadronic tau lepton decays using neural networks in the ATLAS experiment*, ATL-PHYS-PUB-2019-033, 2019, URL: <https://cds.cern.ch/record/2688062>.

- [130] ATLAS Collaboration, *ATLAS b-jet identification performance and efficiency measurement with $t\bar{t}$ events in pp collisions at $\sqrt{s} = 13$ TeV*, *Eur. Phys. J. C* **79** (2019) 970, arXiv: [1907.05120 \[hep-ex\]](#).
- [131] ATLAS Collaboration, *Calibration of the light-flavour jet mistagging efficiency of the b-tagging algorithms with Z+jets events using 139fb^{-1} of ATLAS proton–proton collision data at $\sqrt{s} = 13$ TeV*, *Eur. Phys. J. C* **83** (2023) 728, arXiv: [2301.06319 \[hep-ex\]](#).
- [132] ATLAS Collaboration, *The performance of missing transverse momentum reconstruction and its significance with the ATLAS detector using 140fb^{-1} of $\sqrt{s} = 13$ TeV pp collisions*, *Eur. Phys. J. C* **85** (2025) 606, arXiv: [2402.05858 \[hep-ex\]](#).
- [133] ATLAS Collaboration, *Jet energy scale and resolution measured in proton–proton collisions at $\sqrt{s} = 13$ TeV with the ATLAS detector*, *Eur. Phys. J. C* **81** (2021) 689, arXiv: [2007.02645 \[hep-ex\]](#).
- [134] ATLAS Collaboration, *Performance of pile-up mitigation techniques for jets in pp collisions at $\sqrt{s} = 8$ TeV using the ATLAS detector*, *Eur. Phys. J. C* **76** (2016) 581, arXiv: [1510.03823 \[hep-ex\]](#).
- [135] ATLAS Collaboration, *Studies on top-quark Monte Carlo modelling with Sherpa and MG5_aMC@NLO*, ATL-PHYS-PUB-2017-007, 2017, URL: <https://cds.cern.ch/record/2261938>.
- [136] J. Bellm et al., *Herwig 7.1 Release Note*, (2017), arXiv: [1705.06919 \[hep-ph\]](#).
- [137] ATLAS Collaboration, *Evaluation of QCD uncertainties for Higgs boson production through gluon fusion and in association with two top quarks for simplified template cross-section measurements*, ATL-PHYS-PUB-2023-031, 2023, URL: <https://cds.cern.ch/record/2878797>.
- [138] A. Pinto et al., *Uncertainty components in profile likelihood fits*, *Eur. Phys. J. C* **84** (2024) 593, arXiv: [2307.04007 \[physics.data-an\]](#).
- [139] ATLAS Collaboration, *ATLAS Computing Acknowledgements*, ATL-SOFT-PUB-2025-001, 2025, URL: <https://cds.cern.ch/record/2922210>.

The ATLAS Collaboration

G. Aad [ID¹⁰⁴](#), E. Aakvaag [ID¹⁷](#), B. Abbott [ID¹²³](#), S. Abdelhameed [ID^{119a}](#), K. Abeling [ID⁵⁵](#), N.J. Abicht [ID⁴⁹](#), S.H. Abidi [ID³⁰](#), M. Aboelela [ID⁴⁵](#), A. Aboulhorma [ID^{36e}](#), H. Abramowicz [ID¹⁵⁷](#), Y. Abulaiti [ID¹²⁰](#), B.S. Acharya [ID^{69a,69b,m}](#), A. Ackermann [ID^{63a}](#), C. Adam Bourdarios [ID⁴](#), L. Adamczyk [ID^{86a}](#), S.V. Addepalli [ID¹⁴⁹](#), M.J. Addison [ID¹⁰³](#), J. Adelman [ID¹¹⁸](#), A. Adiguzel [ID^{22c}](#), T. Adye [ID¹³⁷](#), A.A. Affolder [ID¹³⁹](#), Y. Afik [ID⁴⁰](#), M.N. Agaras [ID¹³](#), A. Aggarwal [ID¹⁰²](#), C. Agheorghiesei [ID^{28c}](#), F. Ahmadov [ID^{39,ad}](#), S. Ahuja [ID⁹⁷](#), X. Ai [ID^{143b}](#), G. Aielli [ID^{76a,76b}](#), A. Aikot [ID¹⁶⁹](#), M. Ait Tamlihat [ID^{36e}](#), B. Aitbenchikh [ID^{36a}](#), M. Akbiyik [ID¹⁰²](#), T.P.A. Åkesson [ID¹⁰⁰](#), A.V. Akimov [ID¹⁵¹](#), D. Akiyama [ID¹⁷⁴](#), N.N. Akolkar [ID²⁵](#), S. Aktas [ID^{22a}](#), G.L. Alberghi [ID^{24b}](#), J. Albert [ID¹⁷¹](#), U. Alberti [ID²⁰](#), P. Albicocco [ID⁵³](#), G.L. Albouy [ID⁶⁰](#), S. Alderweireldt [ID⁵²](#), Z.L. Alegria [ID¹²⁴](#), M. Aleksa [ID³⁷](#), I.N. Aleksandrov [ID³⁹](#), C. Alexa [ID^{28b}](#), T. Alexopoulos [ID¹⁰](#), F. Alfonsi [ID^{24b}](#), M. Algren [ID⁵⁶](#), M. Alhroob [ID¹⁷³](#), B. Ali [ID¹³⁵](#), H.M.J. Ali [ID^{93,w}](#), S. Ali [ID³²](#), S.W. Alibocus [ID⁹⁴](#), M. Aliev [ID^{34c}](#), G. Alimonti [ID^{71a}](#), W. Alkakhi [ID⁵⁵](#), C. Allaire [ID⁶⁶](#), B.M.M. Allbrooke [ID¹⁵²](#), J.S. Allen [ID¹⁰³](#), J.F. Allen [ID⁵²](#), P.P. Allport [ID²¹](#), A. Aloisio [ID^{72a,72b}](#), F. Alonso [ID⁹²](#), C. Alpigiani [ID¹⁴²](#), Z.M.K. Alsolami [ID⁹³](#), A. Alvarez Fernandez [ID¹⁰²](#), M. Alves Cardoso [ID⁵⁶](#), M.G. Alvaggi [ID^{72a,72b}](#), M. Aly [ID¹⁰³](#), Y. Amaral Coutinho [ID^{83b}](#), A. Ambler [ID¹⁰⁶](#), C. Amelung [ID³⁷](#), M. Amerl [ID¹⁰³](#), C.G. Ames [ID¹¹¹](#), T. Amezza [ID¹³⁰](#), D. Amidei [ID¹⁰⁸](#), B. Amini [ID⁵⁴](#), K. Amirie [ID¹⁶¹](#), A. Amirkhanov [ID³⁹](#), S.P. Amor Dos Santos [ID^{133a}](#), K.R. Amos [ID¹⁶⁹](#), D. Amperiadou [ID¹⁵⁸](#), S. An [ID⁸⁴](#), C. Anastopoulos [ID¹⁴⁵](#), T. Andeen [ID¹¹](#), J.K. Anders [ID⁹⁴](#), A.C. Anderson [ID⁵⁹](#), A. Andreazza [ID^{71a,71b}](#), S. Angelidakis [ID⁹](#), A. Angerami [ID⁴²](#), A.V. Anisenkov [ID³⁹](#), A. Annovi [ID^{74a}](#), C. Antel [ID³⁷](#), E. Antipov [ID¹⁵¹](#), M. Antonelli [ID⁵³](#), F. Anulli [ID^{75a}](#), M. Aoki [ID⁸⁴](#), T. Aoki [ID¹⁵⁹](#), M.A. Aparo [ID¹⁵²](#), L. Aperio Bella [ID⁴⁸](#), M. Apicella [ID³¹](#), C. Appelt [ID¹⁵⁷](#), A. Apyan [ID²⁷](#), M. Arampatzi [ID¹⁰](#), S.J. Arbiol Val [ID⁸⁷](#), C. Arcangeletti [ID⁵³](#), A.T.H. Arce [ID⁵¹](#), J-F. Arguin [ID¹¹⁰](#), S. Argyropoulos [ID¹⁵⁸](#), J.-H. Arling [ID⁴⁸](#), O. Arnaez [ID⁴](#), H. Arnold [ID¹⁵¹](#), G. Artoni [ID^{75a,75b}](#), H. Asada [ID¹¹³](#), K. Asai [ID¹²¹](#), S. Asatryan [ID¹⁷⁹](#), N.A. Asbah [ID³⁷](#), R.A. Ashby Pickering [ID¹⁷³](#), A.M. Aslam [ID⁹⁷](#), K. Assamagan [ID³⁰](#), R. Astalos [ID^{29a}](#), K.S.V. Astrand [ID¹⁰⁰](#), S. Atashi [ID¹⁶⁵](#), R.J. Atkin [ID^{34a}](#), H. Atmani [ID^{36f}](#), P.A. Atmasiddha [ID¹³¹](#), K. Augsten [ID¹³⁵](#), A.D. Auriol [ID⁴¹](#), V.A. Aastrup [ID¹⁰³](#), G. Avolio [ID³⁷](#), K. Axiotis [ID⁵⁶](#), A. Azzam [ID¹³](#), D. Babal [ID^{29b}](#), H. Bachacou [ID¹³⁸](#), K. Bachas [ID^{158,q}](#), A. Bachiu [ID³⁵](#), E. Bachmann [ID⁵⁰](#), M.J. Backes [ID^{63a}](#), A. Badea [ID⁴⁰](#), T.M. Baer [ID¹⁰⁸](#), P. Bagnaia [ID^{75a,75b}](#), M. Bahmani [ID¹⁹](#), D. Bahner [ID⁵⁴](#), K. Bai [ID¹²⁶](#), J.T. Baines [ID¹³⁷](#), L. Baines [ID⁹⁶](#), O.K. Baker [ID¹⁷⁸](#), E. Bakos [ID¹⁶](#), D. Bakshi Gupta [ID⁸](#), L.E. Balabram Filho [ID^{83b}](#), V. Balakrishnan [ID¹²³](#), R. Balasubramanian [ID⁴](#), E.M. Baldin [ID³⁸](#), P. Balek [ID^{86a}](#), E. Ballabene [ID^{24b,24a}](#), F. Balli [ID¹³⁸](#), L.M. Baltes [ID^{63a}](#), W.K. Balunas [ID³³](#), J. Balz [ID¹⁰²](#), I. Bamwidhi [ID^{119b}](#), E. Banas [ID⁸⁷](#), M. Bandieramonte [ID¹³²](#), A. Bandyopadhyay [ID²⁵](#), S. Bansal [ID²⁵](#), L. Barak [ID¹⁵⁷](#), M. Barakat [ID⁴⁸](#), E.L. Barberio [ID¹⁰⁷](#), D. Barberis [ID^{18b}](#), M. Barbero [ID¹⁰⁴](#), M.Z. Barel [ID¹¹⁷](#), T. Barillari [ID¹¹²](#), M-S. Barisits [ID³⁷](#), T. Barklow [ID¹⁴⁹](#), P. Baron [ID¹³⁶](#), D.A. Baron Moreno [ID¹⁰³](#), A. Baroncelli [ID⁶²](#), A.J. Barr [ID¹²⁹](#), J.D. Barr [ID⁹⁸](#), F. Barreiro [ID¹⁰¹](#), J. Barreiro Guimaraes da Costa [ID¹⁴](#), M.G. Barros Teixeira [ID^{133a}](#), S. Barsov [ID³⁸](#), F. Bartels [ID^{63a}](#), R. Bartoldus [ID¹⁴⁹](#), A.E. Barton [ID⁹³](#), P. Bartos [ID^{29a}](#), A. Basan [ID¹⁰²](#), M. Baselga [ID⁴⁹](#), S. Bashiri [ID⁸⁷](#), A. Bassalat [ID^{66,b}](#), M.J. Basso [ID^{162a}](#), S. Bataju [ID⁴⁵](#), R. Bate [ID¹⁷⁰](#), R.L. Bates [ID⁵⁹](#), S. Batlamous [ID¹⁰¹](#), M. Battaglia [ID¹³⁹](#), D. Battulga [ID¹⁹](#), M. Bauce [ID^{75a,75b}](#), M. Bauer [ID⁷⁹](#), P. Bauer [ID²⁵](#), L.T. Bayer [ID⁴⁸](#), L.T. Bazzano Hurrell [ID³¹](#), J.B. Beacham [ID¹¹²](#), T. Beau [ID¹³⁰](#), J.Y. Beauchamp [ID⁹²](#), P.H. Beauchemin [ID¹⁶⁴](#), P. Bechtle [ID²⁵](#), H.P. Beck [ID^{20,p}](#), K. Becker [ID¹⁷³](#), A.J. Beddall [ID⁸²](#), V.A. Bednyakov [ID³⁹](#), C.P. Bee [ID¹⁵¹](#), L.J. Beemster [ID¹⁶](#), M. Begalli [ID^{83d}](#), M. Begel [ID³⁰](#), J.K. Behr [ID⁴⁸](#), J.F. Beirer [ID³⁷](#), F. Beisiegel [ID²⁵](#), M. Belfkir [ID^{119b}](#), G. Bella [ID¹⁵⁷](#), L. Bellagamba [ID^{24b}](#), A. Bellerive [ID³⁵](#), C.D. Bellgraph [ID⁶⁸](#), P. Bellos [ID²¹](#), K. Beloborodov [ID³⁸](#), D. Benchekroun [ID^{36a}](#), F. Bendebba [ID^{36a}](#), Y. Benhammou [ID¹⁵⁷](#),

K.C. Benkendorfer [ID⁶¹](#), L. Beresford [ID⁴⁸](#), M. Beretta [ID⁵³](#), E. Bergeaas Kuutmann [ID¹⁶⁷](#), N. Berger [ID⁴](#),
 B. Bergmann [ID¹³⁵](#), J. Beringer [ID^{18a}](#), G. Bernardi [ID⁵](#), C. Bernius [ID¹⁴⁹](#), F.U. Bernlochner [ID²⁵](#),
 F. Bernon [ID³⁷](#), A. Berrocal Guardia [ID¹³](#), T. Berry [ID⁹⁷](#), P. Berta [ID¹³⁶](#), A. Berthold [ID⁵⁰](#), A. Berti [ID^{133a}](#),
 R. Bertrand [ID¹⁰⁴](#), S. Bethke [ID¹¹²](#), A. Betti [ID^{75a,75b}](#), A.J. Bevan [ID⁹⁶](#), L. Bezio [ID⁵⁶](#), N.K. Bhalla [ID⁵⁴](#),
 S. Bharthuar [ID¹¹²](#), S. Bhatta [ID¹⁵¹](#), P. Bhattacharai [ID¹⁴⁹](#), Z.M. Bhatti [ID¹²⁰](#), K.D. Bhide [ID⁵⁴](#),
 V.S. Bhopatkar [ID¹²⁴](#), R.M. Bianchi [ID¹³²](#), G. Bianco [ID^{24b,24a}](#), O. Biebel [ID¹¹¹](#), M. Biglietti [ID^{77a}](#),
 C.S. Billingsley [ID⁴⁵](#), Y. Bimgni [ID^{36f}](#), M. Bindl [ID⁵⁵](#), A. Bingham [ID¹⁷⁷](#), A. Bingul [ID^{22b}](#), C. Bini [ID^{75a,75b}](#),
 G.A. Bird [ID³³](#), M. Birman [ID¹⁷⁵](#), M. Biros [ID¹³⁶](#), S. Biryukov [ID¹⁵²](#), T. Bisanz [ID⁴⁹](#), E. Bisceglie [ID^{24b,24a}](#),
 J.P. Biswal [ID¹³⁷](#), D. Biswas [ID¹⁴⁷](#), I. Bloch [ID⁴⁸](#), A. Blue [ID⁵⁹](#), U. Blumenschein [ID⁹⁶](#), J. Blumenthal [ID¹⁰²](#),
 V.S. Bobrovnikov [ID³⁹](#), L. Boccardo [ID^{57b,57a}](#), M. Boehler [ID⁵⁴](#), B. Boehm [ID¹⁷²](#), D. Bogavac [ID¹³](#),
 A.G. Bogdanchikov [ID³⁸](#), L.S. Boggia [ID¹³⁰](#), V. Boisvert [ID⁹⁷](#), P. Bokan [ID³⁷](#), T. Bold [ID^{86a}](#), M. Bomben [ID⁵](#),
 M. Bona [ID⁹⁶](#), M. Boonekamp [ID¹³⁸](#), A.G. Borbely [ID⁵⁹](#), I.S. Bordulev [ID³⁸](#), G. Borissov [ID⁹³](#),
 D. Bortoletto [ID¹²⁹](#), D. Boscherini [ID^{24b}](#), M. Bosman [ID¹³](#), K. Bouaouda [ID^{36a}](#), N. Bouchhar [ID¹⁶⁹](#),
 L. Boudet [ID⁴](#), J. Boudreau [ID¹³²](#), E.V. Bouhova-Thacker [ID⁹³](#), D. Boumediene [ID⁴¹](#), R. Bouquet [ID^{57b,57a}](#),
 A. Boveia [ID¹²²](#), J. Boyd [ID³⁷](#), D. Boye [ID³⁰](#), I.R. Boyko [ID³⁹](#), L. Bozianu [ID⁵⁶](#), J. Bracinik [ID²¹](#),
 N. Brahimi [ID⁴](#), G. Brandt [ID¹⁷⁷](#), O. Brandt [ID³³](#), B. Brau [ID¹⁰⁵](#), J.E. Brau [ID¹²⁶](#), R. Brener [ID¹⁷⁵](#),
 L. Brenner [ID¹¹⁷](#), R. Brenner [ID¹⁶⁷](#), S. Bressler [ID¹⁷⁵](#), G. Brianti [ID^{78a,78b}](#), D. Britton [ID⁵⁹](#), D. Britzger [ID¹¹²](#),
 I. Brock [ID²⁵](#), R. Brock [ID¹⁰⁹](#), G. Brooijmans [ID⁴²](#), A.J. Brooks [ID⁶⁸](#), E.M. Brooks [ID^{162b}](#), E. Brost [ID³⁰](#),
 L.M. Brown [ID^{171,162a}](#), L.E. Bruce [ID⁶¹](#), T.L. Bruckler [ID¹²⁹](#), P.A. Bruckman de Renstrom [ID⁸⁷](#),
 B. Brüers [ID⁴⁸](#), A. Bruni [ID^{24b}](#), G. Bruni [ID^{24b}](#), D. Brunner [ID^{47a,47b}](#), M. Bruschi [ID^{24b}](#), N. Bruscino [ID^{75a,75b}](#),
 T. Buanes [ID¹⁷](#), Q. Buat [ID¹⁴²](#), D. Buchin [ID¹¹²](#), A.G. Buckley [ID⁵⁹](#), O. Bulekov [ID⁸²](#), B.A. Bullard [ID¹⁴⁹](#),
 S. Burdin [ID⁹⁴](#), C.D. Burgard [ID⁴⁹](#), A.M. Burger [ID⁹¹](#), B. Burghgrave [ID⁸](#), O. Burlayenko [ID⁵⁴](#),
 J. Burleson [ID¹⁶⁸](#), J.C. Burzynski [ID¹⁴⁸](#), E.L. Busch [ID⁴²](#), V. Büscher [ID¹⁰²](#), P.J. Bussey [ID⁵⁹](#),
 J.M. Butler [ID²⁶](#), C.M. Buttar [ID⁵⁹](#), J.M. Butterworth [ID⁹⁸](#), W. Buttlinger [ID¹³⁷](#), C.J. Buxo Vazquez [ID¹⁰⁹](#),
 A.R. Buzykaev [ID³⁹](#), S. Cabrera Urbán [ID¹⁶⁹](#), L. Cadamuro [ID⁶⁶](#), H. Cai [ID¹³²](#), Y. Cai [ID^{24b,114c,24a}](#),
 Y. Cai [ID^{114a}](#), V.M.M. Cairo [ID³⁷](#), O. Cakir [ID^{3a}](#), N. Calace [ID³⁷](#), P. Calafiura [ID^{18a}](#), G. Calderini [ID¹³⁰](#),
 P. Calfayan [ID³⁵](#), L. Calic [ID¹⁰⁰](#), G. Callea [ID⁵⁹](#), L.P. Caloba [ID^{83b}](#), D. Calvet [ID⁴¹](#), S. Calvet [ID⁴¹](#),
 R. Camacho Toro [ID¹³⁰](#), S. Camarda [ID³⁷](#), D. Camarero Munoz [ID²⁷](#), P. Camarri [ID^{76a,76b}](#),
 C. Camincher [ID¹⁷¹](#), M. Campanelli [ID⁹⁸](#), A. Camplani [ID⁴³](#), V. Canale [ID^{72a,72b}](#), A.C. Canbay [ID^{3a}](#),
 E. Canonero [ID⁹⁷](#), J. Cantero [ID¹⁶⁹](#), Y. Cao [ID¹⁶⁸](#), F. Capocasa [ID²⁷](#), M. Capua [ID^{44b,44a}](#), A. Carbone [ID^{71a,71b}](#),
 R. Cardarelli [ID^{76a}](#), J.C.J. Cardenas [ID⁸](#), M.P. Cardiff [ID²⁷](#), G. Carducci [ID^{44b,44a}](#), T. Carli [ID³⁷](#),
 G. Carlino [ID^{72a}](#), J.I. Carlotto [ID¹³](#), B.T. Carlson [ID^{132,r}](#), E.M. Carlson [ID¹⁷¹](#), J. Carmignani [ID⁹⁴](#),
 L. Carminati [ID^{71a,71b}](#), A. Carnelli [ID⁴](#), M. Carnesale [ID³⁷](#), S. Caron [ID¹¹⁶](#), E. Carquin [ID^{140g}](#), I.B. Carr [ID¹⁰⁷](#),
 S. Carrá [ID^{73a,73b}](#), G. Carratta [ID^{24b,24a}](#), A.M. Carroll [ID¹²⁶](#), M.P. Casado [ID^{13,h}](#), P. Casolaro [ID^{72a,72b}](#),
 M. Caspar [ID⁴⁸](#), F.L. Castillo [ID⁴](#), L. Castillo Garcia [ID¹³](#), V. Castillo Gimenez [ID¹⁶⁹](#), N.F. Castro [ID^{133a,133e}](#),
 A. Catinaccio [ID³⁷](#), J.R. Catmore [ID¹²⁸](#), T. Cavaliere [ID⁴](#), V. Cavaliere [ID³⁰](#), L.J. Caviedes Betancourt [ID^{23b}](#),
 E. Celebi [ID⁸²](#), S. Cella [ID³⁷](#), V. Cepaitis [ID⁵⁶](#), K. Cerny [ID¹²⁵](#), A.S. Cerqueira [ID^{83a}](#), A. Cerri [ID^{74a,74b,ak}](#),
 L. Cerrito [ID^{76a,76b}](#), F. Cerutti [ID^{18a}](#), B. Cervato [ID^{71a,71b}](#), A. Cervelli [ID^{24b}](#), G. Cesarini [ID⁵³](#), S.A. Cetin [ID⁸²](#),
 P.M. Chabrillat [ID¹³⁰](#), R. Chakkappai [ID⁶⁶](#), S. Chakraborty [ID¹⁷³](#), J. Chan [ID^{18a}](#), W.Y. Chan [ID¹⁵⁹](#),
 J.D. Chapman [ID³³](#), E. Chapon [ID¹³⁸](#), B. Chargeishvili [ID^{155b}](#), D.G. Charlton [ID²¹](#), C. Chauhan [ID¹³⁶](#),
 Y. Che [ID^{114a}](#), S. Chekanov [ID⁶](#), S.V. Chekulaev [ID^{162a}](#), G.A. Chelkov [ID^{39,a}](#), B. Chen [ID¹⁵⁷](#), B. Chen [ID¹⁷¹](#),
 H. Chen [ID^{114a}](#), H. Chen [ID³⁰](#), J. Chen [ID^{144a}](#), J. Chen [ID¹⁴⁸](#), M. Chen [ID¹²⁹](#), S. Chen [ID⁸⁹](#), S.J. Chen [ID^{114a}](#),
 X. Chen [ID^{144a}](#), X. Chen [ID^{15,ag}](#), Z. Chen [ID⁶²](#), C.L. Cheng [ID¹⁷⁶](#), H.C. Cheng [ID^{64a}](#), S. Cheong [ID¹⁴⁹](#),
 A. Cheplakov [ID³⁹](#), E. Cherepanova [ID¹¹⁷](#), R. Cherkaoui El Moursli [ID^{36e}](#), E. Cheu [ID⁷](#), K. Cheung [ID⁶⁵](#),
 L. Chevalier [ID¹³⁸](#), V. Chiarella [ID⁵³](#), G. Chiarelli [ID^{74a}](#), G. Chiodini [ID^{70a}](#), A.S. Chisholm [ID²¹](#),
 A. Chitan [ID^{28b}](#), M. Chitishvili [ID¹⁶⁹](#), M.V. Chizhov [ID^{39,s}](#), K. Choi [ID¹¹](#), Y. Chou [ID¹⁴²](#), E.Y.S. Chow [ID¹¹⁶](#),
 K.L. Chu [ID¹⁷⁵](#), M.C. Chu [ID^{64a}](#), X. Chu [ID^{14,114c}](#), Z. Chubinidze [ID⁵³](#), J. Chudoba [ID¹³⁴](#),

J.J. Chwastowski [ID⁸⁷](#), D. Cieri [ID¹¹²](#), K.M. Ciesla [ID^{86a}](#), V. Cindro [ID⁹⁵](#), A. Ciocio [ID^{18a}](#), F. Cirotto [ID^{72a,72b}](#), Z.H. Citron [ID¹⁷⁵](#), M. Citterio [ID^{71a}](#), D.A. Ciubotaru [ID^{28b}](#), A. Clark [ID⁵⁶](#), P.J. Clark [ID⁵²](#), N. Clarke Hall [ID⁹⁸](#), C. Clarry [ID¹⁶¹](#), S.E. Clawson [ID⁴⁸](#), C. Clement [ID^{47a,47b}](#), Y. Coadou [ID¹⁰⁴](#), M. Cobal [ID^{69a,69c}](#), A. Coccaro [ID^{57b}](#), R.F. Coelho Barrue [ID^{133a}](#), R. Coelho Lopes De Sa [ID¹⁰⁵](#), S. Coelli [ID^{71a}](#), L.S. Colangeli [ID¹⁶¹](#), B. Cole [ID⁴²](#), P. Collado Soto [ID¹⁰¹](#), J. Collot [ID⁶⁰](#), R. Coluccia [ID^{70a,70b}](#), P. Conde Muiño [ID^{133a,133g}](#), M.P. Connell [ID^{34c}](#), S.H. Connell [ID^{34c}](#), E.I. Conroy [ID¹²⁹](#), M. Contreras Cossio [ID¹¹](#), F. Conventi [ID^{72a,ai}](#), A.M. Cooper-Sarkar [ID¹²⁹](#), L. Corazzina [ID^{75a,75b}](#), F.A. Corchia [ID^{24b,24a}](#), A. Cordeiro Oudot Choi [ID¹⁴²](#), L.D. Corpe [ID⁴¹](#), M. Corradi [ID^{75a,75b}](#), F. Corriveau [ID^{106,ab}](#), A. Cortes-Gonzalez [ID¹⁵⁹](#), M.J. Costa [ID¹⁶⁹](#), F. Costanza [ID⁴](#), D. Costanzo [ID¹⁴⁵](#), B.M. Cote [ID¹²²](#), J. Couthures [ID⁴](#), G. Cowan [ID⁹⁷](#), K. Cranmer [ID¹⁷⁶](#), L. Cremer [ID⁴⁹](#), D. Cremonini [ID^{24b,24a}](#), S. Crépé-Renaudin [ID⁶⁰](#), F. Crescioli [ID¹³⁰](#), T. Cresta [ID^{73a,73b}](#), M. Cristinziani [ID¹⁴⁷](#), M. Cristoforetti [ID^{78a,78b}](#), V. Croft [ID¹¹⁷](#), J.E. Crosby [ID¹²⁴](#), G. Crosetti [ID^{44b,44a}](#), A. Cueto [ID¹⁰¹](#), H. Cui [ID⁹⁸](#), Z. Cui [ID⁷](#), B.M. Cunnnett [ID¹⁵²](#), W.R. Cunningham [ID⁵⁹](#), F. Curcio [ID¹⁶⁹](#), J.R. Curran [ID⁵²](#), M.J. Da Cunha Sargedas De Sousa [ID^{57b,57a}](#), J.V. Da Fonseca Pinto [ID^{83b}](#), C. Da Via [ID¹⁰³](#), W. Dabrowski [ID^{86a}](#), T. Dado [ID³⁷](#), S. Dahbi [ID¹⁵⁴](#), T. Dai [ID¹⁰⁸](#), D. Dal Santo [ID²⁰](#), C. Dallapiccola [ID¹⁰⁵](#), M. Dam [ID⁴³](#), G. D'amen [ID³⁰](#), V. D'Amico [ID¹¹¹](#), J. Damp [ID¹⁰²](#), J.R. Dandoy [ID³⁵](#), M. D'andrea [ID^{57b,57a}](#), D. Dannheim [ID³⁷](#), G. D'anniballe [ID^{74a,74b}](#), M. Danninger [ID¹⁴⁸](#), V. Dao [ID¹⁵¹](#), G. Darbo [ID^{57b}](#), S.J. Das [ID³⁰](#), F. Dattola [ID⁴⁸](#), S. D'Auria [ID^{71a,71b}](#), A. D'Avanzo [ID^{72a,72b}](#), T. Davidek [ID¹³⁶](#), J. Davidson [ID¹⁷³](#), I. Dawson [ID⁹⁶](#), K. De [ID⁸](#), C. De Almeida Rossi [ID¹⁶¹](#), R. De Asmundis [ID^{72a}](#), N. De Biase [ID⁴⁸](#), S. De Castro [ID^{24b,24a}](#), N. De Groot [ID¹¹⁶](#), P. de Jong [ID¹¹⁷](#), H. De la Torre [ID¹¹⁸](#), A. De Maria [ID^{114a}](#), A. De Salvo [ID^{75a}](#), U. De Sanctis [ID^{76a,76b}](#), F. De Santis [ID^{70a,70b}](#), A. De Santo [ID¹⁵²](#), J.B. De Vivie De Regie [ID⁶⁰](#), J. Debevc [ID⁹⁵](#), D.V. Dedovich³⁹, J. Degens [ID⁹⁴](#), A.M. Deiana [ID⁴⁵](#), J. Del Peso [ID¹⁰¹](#), L. Delagrange [ID¹³⁰](#), F. Deliot [ID¹³⁸](#), C.M. Delitzsch [ID⁴⁹](#), M. Della Pietra [ID^{72a,72b}](#), D. Della Volpe [ID⁵⁶](#), A. Dell'Acqua [ID³⁷](#), L. Dell'Asta [ID^{71a,71b}](#), M. Delmastro [ID⁴](#), C.C. Delogu [ID¹⁰²](#), P.A. Delsart [ID⁶⁰](#), S. Demers [ID¹⁷⁸](#), M. Demichev [ID³⁹](#), S.P. Denisov [ID³⁸](#), H. Denizli [ID^{22a,l}](#), L. D'Eramo [ID⁴¹](#), D. Derendarz [ID⁸⁷](#), F. Derue [ID¹³⁰](#), P. Dervan [ID⁹⁴](#), A.M. Desai [ID¹](#), K. Desch [ID²⁵](#), F.A. Di Bello [ID^{57b,57a}](#), A. Di Ciaccio [ID^{76a,76b}](#), L. Di Ciaccio [ID⁴](#), A. Di Domenico [ID^{75a,75b}](#), C. Di Donato [ID^{72a,72b}](#), A. Di Girolamo [ID³⁷](#), G. Di Gregorio [ID³⁷](#), A. Di Luca [ID^{78a,78b}](#), B. Di Micco [ID^{77a,77b}](#), R. Di Nardo [ID^{77a,77b}](#), K.F. Di Petrillo [ID⁴⁰](#), M. Diamantopoulou [ID³⁵](#), F.A. Dias [ID¹¹⁷](#), M.A. Diaz [ID^{140a,140b}](#), A.R. Didenko [ID³⁹](#), M. Didenko [ID¹⁶⁹](#), S.D. Diefenbacher [ID^{18a}](#), E.B. Diehl [ID¹⁰⁸](#), S. Díez Cornell [ID⁴⁸](#), C. Diez Pardos [ID¹⁴⁷](#), C. Dimitriadi [ID¹⁵⁰](#), A. Dimitrieva [ID²¹](#), A. Dimri [ID¹⁵¹](#), Y. Ding⁶², J. Dingfelder [ID²⁵](#), T. Dingley [ID¹²⁹](#), I-M. Dinu [ID^{28b}](#), S.J. Dittmeier [ID^{63b}](#), F. Dittus [ID³⁷](#), M. Divisek [ID¹³⁶](#), B. Dixit [ID⁹⁴](#), F. Djama [ID¹⁰⁴](#), T. Djobava [ID^{155b}](#), C. Doglioni [ID^{103,100}](#), A. Dohnalova [ID^{29a}](#), Z. Dolezal [ID¹³⁶](#), K. Domijan [ID^{86a}](#), K.M. Dona [ID⁴⁰](#), M. Donadelli [ID^{83d}](#), B. Dong [ID¹⁰⁹](#), J. Donini [ID⁴¹](#), A. D'Onofrio [ID^{72a,72b}](#), M. D'Onofrio [ID⁹⁴](#), J. Dopke [ID¹³⁷](#), A. Doria [ID^{72a}](#), N. Dos Santos Fernandes [ID^{133a}](#), I.A. Dos Santos Luz [ID^{83e}](#), P. Dougan [ID¹⁰³](#), M.T. Dova [ID⁹²](#), A.T. Doyle [ID⁵⁹](#), M.P. Drescher [ID⁵⁵](#), E. Dreyer [ID¹⁷⁵](#), I. Drivas-koulouris [ID¹⁰](#), M. Drnevich [ID¹²⁰](#), D. Du [ID⁶²](#), T.A. du Pree [ID¹¹⁷](#), Z. Duan^{114a}, M. Dubau [ID⁴](#), F. Dubinin [ID³⁹](#), M. Dubovsky [ID^{29a}](#), E. Duchovni [ID¹⁷⁵](#), G. Duckeck [ID¹¹¹](#), P.K. Duckett⁹⁸, O.A. Ducu [ID^{28b}](#), D. Duda [ID⁵²](#), A. Dudarev [ID³⁷](#), E.R. Duden [ID²⁷](#), M. D'uffizi [ID¹⁰³](#), L. Duflot [ID⁶⁶](#), M. Dührssen [ID³⁷](#), I. Duminica [ID^{28g}](#), A.E. Dumitriu [ID^{28b}](#), M. Dunford [ID^{63a}](#), K. Dunne [ID^{47a,47b}](#), A. Duperrin [ID¹⁰⁴](#), H. Duran Yildiz [ID^{3a}](#), A. Durglishvili [ID^{155b}](#), D. Duvnjak [ID³⁵](#), G.I. Dyckes [ID^{18a}](#), M. Dyndal [ID^{86a}](#), B.S. Dziedzic [ID³⁷](#), Z.O. Earnshaw [ID¹⁵²](#), G.H. Eberwein [ID¹²⁹](#), B. Eckerova [ID^{29a}](#), S. Eggebrecht [ID⁵⁵](#), E. Egidio Purcino De Souza [ID^{83e}](#), G. Eigen [ID¹⁷](#), K. Einsweiler [ID^{18a}](#), T. Ekelof [ID¹⁶⁷](#), P.A. Ekman [ID¹⁰⁰](#), S. El Farkh [ID^{36b}](#), Y. El Ghazali [ID⁶²](#), H. El Jarrari [ID³⁷](#), A. El Moussaoui [ID^{36a}](#), M. Ellert [ID¹⁶⁷](#), F. Ellinghaus [ID¹⁷⁷](#), T.A. Elliot [ID⁹⁷](#), N. Ellis [ID³⁷](#), J. Elmsheuser [ID³⁰](#), M. Elsawy [ID^{119a}](#), M. Elsing [ID³⁷](#), D. Emeliyanov [ID¹³⁷](#), Y. Enari [ID⁸⁴](#), I. Ene [ID^{18a}](#), S. Epari [ID¹¹⁰](#), D. Ernani Martins Neto [ID⁸⁷](#), F. Ernst³⁷,

M. Errenst ID^{177} , M. Escalier ID^{66} , C. Escobar ID^{169} , E. Etzion ID^{157} , G. Evans $\text{ID}^{133a,133b}$, H. Evans ID^{68} , L.S. Evans ID^{97} , A. Ezhilov ID^{38} , S. Ezzarqtouni ID^{36a} , F. Fabbri $\text{ID}^{24b,24a}$, L. Fabbri $\text{ID}^{24b,24a}$, G. Facini ID^{98} , V. Fadeyev ID^{139} , R.M. Fakhrutdinov ID^{38} , D. Fakoudis ID^{102} , S. Falciano ID^{75a} , L.F. Falda Ulhoa Coelho ID^{133a} , F. Fallavollita ID^{112} , G. Falsetti $\text{ID}^{44b,44a}$, J. Faltova ID^{136} , C. Fan ID^{168} , K.Y. Fan ID^{64b} , Y. Fan ID^{14} , Y. Fang $\text{ID}^{14,114c}$, M. Fanti $\text{ID}^{71a,71b}$, M. Faraj $\text{ID}^{69a,69b}$, Z. Farazpay ID^{99} , A. Farbin ID^8 , A. Farilla ID^{77a} , K. Farman ID^{154} , T. Farooque ID^{109} , J.N. Farr ID^{178} , S.M. Farrington $\text{ID}^{137,52}$, F. Fassi ID^{36e} , D. Fassouliotis ID^9 , L. Fayard ID^{66} , P. Federic ID^{136} , P. Federicova ID^{134} , O.L. Fedin $\text{ID}^{38,a}$, M. Feickert ID^{176} , L. Feligioni ID^{104} , D.E. Fellers ID^{18a} , C. Feng ID^{143a} , Y. Feng ID^{14} , Z. Feng ID^{117} , M.J. Fenton ID^{165} , L. Ferencz ID^{48} , B. Fernandez Barbadillo ID^{93} , P. Fernandez Martinez ID^{67} , M.J.V. Fernoux ID^{104} , J. Ferrando ID^{93} , A. Ferrari ID^{167} , P. Ferrari $\text{ID}^{117,116}$, R. Ferrari ID^{73a} , D. Ferrere ID^{56} , C. Ferretti ID^{108} , M.P. Fewell ID^1 , D. Fiacco $\text{ID}^{75a,75b}$, F. Fiedler ID^{102} , P. Fiedler ID^{135} , S. Filimonov ID^{39} , M.S. Filip $\text{ID}^{28b,t}$, A. Filipčić ID^{95} , E.K. Filmer ID^{162a} , F. Filthaut ID^{116} , M.C.N. Fiolhais $\text{ID}^{133a,133c,c}$, L. Fiorini ID^{169} , W.C. Fisher ID^{109} , T. Fitschen ID^{103} , P.M. Fitzhugh ID^{138} , I. Fleck ID^{147} , P. Fleischmann ID^{108} , T. Flick ID^{177} , M. Flores $\text{ID}^{34d,af}$, L.R. Flores Castillo ID^{64a} , L. Flores Sanz De Acedo ID^{37} , F.M. Follega $\text{ID}^{78a,78b}$, N. Fomin ID^{33} , J.H. Foo ID^{161} , A. Formica ID^{138} , A.C. Forti ID^{103} , E. Fortin ID^{37} , A.W. Fortman ID^{18a} , L. Foster ID^{18a} , L. Fountas $\text{ID}^{9,i}$, D. Fournier ID^{66} , H. Fox ID^{93} , P. Francavilla $\text{ID}^{74a,74b}$, S. Francescato ID^{61} , S. Franchellucci ID^{56} , M. Franchini $\text{ID}^{24b,24a}$, S. Franchino ID^{63a} , D. Francis ID^{37} , L. Franco ID^{116} , V. Franco Lima ID^{37} , L. Franconi ID^{48} , M. Franklin ID^{61} , G. Frattari ID^{27} , Y.Y. Frid ID^{157} , J. Friend ID^{59} , N. Fritzsche ID^{37} , A. Froch ID^{56} , D. Froidevaux ID^{37} , J.A. Frost ID^{129} , Y. Fu ID^{109} , S. Fuenzalida Garrido ID^{140g} , M. Fujimoto ID^{104} , K.Y. Fung ID^{64a} , E. Furtado De Simas Filho ID^{83e} , M. Furukawa ID^{159} , J. Fuster ID^{169} , A. Gaa ID^{55} , A. Gabrielli $\text{ID}^{24b,24a}$, A. Gabrielli ID^{161} , P. Gadow ID^{37} , G. Gagliardi $\text{ID}^{57b,57a}$, L.G. Gagnon ID^{18a} , S. Gaid ID^{88b} , S. Galantzan ID^{157} , J. Gallagher ID^1 , E.J. Gallas ID^{129} , A.L. Gallen ID^{167} , B.J. Gallop ID^{137} , K.K. Gan ID^{122} , S. Ganguly ID^{159} , Y. Gao ID^{52} , A. Garabaglu ID^{142} , F.M. Garay Walls $\text{ID}^{140a,140b}$, C. García ID^{169} , A. Garcia Alonso ID^{117} , A.G. Garcia Caffaro ID^{178} , J.E. García Navarro ID^{169} , M.A. Garcia Ruiz ID^{23b} , M. Garcia-Sciveres ID^{18a} , G.L. Gardner ID^{131} , R.W. Gardner ID^{40} , N. Garelli ID^{164} , R.B. Garg ID^{149} , J.M. Gargan ID^{52} , C.A. Garner ID^{161} , C.M. Garvey ID^{34a} , V.K. Gassmann ID^{164} , G. Gaudio ID^{73a} , V. Gautam ID^{13} , P. Gauzzi $\text{ID}^{75a,75b}$, J. Gavranovic ID^{95} , I.L. Gavrilenco ID^{133a} , A. Gavrilyuk ID^{38} , C. Gay ID^{170} , G. Gaycken ID^{126} , E.N. Gazis ID^{10} , A. Gekow ID^{122} , C. Gemme ID^{57b} , M.H. Genest ID^{60} , A.D. Gentry ID^{115} , S. George ID^{97} , T. Geralis ID^{46} , A.A. Gerwin ID^{123} , P. Gessinger-Befurt ID^{37} , M.E. Geyik ID^{177} , M. Ghani ID^{173} , K. Ghorbanian ID^{96} , A. Ghosal ID^{147} , A. Ghosh ID^{165} , A. Ghosh ID^7 , B. Giacobbe ID^{24b} , S. Giagu $\text{ID}^{75a,75b}$, T. Giani ID^{117} , A. Giannini ID^{62} , S.M. Gibson ID^{97} , M. Gignac ID^{139} , D.T. Gil ID^{86b} , A.K. Gilbert ID^{86a} , B.J. Gilbert ID^{42} , D. Gillberg ID^{35} , G. Gilles ID^{117} , D.M. Gingrich $\text{ID}^{2,ah}$, M.P. Giordani $\text{ID}^{69a,69c}$, P.F. Giraud ID^{138} , G. Giugliarelli $\text{ID}^{69a,69c}$, D. Giugni ID^{71a} , F. Giuli $\text{ID}^{76a,76b}$, I. Gkialas $\text{ID}^{9,i}$, L.K. Gladilin ID^{38} , C. Glasman ID^{101} , M. Glazewska ID^{20} , R.M. Gleason ID^{165} , G. Glemža ID^{48} , M. Glisic ID^{126} , I. Gnesi ID^{44b} , Y. Go ID^{30} , M. Goblirsch-Kolb ID^{37} , B. Gocke ID^{49} , D. Godin ID^{110} , B. Gokturk ID^{22a} , S. Goldfarb ID^{107} , T. Golling ID^{56} , M.G.D. Gololo ID^{34c} , D. Golubkov ID^{38} , J.P. Gombas ID^{109} , A. Gomes $\text{ID}^{133a,133b}$, G. Gomes Da Silva ID^{147} , A.J. Gomez Delegido ID^{37} , R. Gonçalo ID^{133a} , L. Gonella ID^{21} , A. Gongadze ID^{155c} , F. Gonnella ID^{21} , J.L. Gonski ID^{149} , R.Y. González Andana ID^{52} , S. González de la Hoz ID^{169} , M.V. Gonzalez Rodrigues ID^{48} , R. Gonzalez Suarez ID^{167} , S. Gonzalez-Sevilla ID^{56} , L. Goossens ID^{37} , B. Gorini ID^{37} , E. Gorini $\text{ID}^{70a,70b}$, A. Gorišek ID^{95} , T.C. Gosart ID^{131} , A.T. Goshaw ID^{51} , M.I. Gostkin ID^{39} , S. Goswami ID^{124} , C.A. Gottardo ID^{37} , S.A. Gotz ID^{111} , M. Gouighri ID^{36b} , A.G. Goussiou ID^{142} , N. Govender ID^{34c} , R.P. Grabarczyk ID^{129} , I. Grabowska-Bold ID^{86a} , K. Graham ID^{35} , E. Gramstad ID^{128} , S. Grancagnolo $\text{ID}^{70a,70b}$, C.M. Grant ID^1 , P.M. Gravila ID^{28f} , F.G. Gravili $\text{ID}^{70a,70b}$, H.M. Gray ID^{18a} , M. Greco ID^{112} , M.J. Green ID^1 , C. Grefe ID^{25} , A.S. Grefsrud ID^{17} , I.M. Gregor ID^{48} , K.T. Greif ID^{165} , P. Grenier ID^{149} , S.G. Grewe ID^{112} , A.A. Grillo ID^{139} , K. Grimm ID^{32} , S. Grinstein $\text{ID}^{13,x}$, J.-F. Grivaz ID^{66} ,

E. Gross [ID¹⁷⁵](#), J. Grosse-Knetter [ID⁵⁵](#), L. Guan [ID¹⁰⁸](#), G. Guerrieri [ID³⁷](#), R. Guevara [ID¹²⁸](#), R. Gugel [ID¹⁰²](#), J.A.M. Guhit [ID¹⁰⁸](#), A. Guida [ID¹⁹](#), E. Guilloton [ID¹⁷³](#), S. Guindon [ID³⁷](#), F. Guo [ID^{14,114c}](#), J. Guo [ID^{144a}](#), L. Guo [ID⁴⁸](#), L. Guo [ID^{114b,v}](#), Y. Guo [ID¹⁰⁸](#), A. Gupta [ID⁴⁹](#), R. Gupta [ID¹³²](#), S. Gupta [ID²⁷](#), S. Gurbuz [ID²⁵](#), S.S. Gurdasani [ID⁴⁸](#), G. Gustavino [ID^{75a,75b}](#), P. Gutierrez [ID¹²³](#), L.F. Gutierrez Zagazeta [ID¹³¹](#), M. Gutsche [ID⁵⁰](#), C. Gutschow [ID⁹⁸](#), C. Gwenlan [ID¹²⁹](#), C.B. Gwilliam [ID⁹⁴](#), E.S. Haaland [ID¹²⁸](#), A. Haas [ID¹²⁰](#), M. Habedank [ID⁵⁹](#), C. Haber [ID^{18a}](#), H.K. Hadavand [ID⁸](#), A. Haddad [ID⁴¹](#), A. Hadef [ID⁵⁰](#), A.I. Hagan [ID⁹³](#), J.J. Hahn [ID¹⁴⁷](#), E.H. Haines [ID⁹⁸](#), M. Haleem [ID¹⁷²](#), J. Haley [ID¹²⁴](#), G.D. Hallewell [ID¹⁰⁴](#), K. Hamano [ID¹⁷¹](#), H. Hamdaoui [ID¹⁶⁷](#), M. Hamer [ID²⁵](#), S.E.D. Hammoud [ID⁶⁶](#), E.J. Hampshire [ID⁹⁷](#), J. Han [ID^{143a}](#), L. Han [ID^{114a}](#), L. Han [ID⁶²](#), S. Han [ID¹⁴](#), K. Hanagaki [ID⁸⁴](#), M. Hance [ID¹³⁹](#), D.A. Hangal [ID⁴²](#), H. Hanif [ID¹⁴⁸](#), M.D. Hank [ID¹³¹](#), J.B. Hansen [ID⁴³](#), P.H. Hansen [ID⁴³](#), D. Harada [ID⁵⁶](#), T. Harenberg [ID¹⁷⁷](#), S. Harkusha [ID¹⁷⁹](#), M.L. Harris [ID¹⁰⁵](#), Y.T. Harris [ID²⁵](#), J. Harrison [ID¹³](#), N.M. Harrison [ID¹²²](#), P.F. Harrison [ID¹⁷³](#), M.L.E. Hart [ID⁹⁸](#), N.M. Hartman [ID¹¹²](#), N.M. Hartmann [ID¹¹¹](#), R.Z. Hasan [ID^{97,137}](#), Y. Hasegawa [ID¹⁴⁶](#), F. Haslbeck [ID¹²⁹](#), S. Hassan [ID¹⁷](#), R. Hauser [ID¹⁰⁹](#), M. Havichernik [ID¹³⁶](#), C.M. Hawkes [ID²¹](#), R.J. Hawkings [ID³⁷](#), Y. Hayashi [ID¹⁵⁹](#), D. Hayden [ID¹⁰⁹](#), C. Hayes [ID¹⁰⁸](#), R.L. Hayes [ID¹¹⁷](#), C.P. Hays [ID¹²⁹](#), J.M. Hays [ID⁹⁶](#), H.S. Hayward [ID⁹⁴](#), M. He [ID^{14,114c}](#), Y. He [ID⁴⁸](#), Y. He [ID⁹⁸](#), N.B. Heatley [ID⁹⁶](#), V. Hedberg [ID¹⁰⁰](#), C. Heidegger [ID⁵⁴](#), K.K. Heidegger [ID⁵⁴](#), J. Heilman [ID³⁵](#), S. Heim [ID⁴⁸](#), T. Heim [ID^{18a}](#), J.G. Heinlein [ID¹³¹](#), J.J. Heinrich [ID¹²⁶](#), L. Heinrich [ID¹¹²](#), J. Hejbal [ID¹³⁴](#), M. Helbig [ID⁵⁰](#), A. Held [ID¹⁷⁶](#), S. Hellesund [ID¹⁷](#), C.M. Hellling [ID¹⁷⁰](#), S. Hellman [ID^{47a,47b}](#), A.M. Henriques Correia [ID³⁷](#), H. Herde [ID¹⁰⁰](#), Y. Hernández Jiménez [ID¹⁵¹](#), L.M. Herrmann [ID²⁵](#), T. Herrmann [ID⁵⁰](#), G. Herten [ID⁵⁴](#), R. Hertenberger [ID¹¹¹](#), L. Hervas [ID³⁷](#), M.E. Hesping [ID¹⁰²](#), N.P. Hessey [ID^{162a}](#), J. Hessler [ID¹¹²](#), M. Hidaoui [ID^{36b}](#), N. Hidic [ID¹³⁶](#), E. Hill [ID¹⁶¹](#), T.S. Hillersoy [ID¹⁷](#), S.J. Hillier [ID²¹](#), J.R. Hinds [ID¹⁰⁹](#), F. Hinterkeuser [ID²⁵](#), M. Hirose [ID¹²⁷](#), S. Hirose [ID¹⁶³](#), D. Hirschbuehl [ID¹⁷⁷](#), T.G. Hitchings [ID¹⁰³](#), B. Hiti [ID⁹⁵](#), J. Hobbs [ID¹⁵¹](#), R. Hobincu [ID^{28e}](#), N. Hod [ID¹⁷⁵](#), A.M. Hodges [ID¹⁶⁸](#), M.C. Hodgkinson [ID¹⁴⁵](#), B.H. Hodgkinson [ID¹²⁹](#), A. Hoecker [ID³⁷](#), D.D. Hofer [ID¹⁰⁸](#), J. Hofer [ID¹⁶⁹](#), M. Holzbock [ID³⁷](#), L.B.A.H. Hommels [ID³³](#), V. Homsak [ID¹²⁹](#), B.P. Honan [ID¹⁰³](#), J.J. Hong [ID⁶⁸](#), T.M. Hong [ID¹³²](#), B.H. Hooberman [ID¹⁶⁸](#), W.H. Hopkins [ID⁶](#), M.C. Hoppesch [ID¹⁶⁸](#), Y. Horii [ID¹¹³](#), M.E. Horstmann [ID¹¹²](#), S. Hou [ID¹⁵⁴](#), M.R. Housenga [ID¹⁶⁸](#), J. Howarth [ID⁵⁹](#), J. Hoya [ID⁶](#), M. Hrabovsky [ID¹²⁵](#), T. Hrynn'ova [ID⁴](#), P.J. Hsu [ID⁶⁵](#), S.-C. Hsu [ID¹⁴²](#), T. Hsu [ID⁶⁶](#), M. Hu [ID^{18a}](#), Q. Hu [ID⁶²](#), S. Huang [ID³³](#), X. Huang [ID^{14,114c}](#), Y. Huang [ID¹³⁶](#), Y. Huang [ID^{114b}](#), Y. Huang [ID¹⁰²](#), Y. Huang [ID¹⁴](#), Z. Huang [ID⁶⁶](#), Z. Hubacek [ID¹³⁵](#), M. Huebner [ID²⁵](#), F. Huegging [ID²⁵](#), T.B. Huffman [ID¹²⁹](#), M. Hufnagel Maranha De Faria [ID^{83a}](#), C.A. Hugli [ID⁴⁸](#), M. Huhtinen [ID³⁷](#), S.K. Huiberts [ID¹⁷](#), R. Hulskens [ID¹⁰⁶](#), C.E. Hultquist [ID^{18a}](#), D.L. Humphreys [ID¹⁰⁵](#), N. Huseynov [ID¹²](#), J. Huston [ID¹⁰⁹](#), J. Huth [ID⁶¹](#), R. Hyneman [ID⁷](#), G. Iacobucci [ID⁵⁶](#), G. Iakovidis [ID³⁰](#), L. Iconomidou-Fayard [ID⁶⁶](#), J.P. Iddon [ID³⁷](#), P. Iengo [ID^{72a,72b}](#), R. Iguchi [ID¹⁵⁹](#), Y. Iiyama [ID¹⁵⁹](#), T. Iizawa [ID¹⁵⁹](#), Y. Ikegami [ID⁸⁴](#), D. Iliadis [ID¹⁵⁸](#), N. Ilic [ID¹⁶¹](#), H. Imam [ID^{36a}](#), G. Inacio Goncalves [ID^{83d}](#), S.A. Infante Cabanas [ID^{140c}](#), T. Ingebretsen Carlson [ID^{47a,47b}](#), J.M. Inglis [ID⁹⁶](#), G. Introzzi [ID^{73a,73b}](#), M. Iodice [ID^{77a}](#), V. Ippolito [ID^{75a,75b}](#), R.K. Irwin [ID⁹⁴](#), M. Ishino [ID¹⁵⁹](#), W. Islam [ID¹⁷⁶](#), C. Issever [ID¹⁹](#), S. Istin [ID^{22a,am}](#), K. Itabashi [ID⁸⁴](#), H. Ito [ID¹⁷⁴](#), R. Iuppa [ID^{78a,78b}](#), A. Ivina [ID¹⁷⁵](#), V. Izzo [ID^{72a}](#), P. Jacka [ID¹³⁵](#), P. Jackson [ID¹](#), P. Jain [ID⁴⁸](#), K. Jakobs [ID⁵⁴](#), T. Jakoubek [ID¹⁷⁵](#), J. Jamieson [ID⁵⁹](#), W. Jang [ID¹⁵⁹](#), S. Jankovych [ID¹³⁶](#), M. Javurkova [ID¹⁰⁵](#), P. Jawahar [ID¹⁰³](#), L. Jeanty [ID¹²⁶](#), J. Jejelava [ID^{155a,ae}](#), P. Jenni [ID^{54,f}](#), C.E. Jessiman [ID³⁵](#), C. Jia [ID^{143a}](#), H. Jia [ID¹⁷⁰](#), J. Jia [ID¹⁵¹](#), X. Jia [ID^{112,114c}](#), Z. Jia [ID^{114a}](#), C. Jiang [ID⁵²](#), Q. Jiang [ID^{64b}](#), S. Jiggins [ID⁴⁸](#), M. Jimenez Ortega [ID¹⁶⁹](#), J. Jimenez Pena [ID¹³](#), S. Jin [ID^{114a}](#), A. Jinaru [ID^{28b}](#), O. Jinnouchi [ID¹⁴¹](#), P. Johansson [ID¹⁴⁵](#), K.A. Johns [ID⁷](#), J.W. Johnson [ID¹³⁹](#), F.A. Jolly [ID⁴⁸](#), D.M. Jones [ID¹⁵²](#), E. Jones [ID⁴⁸](#), K.S. Jones [ID⁸](#), P. Jones [ID³³](#), R.W.L. Jones [ID⁹³](#), T.J. Jones [ID⁹⁴](#), H.L. Joos [ID⁵⁵](#), R. Joshi [ID¹²²](#), J. Jovicevic [ID¹⁶](#), X. Ju [ID^{18a}](#), J.J. Junggeburth [ID³⁷](#), T. Junkermann [ID^{63a}](#), A. Juste Rozas [ID^{13,x}](#), M.K. Juzek [ID⁸⁷](#), S. Kabana [ID^{140f}](#), A. Kaczmarska [ID⁸⁷](#), S.A. Kadir [ID¹⁴⁹](#), M. Kado [ID¹¹²](#), H. Kagan [ID¹²²](#), M. Kagan [ID¹⁴⁹](#), A. Kahn [ID¹³¹](#), C. Kahra [ID¹⁰²](#), T. Kaji [ID¹⁵⁹](#), E. Kajomovitz [ID¹⁵⁶](#), N. Kakati [ID¹⁷⁵](#),

N. Kakoty [ID¹³](#), I. Kalaitzidou [ID⁵⁴](#), S. Kandel [ID⁸](#), N.J. Kang [ID¹³⁹](#), D. Kar [ID^{34h}](#), E. Karentzos [ID²⁵](#), O. Karkout [ID¹¹⁷](#), S.N. Karpov [ID³⁹](#), Z.M. Karpova [ID³⁹](#), V. Kartvelishvili [ID⁹³](#), A.N. Karyukhin [ID³⁸](#), E. Kasimi [ID¹⁵⁸](#), J. Katzy [ID⁴⁸](#), S. Kaur [ID³⁵](#), K. Kawade [ID¹⁴⁶](#), M.P. Kawale [ID¹²³](#), C. Kawamoto [ID⁸⁹](#), T. Kawamoto [ID⁶²](#), E.F. Kay [ID³⁷](#), F.I. Kaya [ID¹⁶⁴](#), S. Kazakos [ID¹⁰⁹](#), V.F. Kazanin [ID³⁸](#), J.M. Keaveney [ID^{34a}](#), R. Keeler [ID¹⁷¹](#), G.V. Kehris [ID⁶¹](#), J.S. Keller [ID³⁵](#), J.M. Kelly [ID¹⁷¹](#), J.J. Kempster [ID¹⁵²](#), O. Kepka [ID¹³⁴](#), J. Kerr [ID^{162b}](#), B.P. Kerridge [ID¹³⁷](#), B.P. Kerševan [ID⁹⁵](#), L. Keszeghova [ID^{29a}](#), R.A. Khan [ID¹³²](#), A. Khanov [ID¹²⁴](#), A.G. Kharlamov [ID³⁸](#), T. Kharlamova [ID³⁸](#), E.E. Khoda [ID¹⁴²](#), M. Kholodenko [ID^{133a}](#), T.J. Khoo [ID¹⁹](#), G. Khoriauli [ID¹⁷²](#), Y. Khoulaki [ID^{36a}](#), J. Khubua [ID^{155b,*}](#), Y.A.R. Khwaira [ID¹³⁰](#), B. Kibirige [ID^{34h}](#), D. Kim [ID⁶](#), D.W. Kim [ID^{47a,47b}](#), Y.K. Kim [ID⁴⁰](#), N. Kimura [ID⁹⁸](#), M.K. Kingston [ID⁵⁵](#), A. Kirchhoff [ID⁵⁵](#), C. Kirlfel [ID²⁵](#), F. Kirfel [ID²⁵](#), J. Kirk [ID¹³⁷](#), A.E. Kiryunin [ID¹¹²](#), S. Kita [ID¹⁶³](#), O. Kivernyk [ID²⁵](#), M. Klassen [ID¹⁶⁴](#), C. Klein [ID³⁵](#), L. Klein [ID¹⁷²](#), M.H. Klein [ID⁴⁵](#), S.B. Klein [ID⁵⁶](#), U. Klein [ID⁹⁴](#), A. Klimentov [ID³⁰](#), T. Klioutchnikova [ID³⁷](#), P. Kluit [ID¹¹⁷](#), S. Kluth [ID¹¹²](#), E. Kneringer [ID⁷⁹](#), T.M. Knight [ID¹⁶¹](#), A. Knue [ID⁴⁹](#), M. Kobel [ID⁵⁰](#), D. Kobylanskii [ID¹⁷⁵](#), S.F. Koch [ID¹²⁹](#), M. Kocian [ID¹⁴⁹](#), P. Kodyš [ID¹³⁶](#), D.M. Koeck [ID¹²⁶](#), T. Koffas [ID³⁵](#), O. Kolay [ID⁵⁰](#), I. Koletsou [ID⁴](#), T. Komarek [ID⁸⁷](#), K. Köneke [ID⁵⁵](#), A.X.Y. Kong [ID¹](#), T. Kono [ID¹²¹](#), N. Konstantinidis [ID⁹⁸](#), P. Kontaxakis [ID⁵⁶](#), B. Konya [ID¹⁰⁰](#), R. Kopeliansky [ID⁴²](#), S. Koperny [ID^{86a}](#), K. Korcyl [ID⁸⁷](#), K. Kordas [ID^{158,d}](#), A. Korn [ID⁹⁸](#), S. Korn [ID⁵⁵](#), I. Korolkov [ID¹³](#), N. Korotkova [ID³⁸](#), B. Kortman [ID¹¹⁷](#), O. Kortner [ID¹¹²](#), S. Kortner [ID¹¹²](#), W.H. Kostecka [ID¹¹⁸](#), M. Kostov [ID^{29a}](#), V.V. Kostyukhin [ID¹⁴⁷](#), A. Kotsokechagia [ID³⁷](#), A. Kotwal [ID⁵¹](#), A. Koulouris [ID³⁷](#), A. Kourkoumeli-Charalampidi [ID^{73a,73b}](#), C. Kourkoumelis [ID⁹](#), E. Kourlitis [ID¹¹²](#), O. Kovanda [ID¹²⁶](#), R. Kowalewski [ID¹⁷¹](#), W. Kozanecki [ID¹²⁶](#), A.S. Kozhin [ID³⁸](#), V.A. Kramarenko [ID³⁸](#), G. Kramberger [ID⁹⁵](#), P. Kramer [ID²⁵](#), M.W. Krasny [ID¹³⁰](#), A. Krasznahorkay [ID¹⁰⁵](#), A.C. Kraus [ID¹¹⁸](#), J.W. Kraus [ID¹⁷⁷](#), J.A. Kremer [ID⁴⁸](#), N.B. Krengel [ID¹⁴⁷](#), T. Kresse [ID⁵⁰](#), L. Kretschmann [ID¹⁷⁷](#), J. Kretzschmar [ID⁹⁴](#), P. Krieger [ID¹⁶¹](#), K. Krizka [ID²¹](#), K. Kroeninger [ID⁴⁹](#), H. Kroha [ID¹¹²](#), J. Kroll [ID¹³⁴](#), J. Kroll [ID¹³¹](#), K.S. Krowpman [ID¹⁰⁹](#), U. Kruchonak [ID³⁹](#), H. Krüger [ID²⁵](#), N. Krumnack ⁸¹, M.C. Kruse [ID⁵¹](#), O. Kuchinskaia [ID³⁹](#), S. Kuday [ID^{3a}](#), S. Kuehn [ID³⁷](#), R. Kuesters [ID⁵⁴](#), T. Kuhl [ID⁴⁸](#), V. Kukhtin [ID³⁹](#), Y. Kulchitsky [ID³⁹](#), S. Kuleshov [ID^{140d,140b}](#), J. Kull [ID¹](#), E.V. Kumar [ID¹¹¹](#), M. Kumar [ID^{34h}](#), N. Kumar [ID⁴⁸](#), P. Kumari [ID^{162b}](#), A. Kupco [ID¹³⁴](#), T. Kupfer ⁴⁹, A. Kupich [ID³⁸](#), O. Kuprash [ID⁵⁴](#), H. Kurashige [ID⁸⁵](#), L.L. Kurchaninov [ID^{162a}](#), O. Kurdysh [ID⁴](#), Y.A. Kurochkin [ID³⁸](#), A. Kurova [ID³⁸](#), M. Kuze [ID¹⁴¹](#), A.K. Kvam [ID¹⁰⁵](#), J. Kvita [ID¹²⁵](#), N.G. Kyriacou [ID¹⁰⁸](#), C. Lacasta [ID¹⁶⁹](#), F. Lacava [ID^{75a,75b}](#), H. Lacker [ID¹⁹](#), D. Lacour [ID¹³⁰](#), N.N. Lad [ID⁹⁸](#), E. Ladygin [ID³⁹](#), A. Lafarge [ID⁴¹](#), B. Laforge [ID¹³⁰](#), T. Lagouri [ID¹⁷⁸](#), F.Z. Lahbabí [ID^{36a}](#), S. Lai [ID⁵⁵](#), W.S. Lai [ID⁹⁸](#), J.E. Lambert [ID¹⁷¹](#), S. Lammers [ID⁶⁸](#), W. Lampl [ID⁷](#), C. Lampoudis [ID^{158,d}](#), G. Lamprinoudis [ID¹⁰²](#), A.N. Lancaster [ID¹¹⁸](#), E. Lançon [ID³⁰](#), U. Landgraf [ID⁵⁴](#), M.P.J. Landon [ID⁹⁶](#), V.S. Lang [ID⁵⁴](#), O.K.B. Langrekken [ID¹²⁸](#), A.J. Lankford [ID¹⁶⁵](#), F. Lanni [ID³⁷](#), K. Lantzsch [ID²⁵](#), A. Lanza [ID^{73a}](#), M. Lanzac Berrocal [ID¹⁶⁹](#), J.F. Laporte [ID¹³⁸](#), T. Lari [ID^{71a}](#), D. Larsen [ID¹⁷](#), L. Larson [ID¹¹](#), F. Lasagni Manghi [ID^{24b}](#), M. Lassnig [ID³⁷](#), S.D. Lawlor [ID¹⁴⁵](#), R. Lazaridou ¹⁶⁵, M. Lazzaroni [ID^{71a,71b}](#), H.D.M. Le [ID¹⁰⁹](#), E.M. Le Boulicaut [ID¹⁷⁸](#), L.T. Le Pottier [ID^{18a}](#), B. Leban [ID^{24b,24a}](#), F. Ledroit-Guillon [ID⁶⁰](#), T.F. Lee [ID^{162b}](#), L.L. Leeuw [ID^{34c}](#), M. Lefebvre [ID¹⁷¹](#), C. Leggett [ID^{18a}](#), G. Lehmann Miotto [ID³⁷](#), M. Leigh [ID⁵⁶](#), W.A. Leight [ID¹⁰⁵](#), W. Leinonen [ID¹¹⁶](#), A. Leisos [ID^{158,u}](#), M.A.L. Leite [ID^{83c}](#), C.E. Leitgeb [ID¹⁹](#), R. Leitner [ID¹³⁶](#), K.J.C. Leney [ID⁴⁵](#), T. Lenz [ID²⁵](#), S. Leone [ID^{74a}](#), C. Leonidopoulos [ID⁵²](#), A. Leopold [ID¹⁵⁰](#), J.H. Lepage Bourbonnais [ID³⁵](#), R. Les [ID¹⁰⁹](#), C.G. Lester [ID³³](#), M. Levchenko [ID³⁸](#), J. Levêque [ID⁴](#), L.J. Levinson [ID¹⁷⁵](#), G. Levrini [ID^{24b,24a}](#), M.P. Lewicki [ID⁸⁷](#), C. Lewis [ID¹⁴²](#), D.J. Lewis [ID⁴](#), L. Lewitt [ID¹⁴⁵](#), A. Li [ID³⁰](#), B. Li [ID^{143a}](#), C. Li [ID¹⁰⁸](#), C-Q. Li [ID¹¹²](#), H. Li [ID^{143a}](#), H. Li [ID¹⁰³](#), H. Li [ID¹⁵](#), H. Li [ID⁶²](#), H. Li [ID^{143a}](#), J. Li [ID^{144a}](#), K. Li [ID¹⁴](#), L. Li [ID^{144a}](#), R. Li [ID¹⁷⁸](#), S. Li [ID^{14,114c}](#), S. Li [ID^{144b,144a}](#), T. Li [ID⁵](#), X. Li [ID¹⁰⁶](#), Z. Li [ID¹⁵⁹](#), Z. Li [ID^{14,114c}](#), Z. Li [ID⁶²](#), S. Liang [ID^{14,114c}](#), Z. Liang [ID¹⁴](#), M. Liberatore [ID¹³⁸](#), B. Liberti [ID^{76a}](#), K. Lie [ID^{64c}](#), J. Lieber Marin [ID^{83e}](#), H. Lien [ID⁶⁸](#), H. Lin [ID¹⁰⁸](#), S.F. Lin [ID¹⁵¹](#), L. Linden [ID¹¹¹](#), R.E. Lindley [ID⁷](#), J.H. Lindon [ID³⁷](#), J. Ling [ID⁶¹](#), E. Lipeles [ID¹³¹](#), A. Lipniacka [ID¹⁷](#), A. Lister [ID¹⁷⁰](#), J.D. Little [ID⁶⁸](#), B. Liu [ID¹⁴](#), B.X. Liu [ID^{114b}](#), D. Liu [ID^{144b,144a}](#),

D. Liu [ID¹³⁹](#), E.H.L. Liu [ID²¹](#), J.K.K. Liu [ID¹²⁰](#), K. Liu [ID^{144b}](#), K. Liu [ID^{144b,144a}](#), M. Liu [ID⁶²](#), M.Y. Liu [ID⁶²](#), P. Liu [ID¹⁴](#), Q. Liu [ID^{144b,142,144a}](#), X. Liu [ID⁶²](#), X. Liu [ID^{143a}](#), Y. Liu [ID^{114b,114c}](#), Y.L. Liu [ID^{143a}](#), Y.W. Liu [ID⁶²](#), Z. Liu [ID^{66,k}](#), S.L. Lloyd [ID⁹⁶](#), E.M. Lobodzinska [ID⁴⁸](#), P. Loch [ID⁷](#), E. Lodhi [ID¹⁶¹](#), K. Lohwasser [ID¹⁴⁵](#), E. Loiacono [ID⁴⁸](#), J.D. Lomas [ID²¹](#), J.D. Long [ID⁴²](#), I. Longarini [ID¹⁶⁵](#), R. Longo [ID¹⁶⁸](#), A. Lopez Solis [ID¹³](#), N.A. Lopez-canelas [ID⁷](#), N. Lorenzo Martinez [ID⁴](#), A.M. Lory [ID¹¹¹](#), M. Losada [ID^{119a}](#), G. Löschecke Centeno [ID¹⁵²](#), X. Lou [ID^{47a,47b}](#), X. Lou [ID^{14,114c}](#), A. Lounis [ID⁶⁶](#), P.A. Love [ID⁹³](#), M. Lu [ID⁶⁶](#), S. Lu [ID¹³¹](#), Y.J. Lu [ID¹⁵⁴](#), H.J. Lubatti [ID¹⁴²](#), C. Luci [ID^{75a,75b}](#), F.L. Lucio Alves [ID^{114a}](#), F. Luehring [ID⁶⁸](#), B.S. Lunday [ID¹³¹](#), O. Lundberg [ID¹⁵⁰](#), J. Lunde [ID³⁷](#), N.A. Luongo [ID⁶](#), M.S. Lutz [ID³⁷](#), A.B. Lux [ID²⁶](#), D. Lynn [ID³⁰](#), R. Lysak [ID¹³⁴](#), V. Lysenko [ID¹³⁵](#), E. Lytken [ID¹⁰⁰](#), V. Lyubushkin [ID³⁹](#), T. Lyubushkina [ID³⁹](#), M.M. Lyukova [ID¹⁵¹](#), M.Firdaus M. Soberi [ID⁵²](#), H. Ma [ID³⁰](#), K. Ma [ID⁶²](#), L.L. Ma [ID^{143a}](#), W. Ma [ID⁶²](#), Y. Ma [ID¹²⁴](#), J.C. MacDonald [ID¹⁰²](#), P.C. Machado De Abreu Farias [ID^{83e}](#), R. Madar [ID⁴¹](#), T. Madula [ID⁹⁸](#), J. Maeda [ID⁸⁵](#), S. Maeland [ID¹⁷](#), T. Maeno [ID³⁰](#), P.T. Mafa [ID^{34c,j}](#), H. Maguire [ID¹⁴⁵](#), M. Maheshwari [ID³³](#), V. Maiboroda [ID⁶⁶](#), A. Maio [ID^{133a,133b,133d}](#), K. Maj [ID^{86a}](#), O. Majersky [ID⁴⁸](#), S. Majewski [ID¹²⁶](#), R. Makhmanazarov [ID³⁸](#), N. Makovec [ID⁶⁶](#), V. Maksimovic [ID¹⁶](#), B. Malaescu [ID¹³⁰](#), J. Malamant [ID¹²⁸](#), Pa. Malecki [ID⁸⁷](#), V.P. Maleev [ID³⁸](#), F. Malek [ID^{60,o}](#), M. Mali [ID⁹⁵](#), D. Malito [ID⁹⁷](#), U. Mallik [ID^{80,*}](#), A. Maloizel [ID⁵](#), S. Maltezos [ID¹⁰](#), A. Malvezzi Lopes [ID^{83d}](#), S. Malyukov [ID³⁹](#), J. Mamuzic [ID⁹⁵](#), G. Mancini [ID⁵³](#), M.N. Mancini [ID²⁷](#), G. Manco [ID^{73a,73b}](#), J.P. Mandalia [ID⁹⁶](#), S.S. Mandarry [ID¹⁵²](#), I. Mandić [ID⁹⁵](#), L. Manhaes de Andrade Filho [ID^{83a}](#), I.M. Maniatis [ID¹⁷⁵](#), J. Manjarres Ramos [ID⁹¹](#), D.C. Mankad [ID¹⁷⁵](#), A. Mann [ID¹¹¹](#), T. Manoussos [ID³⁷](#), M.N. Mantinan [ID⁴⁰](#), S. Manzoni [ID³⁷](#), L. Mao [ID^{144a}](#), X. Mapekula [ID^{34c}](#), A. Marantis [ID¹⁵⁸](#), R.R. Marcelo Gregorio [ID⁹⁶](#), G. Marchiori [ID⁵](#), C. Marcon [ID^{71a}](#), E. Maricic [ID¹³⁸](#), M. Marinescu [ID⁴⁸](#), S. Marium [ID⁴⁸](#), M. Marjanovic [ID¹²³](#), A. Markhoos [ID⁵⁴](#), M. Markovitch [ID⁶⁶](#), M.K. Maroun [ID¹⁰⁵](#), M.C. Marr [ID¹⁴⁸](#), G.T. Marsden [ID¹⁰³](#), E.J. Marshall [ID⁹³](#), Z. Marshall [ID^{18a}](#), S. Marti-Garcia [ID¹⁶⁹](#), J. Martin [ID⁹⁸](#), T.A. Martin [ID¹³⁷](#), V.J. Martin [ID⁵²](#), B. Martin dit Latour [ID¹⁷](#), L. Martinelli [ID^{75a,75b}](#), M. Martinez [ID^{13,x}](#), P. Martinez Agullo [ID¹⁶⁹](#), V.I. Martinez Outschoorn [ID¹⁰⁵](#), P. Martinez Suarez [ID³⁷](#), S. Martin-Haugh [ID¹³⁷](#), G. Martinovicova [ID¹³⁶](#), V.S. Martoiu [ID^{28b}](#), A.C. Martyniuk [ID⁹⁸](#), A. Marzin [ID³⁷](#), D. Mascione [ID^{78a,78b}](#), L. Masetti [ID¹⁰²](#), J. Maslik [ID¹⁰³](#), A.L. Maslennikov [ID³⁹](#), S.L. Mason [ID⁴²](#), P. Massarotti [ID^{72a,72b}](#), P. Mastrandrea [ID^{74a,74b}](#), A. Mastroberardino [ID^{44b,44a}](#), T. Masubuchi [ID¹²⁷](#), T.T. Mathew [ID¹²⁶](#), J. Matousek [ID¹³⁶](#), D.M. Mattern [ID⁴⁹](#), J. Maurer [ID^{28b}](#), T. Maurin [ID⁵⁹](#), A.J. Maury [ID⁶⁶](#), B. Maček [ID⁹⁵](#), C. Mavungu Tsava [ID¹⁰⁴](#), D.A. Maximov [ID³⁸](#), A.E. May [ID¹⁰³](#), E. Mayer [ID⁴¹](#), R. Mazini [ID^{34h}](#), I. Maznas [ID¹¹⁸](#), S.M. Mazza [ID¹³⁹](#), E. Mazzeo [ID³⁷](#), J.P. Mc Gowan [ID¹⁷¹](#), S.P. Mc Kee [ID¹⁰⁸](#), C.A. Mc Lean [ID⁶](#), C.C. McCracken [ID¹⁷⁰](#), E.F. McDonald [ID¹⁰⁷](#), A.E. McDougall [ID¹¹⁷](#), L.F. McElhinney [ID⁹³](#), J.A. Mcfayden [ID¹⁵²](#), R.P. McGovern [ID¹³¹](#), R.P. Mckenzie [ID^{34h}](#), T.C. McLachlan [ID⁴⁸](#), D.J. McLaughlin [ID⁹⁸](#), S.J. McMahon [ID¹³⁷](#), C.M. Mcpartland [ID⁹⁴](#), R.A. McPherson [ID^{171,ab}](#), S. Mehlhase [ID¹¹¹](#), A. Mehta [ID⁹⁴](#), D. Melini [ID¹⁶⁹](#), B.R. Mellado Garcia [ID^{34h}](#), A.H. Melo [ID⁵⁵](#), F. Meloni [ID⁴⁸](#), A.M. Mendes Jacques Da Costa [ID¹⁰³](#), L. Meng [ID⁹³](#), S. Menke [ID¹¹²](#), M. Mentink [ID³⁷](#), E. Meoni [ID^{44b,44a}](#), G. Mercado [ID¹¹⁸](#), S. Merianos [ID¹⁵⁸](#), C. Merlassino [ID^{69a,69c}](#), C. Meroni [ID^{71a,71b}](#), J. Metcalfe [ID⁶](#), A.S. Mete [ID⁶](#), E. Meuser [ID¹⁰²](#), C. Meyer [ID⁶⁸](#), J-P. Meyer [ID¹³⁸](#), Y. Miao [ID^{114a}](#), R.P. Middleton [ID¹³⁷](#), M. Mihovilovic [ID⁶⁶](#), L. Mijović [ID⁵²](#), G. Mikenberg [ID¹⁷⁵](#), M. Mikesikova [ID¹³⁴](#), M. Mikuž [ID⁹⁵](#), H. Mildner [ID¹⁰²](#), A. Milic [ID³⁷](#), D.W. Miller [ID⁴⁰](#), E.H. Miller [ID¹⁴⁹](#), A. Milov [ID¹⁷⁵](#), D.A. Milstead [ID^{47a,47b}](#), T. Min [ID^{114a}](#), A.A. Minaenko [ID³⁸](#), I.A. Minashvili [ID^{155b}](#), A.I. Mincer [ID¹²⁰](#), B. Mindur [ID^{86a}](#), M. Mineev [ID³⁹](#), Y. Mino [ID⁸⁹](#), L.M. Mir [ID¹³](#), M. Miralles Lopez [ID⁵⁹](#), M. Mironova [ID^{18a}](#), M.C. Missio [ID¹¹⁶](#), A. Mitra [ID¹⁷³](#), V.A. Mitsou [ID¹⁶⁹](#), Y. Mitsumori [ID¹¹³](#), O. Miu [ID¹⁶¹](#), P.S. Miyagawa [ID⁹⁶](#), T. Mkrtchyan [ID^{63a}](#), M. Mlinarevic [ID⁹⁸](#), T. Mlinarevic [ID⁹⁸](#), M. Mlynarikova [ID¹³⁶](#), S. Mobius [ID²⁰](#), M.H. Mohamed Farook [ID¹¹⁵](#), S. Mohapatra [ID⁴²](#), S. Mohiuddin [ID¹²⁴](#), G. Mokgatitswane [ID^{34h}](#), L. Moleri [ID¹⁷⁵](#), U. Molinatti [ID¹²⁹](#), L.G. Mollier [ID²⁰](#), B. Mondal [ID¹³⁴](#), S. Mondal [ID¹³⁵](#), K. Mönig [ID⁴⁸](#), E. Monnier [ID¹⁰⁴](#), L. Monsonis Romero [ID¹⁶⁹](#), J. Montejo Berlingen [ID¹³](#), A. Montella [ID^{47a,47b}](#), M. Montella [ID¹²²](#), F. Montereali [ID^{77a,77b}](#),

F. Monticelli [ID⁹²](#), S. Monzani [ID^{69a,69c}](#), A. Morancho Tarda [ID⁴³](#), N. Morange [ID⁶⁶](#),
 A.L. Moreira De Carvalho [ID⁴⁸](#), M. Moreno Llácer [ID¹⁶⁹](#), C. Moreno Martinez [ID⁵⁶](#), J.M. Moreno Perez^{23b},
 P. Morettini [ID^{57b}](#), S. Morgenstern [ID³⁷](#), M. Morii [ID⁶¹](#), M. Morinaga [ID¹⁵⁹](#), M. Moritsu [ID⁹⁰](#),
 F. Morodei [ID^{75a,75b}](#), P. Moschovakos [ID³⁷](#), B. Moser [ID⁵⁴](#), M. Mosidze [ID^{155b}](#), T. Moskalets [ID⁴⁵](#),
 P. Moskvitina [ID¹¹⁶](#), J. Moss [ID³²](#), P. Moszkowicz [ID^{86a}](#), A. Moussa [ID^{36d}](#), Y. Moyal [ID¹⁷⁵](#),
 H. Moyano Gomez [ID¹³](#), E.J.W. Moyse [ID¹⁰⁵](#), T.G. Mroz [ID⁸⁷](#), O. Mtintsilana [ID^{34h}](#), S. Muanza [ID¹⁰⁴](#),
 M. Mucha²⁵, J. Mueller [ID¹³²](#), R. Müller [ID³⁷](#), G.A. Mullier [ID¹⁶⁷](#), A.J. Mullin³³, J.J. Mullin⁵¹,
 A.C. Mullins⁴⁵, A.E. Mulski [ID⁶¹](#), D.P. Mungo [ID¹⁶¹](#), D. Munoz Perez [ID¹⁶⁹](#), F.J. Munoz Sanchez [ID¹⁰³](#),
 W.J. Murray [ID^{173,137}](#), M. Muškinja [ID⁹⁵](#), C. Mwewa [ID⁴⁸](#), A.G. Myagkov [ID^{38,a}](#), A.J. Myers [ID⁸](#),
 G. Myers [ID¹⁰⁸](#), M. Myska [ID¹³⁵](#), B.P. Nachman [ID^{18a}](#), K. Nagai [ID¹²⁹](#), K. Nagano [ID⁸⁴](#), R. Nagasaka¹⁵⁹,
 J.L. Nagle [ID^{30,aj}](#), E. Nagy [ID¹⁰⁴](#), A.M. Nairz [ID³⁷](#), Y. Nakahama [ID⁸⁴](#), K. Nakamura [ID⁸⁴](#), K. Nakkalil [ID⁵](#),
 A. Nandi [ID^{63b}](#), H. Nanjo [ID¹²⁷](#), E.A. Narayanan [ID⁴⁵](#), Y. Narukawa [ID¹⁵⁹](#), I. Naryshkin [ID³⁸](#),
 L. Nasella [ID^{71a,71b}](#), S. Nasri [ID^{119b}](#), C. Nass [ID²⁵](#), G. Navarro [ID^{23a}](#), J. Navarro-Gonzalez [ID¹⁶⁹](#),
 A. Nayaz [ID¹⁹](#), P.Y. Nechaeva [ID³⁸](#), S. Nechaeva [ID^{24b,24a}](#), F. Nechansky [ID¹³⁴](#), L. Nedic [ID¹²⁹](#), T.J. Neep [ID²¹](#),
 A. Negri [ID^{73a,73b}](#), M. Negrini [ID^{24b}](#), C. Nellist [ID¹¹⁷](#), C. Nelson [ID¹⁰⁶](#), K. Nelson [ID¹⁰⁸](#), S. Nemecek [ID¹³⁴](#),
 M. Nessi [ID^{37,g}](#), M.S. Neubauer [ID¹⁶⁸](#), J. Newell [ID⁹⁴](#), P.R. Newman [ID²¹](#), Y.W.Y. Ng [ID¹⁶⁸](#), B. Ngair [ID^{119a}](#),
 H.D.N. Nguyen [ID¹¹⁰](#), J.D. Nichols [ID¹²³](#), R.B. Nickerson [ID¹²⁹](#), R. Nicolaïdou [ID¹³⁸](#), J. Nielsen [ID¹³⁹](#),
 M. Niemeyer [ID⁵⁵](#), J. Niermann [ID³⁷](#), N. Nikiforou [ID³⁷](#), V. Nikolaenko [ID^{38,a}](#), I. Nikolic-Audit [ID¹³⁰](#),
 P. Nilsson [ID³⁰](#), I. Ninca [ID⁴⁸](#), G. Ninio [ID¹⁵⁷](#), A. Nisati [ID^{75a}](#), R. Nisius [ID¹¹²](#), N. Nitika [ID^{69a,69c}](#),
 J-E. Nitschke [ID⁵⁰](#), E.K. Nkadameng [ID^{34b}](#), T. Nobe [ID¹⁵⁹](#), D. Noll [ID^{18a}](#), T. Nommensen [ID¹⁵³](#),
 M.B. Norfolk [ID¹⁴⁵](#), B.J. Norman [ID³⁵](#), M. Noury [ID^{36a}](#), J. Novak [ID⁹⁵](#), T. Novak [ID⁹⁵](#), R. Novotny [ID¹³⁵](#),
 L. Nozka [ID¹²⁵](#), K. Ntekas [ID¹⁶⁵](#), N.M.J. Nunes De Moura Junior [ID^{83b}](#), J. Ocariz [ID¹³⁰](#), A. Ochi [ID⁸⁵](#),
 I. Ochoa [ID^{133a}](#), S. Oerdekk [ID^{48,y}](#), J.T. Offermann [ID⁴⁰](#), A. Ogodnik [ID¹³⁶](#), A. Oh [ID¹⁰³](#), C.C. Ohm [ID¹⁵⁰](#),
 H. Oide [ID⁸⁴](#), M.L. Ojeda [ID³⁷](#), Y. Okumura [ID¹⁵⁹](#), L.F. Oleiro Seabra [ID^{133a}](#), I. Oleksiyuk [ID⁵⁶](#),
 G. Oliveira Correa [ID¹³](#), D. Oliveira Damazio [ID³⁰](#), J.L. Oliver [ID¹⁶⁵](#), R. Omar [ID⁶⁸](#), Ö.O. Öncel [ID⁵⁴](#),
 A.P. O'Neill [ID²⁰](#), A. Onofre [ID^{133a,133e,e}](#), P.U.E. Onyisi [ID¹¹](#), M.J. Oreglia [ID⁴⁰](#), D. Orestano [ID^{77a,77b}](#),
 R. Orlandini [ID^{77a,77b}](#), R.S. Orr [ID¹⁶¹](#), L.M. Osojnak [ID¹³¹](#), Y. Osumi [ID¹¹³](#), G. Otero y Garzon [ID³¹](#),
 H. Otono [ID⁹⁰](#), M. Ouchrif [ID^{36d}](#), F. Ould-Saada [ID¹²⁸](#), T. Ovsianikova [ID¹⁴²](#), M. Owen [ID⁵⁹](#),
 R.E. Owen [ID¹³⁷](#), V.E. Ozcan [ID^{22a}](#), F. Ozturk [ID⁸⁷](#), N. Ozturk [ID⁸](#), S. Ozturk [ID⁸²](#), H.A. Pacey [ID¹²⁹](#),
 K. Pachal [ID^{162a}](#), A. Pacheco Pages [ID¹³](#), C. Padilla Aranda [ID¹³](#), G. Padovano [ID^{75a,75b}](#),
 S. Pagan Griso [ID^{18a}](#), G. Palacino [ID⁶⁸](#), A. Palazzo [ID^{70a,70b}](#), J. Pampel [ID²⁵](#), J. Pan [ID¹⁷⁸](#), T. Pan [ID^{64a}](#),
 D.K. Panchal [ID¹¹](#), C.E. Pandini [ID⁶⁰](#), J.G. Panduro Vazquez [ID¹³⁷](#), H.D. Pandya [ID¹](#), H. Pang [ID¹³⁸](#),
 P. Pani [ID⁴⁸](#), G. Panizzo [ID^{69a,69c}](#), L. Panwar [ID¹³⁰](#), L. Paolozzi [ID⁵⁶](#), S. Parajuli [ID¹⁶⁸](#), A. Paramonov [ID⁶](#),
 C. Paraskevopoulos [ID⁵³](#), D. Paredes Hernandez [ID^{64b}](#), A. Pareti [ID^{73a,73b}](#), K.R. Park [ID⁴²](#), T.H. Park [ID¹¹²](#),
 F. Parodi [ID^{57b,57a}](#), J.A. Parsons [ID⁴²](#), U. Parzefall [ID⁵⁴](#), B. Pascual Dias [ID⁴¹](#), L. Pascual Dominguez [ID¹⁰¹](#),
 E. Pasqualucci [ID^{75a}](#), S. Passaggio [ID^{57b}](#), F. Pastore [ID⁹⁷](#), P. Patel [ID⁸⁷](#), U.M. Patel [ID⁵¹](#), J.R. Pater [ID¹⁰³](#),
 T. Pauly [ID³⁷](#), F. Pauwels [ID¹³⁶](#), C.I. Pazos [ID¹⁶⁴](#), M. Pedersen [ID¹²⁸](#), R. Pedro [ID^{133a}](#), S.V. Peleganchuk [ID³⁸](#),
 O. Penc [ID¹³⁴](#), E.A. Pender [ID⁵²](#), S. Peng [ID¹⁵](#), G.D. Penn [ID¹⁷⁸](#), K.E. Penski [ID¹¹¹](#), M. Penzin [ID³⁸](#),
 B.S. Peralva [ID^{83d}](#), A.P. Pereira Peixoto [ID¹⁴²](#), L. Pereira Sanchez [ID¹⁴⁹](#), D.V. Perepelitsa [ID^{30,aj}](#),
 G. Perera [ID¹⁰⁵](#), E. Perez Codina [ID³⁷](#), M. Perganti [ID¹⁰](#), H. Pernegger [ID³⁷](#), S. Perrella [ID^{75a,75b}](#),
 K. Peters [ID⁴⁸](#), R.F.Y. Peters [ID¹⁰³](#), B.A. Petersen [ID³⁷](#), T.C. Petersen [ID⁴³](#), E. Petit [ID¹⁰⁴](#), V. Petousis [ID¹³⁵](#),
 A.R. Petri [ID^{71a,71b}](#), C. Petridou [ID^{158,d}](#), T. Petru [ID¹³⁶](#), A. Petrukhin [ID¹⁴⁷](#), M. Pettee [ID^{18a}](#), A. Petukhov [ID⁸²](#),
 K. Petukhova [ID³⁷](#), R. Pezoa [ID^{140g}](#), L. Pezzotti [ID^{24b,24a}](#), G. Pezzullo [ID¹⁷⁸](#), L. Pfaffenbichler [ID³⁷](#),
 A.J. Pfleger [ID⁷⁹](#), T.M. Pham [ID¹⁷⁶](#), T. Pham [ID¹⁰⁷](#), P.W. Phillips [ID¹³⁷](#), G. Piacquadio [ID¹⁵¹](#), E. Pianori [ID^{18a}](#),
 F. Piazza [ID¹²⁶](#), R. Piegaia [ID³¹](#), D. Pietreanu [ID^{28b}](#), A.D. Pilkington [ID¹⁰³](#), M. Pinamonti [ID^{69a,69c}](#),
 J.L. Pinfold [ID²](#), B.C. Pinheiro Pereira [ID^{133a}](#), J. Pinol Bel [ID¹³](#), A.E. Pinto Pinoargote [ID¹³⁰](#),
 L. Pintucci [ID^{69a,69c}](#), K.M. Piper [ID¹⁵²](#), A. Pirttikoski [ID⁵⁶](#), D.A. Pizzi [ID³⁵](#), L. Pizzimento [ID^{64b}](#),

- A. Plebani [ID³³](#), M.-A. Pleier [ID³⁰](#), V. Pleskot [ID¹³⁶](#), E. Plotnikova [ID³⁹](#), G. Poddar [ID⁹⁶](#), R. Poettgen [ID¹⁰⁰](#),
 L. Poggioli [ID¹³⁰](#), S. Polacek [ID¹³⁶](#), G. Polesello [ID^{73a}](#), A. Poley [ID¹⁴⁸](#), A. Polini [ID^{24b}](#), C.S. Pollard [ID¹⁷³](#),
 Z.B. Pollock [ID¹²²](#), E. Pompa Pacchi [ID¹²³](#), N.I. Pond [ID⁹⁸](#), D. Ponomarenko [ID⁶⁸](#), L. Pontecorvo [ID³⁷](#),
 S. Popa [ID^{28a}](#), G.A. Popeneciu [ID^{28d}](#), A. Poreba [ID³⁷](#), D.M. Portillo Quintero [ID^{162a}](#), S. Pospisil [ID¹³⁵](#),
 M.A. Postill [ID¹⁴⁵](#), P. Postolache [ID^{28c}](#), K. Potamianos [ID¹⁷³](#), P.A. Potepa [ID^{86a}](#), I.N. Potrap [ID³⁹](#),
 C.J. Potter [ID³³](#), H. Potti [ID¹⁵³](#), J. Poveda [ID¹⁶⁹](#), M.E. Pozo Astigarraga [ID³⁷](#), R. Pozzi [ID³⁷](#),
 A. Prades Ibanez [ID^{76a,76b}](#), S.R. Pradhan [ID¹⁴⁵](#), J. Pretel [ID¹⁷¹](#), D. Price [ID¹⁰³](#), M. Primavera [ID^{70a}](#),
 L. Primomo [ID^{69a,69c}](#), M.A. Principe Martin [ID¹⁰¹](#), R. Privara [ID¹²⁵](#), T. Procter [ID^{86b}](#), M.L. Proffitt [ID¹⁴²](#),
 N. Proklova [ID¹³¹](#), K. Prokofiev [ID^{64c}](#), G. Proto [ID¹¹²](#), J. Proudfoot [ID⁶](#), M. Przybycien [ID^{86a}](#),
 W.W. Przygoda [ID^{86b}](#), A. Psallidas [ID⁴⁶](#), J.E. Puddefoot [ID¹⁴⁵](#), D. Pudzha [ID⁵³](#), H.I. Purnell [ID¹](#),
 D. Pyatiizbyantseva [ID¹¹⁶](#), J. Qian [ID¹⁰⁸](#), R. Qian [ID¹⁰⁹](#), D. Qichen [ID¹²⁹](#), Y. Qin [ID¹³](#), T. Qiu [ID⁵²](#),
 A. Quadt [ID⁵⁵](#), M. Queitsch-Maitland [ID¹⁰³](#), G. Quetant [ID⁵⁶](#), R.P. Quinn [ID¹⁷⁰](#), G. Rabanal Bolanos [ID⁶¹](#),
 D. Rafanoharana [ID¹¹²](#), F. Raffaeli [ID^{76a,76b}](#), F. Ragusa [ID^{71a,71b}](#), J.L. Rainbolt [ID⁴⁰](#), S. Rajagopalan [ID³⁰](#),
 E. Ramakoti [ID³⁹](#), L. Rambelli [ID^{57b,57a}](#), I.A. Ramirez-Berend [ID³⁵](#), K. Ran [ID^{48,114c}](#), D.S. Rankin [ID¹³¹](#),
 N.P. Rapheeha [ID^{34h}](#), H. Rasheed [ID^{28b}](#), D.F. Rassloff [ID^{63a}](#), A. Rastogi [ID^{18a}](#), S. Rave [ID¹⁰²](#),
 S. Ravera [ID^{57b,57a}](#), B. Ravina [ID³⁷](#), I. Ravinovich [ID¹⁷⁵](#), M. Raymond [ID³⁷](#), A.L. Read [ID¹²⁸](#),
 N.P. Readioff [ID¹⁴⁵](#), D.M. Rebuzzi [ID^{73a,73b}](#), A.S. Reed [ID⁵⁹](#), K. Reeves [ID²⁷](#), J.A. Reidelsturz [ID¹⁷⁷](#),
 D. Reikher [ID¹²⁶](#), A. Rej [ID⁴⁹](#), C. Rembsler [ID³⁷](#), H. Ren [ID⁶²](#), M. Renda [ID^{28b}](#), F. Renner [ID⁴⁸](#),
 A.G. Rennie [ID⁵⁹](#), A.L. Rescia [ID^{57b,57a}](#), S. Resconi [ID^{71a}](#), M. Ressegotti [ID^{57b,57a}](#), S. Rettie [ID³⁷](#),
 W.F. Rettie [ID³⁵](#), M.M. Revering [ID³³](#), E. Reynolds [ID^{18a}](#), O.L. Rezanova [ID³⁹](#), P. Reznicek [ID¹³⁶](#),
 H. Riani [ID^{36d}](#), N. Ribaric [ID⁵¹](#), B. Ricci [ID^{69a,69c}](#), E. Ricci [ID^{78a,78b}](#), R. Richter [ID¹¹²](#), S. Richter [ID^{47a,47b}](#),
 E. Richter-Was [ID^{86b}](#), M. Ridel [ID¹³⁰](#), S. Ridouani [ID^{36d}](#), P. Rieck [ID¹²⁰](#), P. Riedler [ID³⁷](#), E.M. Riefel [ID^{47a,47b}](#),
 J.O. Rieger [ID¹¹⁷](#), M. Rijssenbeek [ID¹⁵¹](#), M. Rimoldi [ID³⁷](#), L. Rinaldi [ID^{24b,24a}](#), P. Rincke [ID^{167,55}](#),
 G. Ripellino [ID¹⁶⁷](#), I. Riu [ID¹³](#), J.C. Rivera Vergara [ID¹⁷¹](#), F. Rizatdinova [ID¹²⁴](#), E. Rizvi [ID⁹⁶](#),
 B.R. Roberts [ID^{18a}](#), S.S. Roberts [ID¹³⁹](#), D. Robinson [ID³³](#), M. Robles Manzano [ID¹⁰²](#), A. Robson [ID⁵⁹](#),
 A. Rocchi [ID^{76a,76b}](#), C. Roda [ID^{74a,74b}](#), S. Rodriguez Bosca [ID³⁷](#), Y. Rodriguez Garcia [ID^{23a}](#),
 A.M. Rodriguez Vera [ID¹¹⁸](#), S. Roe [ID³⁷](#), J.T. Roemer [ID³⁷](#), O. Røhne [ID¹²⁸](#), R.A. Rojas [ID³⁷](#),
 C.P.A. Roland [ID¹³⁰](#), A. Romanouk [ID⁷⁹](#), E. Romano [ID^{73a,73b}](#), M. Romano [ID^{24b}](#),
 A.C. Romero Hernandez [ID¹⁶⁸](#), N. Rompotis [ID⁹⁴](#), L. Roos [ID¹³⁰](#), S. Rosati [ID^{75a}](#), B.J. Rosser [ID⁴⁰](#),
 E. Rossi [ID¹²⁹](#), E. Rossi [ID^{72a,72b}](#), L.P. Rossi [ID⁶¹](#), L. Rossini [ID⁵⁴](#), R. Rosten [ID¹²²](#), M. Rotaru [ID^{28b}](#),
 B. Rottler [ID⁵⁴](#), D. Rousseau [ID⁶⁶](#), D. Rousso [ID⁴⁸](#), S. Roy-Garand [ID¹⁶¹](#), A. Rozanov [ID¹⁰⁴](#),
 Z.M.A. Rozario [ID⁵⁹](#), Y. Rozen [ID¹⁵⁶](#), A. Rubio Jimenez [ID¹⁶⁹](#), V.H. Ruelas Rivera [ID¹⁹](#), T.A. Ruggeri [ID¹](#),
 A. Ruggiero [ID¹²⁹](#), A. Ruiz-Martinez [ID¹⁶⁹](#), A. Rummler [ID³⁷](#), Z. Rurikova [ID⁵⁴](#), N.A. Rusakovich [ID³⁹](#),
 S. Ruscelli [ID⁴⁹](#), H.L. Russell [ID¹⁷¹](#), G. Russo [ID^{75a,75b}](#), J.P. Rutherford [ID⁷](#), S. Rutherford Colmenares [ID³³](#),
 M. Rybar [ID¹³⁶](#), P. Rybczynski [ID^{86a}](#), A. Ryzhov [ID⁴⁵](#), J.A. Sabater Iglesias [ID⁵⁶](#), H.F-W. Sadrozinski [ID¹³⁹](#),
 F. Safai Tehrani [ID^{75a}](#), S. Saha [ID¹](#), M. Sahin soy [ID⁸²](#), B. Sahoo [ID¹⁷⁵](#), A. Saibel [ID¹⁶⁹](#), B.T. Saifuddin [ID¹²³](#),
 M. Saimpert [ID¹³⁸](#), G.T. Saito [ID^{83c}](#), M. Saito [ID¹⁵⁹](#), T. Saito [ID¹⁵⁹](#), A. Sala [ID^{71a,71b}](#), A. Salnikov [ID¹⁴⁹](#),
 J. Salt [ID¹⁶⁹](#), A. Salvador Salas [ID¹⁵⁷](#), F. Salvatore [ID¹⁵²](#), A. Salzburger [ID³⁷](#), D. Sammel [ID⁵⁴](#),
 E. Sampson [ID⁹³](#), D. Sampsonidis [ID^{158,d}](#), D. Sampsonidou [ID¹²⁶](#), J. Sánchez [ID¹⁶⁹](#),
 V. Sanchez Sebastian [ID¹⁶⁹](#), H. Sandaker [ID¹²⁸](#), C.O. Sander [ID⁴⁸](#), J.A. Sandesara [ID¹⁷⁶](#), M. Sandhoff [ID¹⁷⁷](#),
 C. Sandoval [ID^{23b}](#), L. Sanfilippo [ID^{63a}](#), D.P.C. Sankey [ID¹³⁷](#), T. Sano [ID⁸⁹](#), A. Sansoni [ID⁵³](#),
 M. Santana Queiroz [ID^{18b}](#), L. Santi [ID³⁷](#), C. Santoni [ID⁴¹](#), H. Santos [ID^{133a,133b}](#), A. Santra [ID¹⁷⁵](#),
 E. Sanzani [ID^{24b,24a}](#), K.A. Saoucha [ID^{88b}](#), J.G. Saraiva [ID^{133a,133d}](#), J. Sardain [ID⁷](#), O. Sasaki [ID⁸⁴](#),
 K. Sato [ID¹⁶³](#), C. Sauer [ID³⁷](#), E. Sauvan [ID⁴](#), P. Savard [ID^{161,ah}](#), R. Sawada [ID¹⁵⁹](#), C. Sawyer [ID¹³⁷](#),
 L. Sawyer [ID⁹⁹](#), C. Sbarra [ID^{24b}](#), A. Sbrizzi [ID^{24b,24a}](#), T. Scanlon [ID⁹⁸](#), J. Schaarschmidt [ID¹⁴²](#),
 U. Schäfer [ID¹⁰²](#), A.C. Schaffer [ID^{66,45}](#), D. Schaile [ID¹¹¹](#), R.D. Schamberger [ID¹⁵¹](#), C. Scharf [ID¹⁹](#),
 M.M. Schefer [ID²⁰](#), V.A. Schegelsky [ID³⁸](#), D. Scheirich [ID¹³⁶](#), M. Schernau [ID^{140f}](#), C. Scheulen [ID⁵⁶](#)

C. Schiavi [ID^{57b,57a}](#), M. Schioppa [ID^{44b,44a}](#), B. Schlag [ID¹⁴⁹](#), S. Schlenker [ID³⁷](#), J. Schmeing [ID¹⁷⁷](#),
 E. Schmidt [ID¹¹²](#), M.A. Schmidt [ID¹⁷⁷](#), K. Schmieden [ID¹⁰²](#), C. Schmitt [ID¹⁰²](#), N. Schmitt [ID¹⁰²](#),
 S. Schmitt [ID⁴⁸](#), N.A. Schneider [ID¹¹¹](#), L. Schoeffel [ID¹³⁸](#), A. Schoening [ID^{63b}](#), P.G. Scholer [ID³⁵](#),
 E. Schopf [ID¹⁴⁷](#), M. Schott [ID²⁵](#), S. Schramm [ID⁵⁶](#), T. Schroer [ID⁵⁶](#), H-C. Schultz-Coulon [ID^{63a}](#),
 M. Schumacher [ID⁵⁴](#), B.A. Schumm [ID¹³⁹](#), Ph. Schune [ID¹³⁸](#), H.R. Schwartz [ID⁷](#), A. Schwartzman [ID¹⁴⁹](#),
 T.A. Schwarz [ID¹⁰⁸](#), Ph. Schwemling [ID¹³⁸](#), R. Schwienhorst [ID¹⁰⁹](#), F.G. Sciacca [ID²⁰](#), A. Sciandra [ID³⁰](#),
 G. Sciolla [ID²⁷](#), F. Scuri [ID^{74a}](#), C.D. Sebastiani [ID³⁷](#), K. Sedlaczek [ID¹¹⁸](#), S.C. Seidel [ID¹¹⁵](#), A. Seiden [ID¹³⁹](#),
 B.D. Seidlitz [ID⁴²](#), C. Seitz [ID⁴⁸](#), J.M. Seixas [ID^{83b}](#), G. Sekhniaidze [ID^{72a}](#), L. Selem [ID⁶⁰](#),
 N. Semprini-Cesari [ID^{24b,24a}](#), A. Semushin [ID¹⁷⁹](#), D. Sengupta [ID⁵⁶](#), V. Senthilkumar [ID¹⁶⁹](#), L. Serin [ID⁶⁶](#),
 M. Sessa [ID^{72a,72b}](#), H. Severini [ID¹²³](#), F. Sforza [ID^{57b,57a}](#), A. Sfyrla [ID⁵⁶](#), Q. Sha [ID¹⁴](#), E. Shabalina [ID⁵⁵](#),
 H. Shaddix [ID¹¹⁸](#), A.H. Shah [ID³³](#), R. Shaheen [ID¹⁵⁰](#), J.D. Shahinian [ID¹³¹](#), M. Shamim [ID³⁷](#), L.Y. Shan [ID¹⁴](#),
 M. Shapiro [ID^{18a}](#), A. Sharma [ID³⁷](#), A.S. Sharma [ID¹⁷⁰](#), P. Sharma [ID³⁰](#), P.B. Shatalov [ID³⁸](#), K. Shaw [ID¹⁵²](#),
 S.M. Shaw [ID¹⁰³](#), Q. Shen [ID^{144a}](#), D.J. Sheppard [ID¹⁴⁸](#), P. Sherwood [ID⁹⁸](#), L. Shi [ID⁹⁸](#), X. Shi [ID¹⁴](#),
 S. Shimizu [ID⁸⁴](#), C.O. Shimmin [ID¹⁷⁸](#), I.P.J. Shipsey [ID^{129,*}](#), S. Shirabe [ID⁹⁰](#), M. Shiyakova [ID^{39,z}](#),
 M.J. Shochet [ID⁴⁰](#), D.R. Shope [ID¹²⁸](#), B. Shrestha [ID¹²³](#), S. Shrestha [ID^{122,al}](#), I. Shreyber [ID³⁹](#),
 M.J. Shroff [ID¹⁷¹](#), P. Sicho [ID¹³⁴](#), A.M. Sickles [ID¹⁶⁸](#), E. Sideras Haddad [ID^{34h,166}](#), A.C. Sidley [ID¹¹⁷](#),
 A. Sidoti [ID^{24b}](#), F. Siegert [ID⁵⁰](#), Dj. Sijacki [ID¹⁶](#), F. Sili [ID⁹²](#), J.M. Silva [ID⁵²](#), I. Silva Ferreira [ID^{83b}](#),
 M.V. Silva Oliveira [ID³⁰](#), S.B. Silverstein [ID^{47a}](#), S. Simion [ID⁶⁶](#), R. Simonello [ID³⁷](#), E.L. Simpson [ID¹⁰³](#),
 H. Simpson [ID¹⁵²](#), L.R. Simpson [ID⁶](#), S. Simsek [ID⁸²](#), S. Sindhu [ID⁵⁵](#), P. Sinervo [ID¹⁶¹](#), S.N. Singh [ID²⁷](#),
 S. Singh [ID³⁰](#), S. Sinha [ID⁴⁸](#), S. Sinha [ID¹⁰³](#), M. Sioli [ID^{24b,24a}](#), K. Sioulas [ID⁹](#), I. Siral [ID³⁷](#), E. Sitnikova [ID⁴⁸](#),
 J. Sjölin [ID^{47a,47b}](#), A. Skaf [ID⁵⁵](#), E. Skorda [ID²¹](#), P. Skubic [ID¹²³](#), M. Slawinska [ID⁸⁷](#), I. Slazyk [ID¹⁷](#),
 I. Sliusar [ID¹²⁸](#), V. Smakhtin [ID¹⁷⁵](#), B.H. Smart [ID¹³⁷](#), S.Yu. Smirnov [ID^{140b}](#), Y. Smirnov [ID⁸²](#),
 L.N. Smirnova [ID^{38,a}](#), O. Smirnova [ID¹⁰⁰](#), A.C. Smith [ID⁴²](#), D.R. Smith [ID¹⁶⁵](#), J.L. Smith [ID¹⁰³](#), M.B. Smith [ID³⁵](#),
 R. Smith [ID¹⁴⁹](#), H. Smitmanns [ID¹⁰²](#), M. Smizanska [ID⁹³](#), K. Smolek [ID¹³⁵](#), P. Smolyanskiy [ID¹³⁵](#),
 A.A. Snesarev [ID³⁹](#), H.L. Snoek [ID¹¹⁷](#), S. Snyder [ID³⁰](#), R. Sobie [ID^{171,ab}](#), A. Soffer [ID¹⁵⁷](#),
 C.A. Solans Sanchez [ID³⁷](#), E.Yu. Soldatov [ID³⁹](#), U. Soldevila [ID¹⁶⁹](#), A.A. Solodkov [ID^{34h}](#), S. Solomon [ID²⁷](#),
 A. Soloshenko [ID³⁹](#), K. Solovieva [ID⁵⁴](#), O.V. Solovyanov [ID⁴¹](#), P. Sommer [ID⁵⁰](#), A. Sonay [ID¹³](#),
 A. Sopczak [ID¹³⁵](#), A.L. Sopio [ID⁵²](#), F. Sopkova [ID^{29b}](#), J.D. Sorenson [ID¹¹⁵](#), I.R. Sotarriva Alvarez [ID¹⁴¹](#),
 V. Sothilingam [ID^{63a}](#), O.J. Soto Sandoval [ID^{140c,140b}](#), S. Sottocornola [ID⁶⁸](#), R. Soualah [ID^{88a}](#),
 Z. Soumaimi [ID^{36e}](#), D. South [ID⁴⁸](#), N. Soybelman [ID¹⁷⁵](#), S. Spagnolo [ID^{70a,70b}](#), M. Spalla [ID¹¹²](#),
 D. Sperlich [ID⁵⁴](#), B. Spisso [ID^{72a,72b}](#), D.P. Spiteri [ID⁵⁹](#), L. Splendori [ID¹⁰⁴](#), M. Spousta [ID¹³⁶](#), E.J. Staats [ID³⁵](#),
 R. Stamen [ID^{63a}](#), E. Stanecka [ID⁸⁷](#), W. Stanek-Maslouska [ID⁴⁸](#), M.V. Stange [ID⁵⁰](#), B. Stanislaus [ID^{18a}](#),
 M.M. Stanitzki [ID⁴⁸](#), B. Stapf [ID⁴⁸](#), E.A. Starchenko [ID³⁸](#), G.H. Stark [ID¹³⁹](#), J. Stark [ID⁹¹](#), P. Staroba [ID¹³⁴](#),
 P. Starovoitov [ID^{88b}](#), R. Staszewski [ID⁸⁷](#), C. Stauch [ID¹¹¹](#), G. Stavropoulos [ID⁴⁶](#), A. Stefl [ID³⁷](#), A. Stein [ID¹⁰²](#),
 P. Steinberg [ID³⁰](#), B. Stelzer [ID^{148,162a}](#), H.J. Stelzer [ID¹³²](#), O. Stelzer-Chilton [ID^{162a}](#), H. Stenzel [ID⁵⁸](#),
 T.J. Stevenson [ID¹⁵²](#), G.A. Stewart [ID³⁷](#), J.R. Stewart [ID¹²⁴](#), G. Stoica [ID^{28b}](#), M. Stolarski [ID^{133a}](#),
 S. Stonjek [ID¹¹²](#), A. Straessner [ID⁵⁰](#), J. Strandberg [ID¹⁵⁰](#), S. Strandberg [ID^{47a,47b}](#), M. Stratmann [ID¹⁷⁷](#),
 M. Strauss [ID¹²³](#), T. Strebler [ID¹⁰⁴](#), P. Strizenec [ID^{29b}](#), R. Ströhmer [ID¹⁷²](#), D.M. Strom [ID¹²⁶](#),
 R. Stroynowski [ID⁴⁵](#), A. Strubig [ID^{47a,47b}](#), S.A. Stucci [ID³⁰](#), B. Stugu [ID¹⁷](#), J. Stupak [ID¹²³](#), N.A. Styles [ID⁴⁸](#),
 D. Su [ID¹⁴⁹](#), S. Su [ID⁶²](#), X. Su [ID⁶²](#), D. Suchy [ID^{29a}](#), K. Sugizaki [ID¹³¹](#), V.V. Sulin [ID³⁸](#), D.M.S. Sultan [ID¹²⁹](#),
 L. Sultanaliyeva [ID²⁵](#), S. Sultansoy [ID^{3b}](#), S. Sun [ID¹⁷⁶](#), W. Sun [ID¹⁴](#), O. Sunneborn Gudnadottir [ID¹⁶⁷](#),
 N. Sur [ID¹⁰⁰](#), M.R. Sutton [ID¹⁵²](#), M. Svatos [ID¹³⁴](#), P.N. Swallow [ID³³](#), M. Swiatlowski [ID^{162a}](#),
 T. Swirski [ID¹⁷²](#), A. Swoboda [ID³⁷](#), I. Sykora [ID^{29a}](#), M. Sykora [ID¹³⁶](#), T. Sykora [ID¹³⁶](#), D. Ta [ID¹⁰²](#),
 K. Tackmann [ID^{48,y}](#), A. Taffard [ID¹⁶⁵](#), R. Tafirout [ID^{162a}](#), Y. Takubo [ID⁸⁴](#), M. Talby [ID¹⁰⁴](#), A.A. Talyshев [ID³⁸](#),
 K.C. Tam [ID^{64b}](#), N.M. Tamir [ID¹⁵⁷](#), A. Tanaka [ID¹⁵⁹](#), J. Tanaka [ID¹⁵⁹](#), R. Tanaka [ID⁶⁶](#), M. Tanasini [ID¹⁵¹](#),
 Z. Tao [ID¹⁷⁰](#), S. Tapia Araya [ID^{140g}](#), S. Tapprogge [ID¹⁰²](#), A. Tarek Abouelfadl Mohamed [ID¹⁰⁹](#),
 S. Tarem [ID¹⁵⁶](#), K. Tariq [ID¹⁴](#), G. Tarna [ID³⁷](#), G.F. Tartarelli [ID^{71a}](#), M.J. Tartarin [ID⁹¹](#), P. Tas [ID¹³⁶](#),

M. Tasevsky [ID¹³⁴](#), E. Tassi [ID^{44b,44a}](#), A.C. Tate [ID¹⁶⁸](#), Y. Tayalati [ID^{36e,aa}](#), G.N. Taylor [ID¹⁰⁷](#),
 W. Taylor [ID^{162b}](#), A.S. Tegetmeier [ID⁹¹](#), P. Teixeira-Dias [ID⁹⁷](#), J.J. Teoh [ID¹⁶¹](#), K. Terashi [ID¹⁵⁹](#),
 J. Terron [ID¹⁰¹](#), S. Terzo [ID¹³](#), M. Testa [ID⁵³](#), R.J. Teuscher [ID^{161,ab}](#), A. Thaler [ID⁷⁹](#), O. Theiner [ID⁵⁶](#),
 T. Theveneaux-Pelzer [ID¹⁰⁴](#), D.W. Thomas [ID⁹⁷](#), J.P. Thomas [ID²¹](#), E.A. Thompson [ID^{18a}](#), P.D. Thompson [ID²¹](#),
 E. Thomson [ID¹³¹](#), R.E. Thornberry [ID⁴⁵](#), C. Tian [ID⁶²](#), Y. Tian [ID⁵⁶](#), V. Tikhomirov [ID⁸²](#),
 Yu.A. Tikhonov [ID³⁹](#), S. Timoshenko³⁸, D. Timoshyn [ID¹³⁶](#), E.X.L. Ting [ID¹](#), P. Tipton [ID¹⁷⁸](#),
 A. Tishelman-Charny [ID³⁰](#), K. Todome [ID¹⁴¹](#), S. Todorova-Nova [ID¹³⁶](#), L. Toffolin [ID^{69a,69c}](#), M. Togawa [ID⁸⁴](#),
 J. Tojo [ID⁹⁰](#), S. Tokár [ID^{29a}](#), O. Toldaiev [ID⁶⁸](#), G. Tolkachev [ID¹⁰⁴](#), M. Tomoto [ID⁸⁴](#), L. Tompkins [ID^{149,n}](#),
 E. Torrence [ID¹²⁶](#), H. Torres [ID⁹¹](#), E. Torró Pastor [ID¹⁶⁹](#), M. Toscani [ID³¹](#), C. Tosciri [ID⁴⁰](#), M. Tost [ID¹¹](#),
 D.R. Tovey [ID¹⁴⁵](#), T. Trefzger [ID¹⁷²](#), P.M. Tricarico [ID¹³](#), A. Tricoli [ID³⁰](#), I.M. Trigger [ID^{162a}](#),
 S. Trincaz-Duvoid [ID¹³⁰](#), D.A. Trischuk [ID²⁷](#), A. Tropina³⁹, L. Truong [ID^{34c}](#), M. Trzebinski [ID⁸⁷](#),
 A. Trzupek [ID⁸⁷](#), F. Tsai [ID¹⁵¹](#), M. Tsai [ID¹⁰⁸](#), A. Tsiamis [ID¹⁵⁸](#), P.V. Tsiareshka³⁹, S. Tsigaridas [ID^{162a}](#),
 A. Tsirigotis [ID^{158,u}](#), V. Tsiskaridze [ID^{155a}](#), E.G. Tskhadadze [ID^{155a}](#), M. Tsopoulou [ID¹⁵⁸](#), Y. Tsujikawa [ID⁸⁹](#),
 I.I. Tsukerman [ID³⁸](#), V. Tsulaia [ID^{18a}](#), S. Tsuno [ID⁸⁴](#), K. Tsuri [ID¹²¹](#), D. Tsybychev [ID¹⁵¹](#), Y. Tu [ID^{64b}](#),
 A. Tudorache [ID^{28b}](#), V. Tudorache [ID^{28b}](#), S.B. Tuncay [ID¹²⁹](#), S. Turchikhin [ID^{57b,57a}](#), I. Turk Cakir [ID^{3a}](#),
 R. Turra [ID^{71a}](#), T. Turtuvshin [ID^{39,ac}](#), P.M. Tuts [ID⁴²](#), S. Tzamarias [ID^{158,d}](#), E. Tzovara [ID¹⁰²](#), Y. Uematsu [ID⁸⁴](#),
 F. Ukegawa [ID¹⁶³](#), P.A. Ulloa Poblete [ID^{140c,140b}](#), E.N. Umaka [ID³⁰](#), G. Unal [ID³⁷](#), A. Undrus [ID³⁰](#),
 G. Unel [ID¹⁶⁵](#), J. Urban [ID^{29b}](#), P. Urrejola [ID^{140a}](#), G. Usai [ID⁸](#), R. Ushioda [ID¹⁶⁰](#), M. Usman [ID¹¹⁰](#),
 F. Ustuner [ID⁵²](#), Z. Uysal [ID⁸²](#), V. Vacek [ID¹³⁵](#), B. Vachon [ID¹⁰⁶](#), T. Vafeiadis [ID³⁷](#), A. Vaitkus [ID⁹⁸](#),
 C. Valderanis [ID¹¹¹](#), E. Valdes Santurio [ID^{47a,47b}](#), M. Valente [ID³⁷](#), S. Valentinietti [ID^{24b,24a}](#), A. Valero [ID¹⁶⁹](#),
 E. Valiente Moreno [ID¹⁶⁹](#), A. Vallier [ID⁹¹](#), J.A. Valls Ferrer [ID¹⁶⁹](#), D.R. Van Arneman [ID¹¹⁷](#),
 A. Van Der Graaf [ID⁴⁹](#), H.Z. Van Der Schyf [ID^{34h}](#), P. Van Gemmeren [ID⁶](#), M. Van Rijnbach [ID³⁷](#),
 S. Van Stroud [ID⁹⁸](#), I. Van Vulpen [ID¹¹⁷](#), P. Vana [ID¹³⁶](#), M. Vanadia [ID^{76a,76b}](#), U.M. Vande Voorde [ID¹⁵⁰](#),
 W. Vandelli [ID³⁷](#), E.R. Vandewall [ID¹²⁴](#), D. Vannicola [ID¹⁵⁷](#), L. Vannoli [ID⁵³](#), R. Vari [ID^{75a}](#), M. Varma [ID¹⁷⁸](#),
 E.W. Varnes [ID⁷](#), C. Varni [ID¹¹⁸](#), D. Varouchas [ID⁶⁶](#), L. Varriale [ID¹⁶⁹](#), K.E. Varvell [ID¹⁵³](#), M.E. Vasile [ID^{28b}](#),
 L. Vaslin⁸⁴, M.D. Vassilev [ID¹⁴⁹](#), A. Vasyukov [ID³⁹](#), L.M. Vaughan [ID¹²⁴](#), R. Vavricka¹³⁶,
 T. Vazquez Schroeder [ID¹³](#), J. Veatch [ID³²](#), V. Vecchio [ID¹⁰³](#), M.J. Veen [ID¹⁰⁵](#), I. Velisek [ID³⁰](#),
 I. Velkovska [ID⁹⁵](#), L.M. Veloce [ID¹⁶¹](#), F. Veloso [ID^{133a,133c}](#), S. Veneziano [ID^{75a}](#), A. Ventura [ID^{70a,70b}](#),
 A. Verbytskyi [ID¹¹²](#), M. Verducci [ID^{74a,74b}](#), C. Vergis [ID⁹⁶](#), M. Verissimo De Araujo [ID^{83b}](#),
 W. Verkerke [ID¹¹⁷](#), J.C. Vermeulen [ID¹¹⁷](#), C. Vernieri [ID¹⁴⁹](#), M. Vessella [ID¹⁶⁵](#), M.C. Vetterli [ID^{148,ah}](#),
 A. Vgenopoulos [ID¹⁰²](#), N. Viaux Maira [ID^{140g}](#), T. Vickey [ID¹⁴⁵](#), O.E. Vickey Boeriu [ID¹⁴⁵](#),
 G.H.A. Viehhauser [ID¹²⁹](#), L. Vigani [ID^{63b}](#), M. Vigl [ID¹¹²](#), M. Villa [ID^{24b,24a}](#), M. Villaplana Perez [ID¹⁶⁹](#),
 E.M. Villhauer⁴⁰, E. Vilucchi [ID⁵³](#), M. Vincent [ID¹⁶⁹](#), M.G. Vincter [ID³⁵](#), A. Visibile¹¹⁷, C. Vittori [ID³⁷](#),
 I. Vivarelli [ID^{24b,24a}](#), E. Voevodina [ID¹¹²](#), F. Vogel [ID¹¹¹](#), J.C. Voigt [ID⁵⁰](#), P. Vokac [ID¹³⁵](#), Yu. Volkotrub [ID^{86b}](#),
 L. Vomberg [ID²⁵](#), E. Von Toerne [ID²⁵](#), B. Vormwald [ID³⁷](#), K. Vorobev [ID⁵¹](#), M. Vos [ID¹⁶⁹](#), K. Voss [ID¹⁴⁷](#),
 M. Vozak [ID³⁷](#), L. Vozdecky [ID¹²³](#), N. Vranjes [ID¹⁶](#), M. Vranjes Milosavljevic [ID¹⁶](#), M. Vreeswijk [ID¹¹⁷](#),
 N.K. Vu [ID^{144b,144a}](#), R. Vuillermet [ID³⁷](#), O. Vujinovic [ID¹⁰²](#), I. Vukotic [ID⁴⁰](#), I.K. Vyas [ID³⁵](#), J.F. Wack [ID³³](#),
 S. Wada [ID¹⁶³](#), C. Wagner¹⁴⁹, J.M. Wagner [ID^{18a}](#), W. Wagner [ID¹⁷⁷](#), S. Wahdan [ID¹⁷⁷](#), H. Wahlberg [ID⁹²](#),
 C.H. Waits [ID¹²³](#), J. Walder [ID¹³⁷](#), R. Walker [ID¹¹¹](#), K. Walkingshaw Pass⁵⁹, W. Walkowiak [ID¹⁴⁷](#),
 A. Wall [ID¹³¹](#), E.J. Wallin [ID¹⁰⁰](#), T. Wamorkar [ID^{18a}](#), K. Wandall-Christensen [ID¹⁶⁹](#), A. Wang [ID⁶²](#),
 A.Z. Wang [ID¹³⁹](#), C. Wang [ID¹⁰²](#), C. Wang [ID¹¹](#), H. Wang [ID^{18a}](#), J. Wang [ID^{64c}](#), P. Wang [ID¹⁰³](#), P. Wang [ID⁹⁸](#),
 R. Wang [ID⁶¹](#), R. Wang [ID⁶](#), S.M. Wang [ID¹⁵⁴](#), S. Wang [ID¹⁴](#), T. Wang [ID¹¹⁶](#), T. Wang [ID⁶²](#), W.T. Wang [ID⁸⁰](#),
 W. Wang [ID¹⁴](#), X. Wang [ID¹⁶⁸](#), X. Wang [ID^{144a}](#), X. Wang [ID⁴⁸](#), Y. Wang [ID^{114a}](#), Y. Wang [ID⁶²](#), Z. Wang [ID¹⁰⁸](#),
 Z. Wang [ID^{144b}](#), Z. Wang [ID¹⁰⁸](#), C. Wanotayaroj [ID⁸⁴](#), A. Warburton [ID¹⁰⁶](#), A.L. Warnerbring [ID¹⁴⁷](#),
 S. Waterhouse [ID⁹⁷](#), A.T. Watson [ID²¹](#), H. Watson [ID⁵²](#), M.F. Watson [ID²¹](#), E. Watton [ID⁵⁹](#), G. Watts [ID¹⁴²](#),
 B.M. Waugh [ID⁹⁸](#), J.M. Webb [ID⁵⁴](#), C. Weber [ID³⁰](#), H.A. Weber [ID¹⁹](#), M.S. Weber [ID²⁰](#), S.M. Weber [ID^{63a}](#),
 C. Wei [ID⁶²](#), Y. Wei [ID⁵⁴](#), A.R. Weidberg [ID¹²⁹](#), E.J. Weik [ID¹²⁰](#), J. Weingarten [ID⁴⁹](#), C. Weiser [ID⁵⁴](#),

C.J. Wells [ID⁴⁸](#), T. Wenaus [ID³⁰](#), T. Wengler [ID³⁷](#), N.S. Wenke¹¹², N. Wermes [ID²⁵](#), M. Wessels [ID^{63a}](#), A.M. Wharton [ID⁹³](#), A.S. White [ID⁶¹](#), A. White [ID⁸](#), M.J. White [ID¹](#), D. Whiteson [ID¹⁶⁵](#), L. Wickremasinghe [ID¹²⁷](#), W. Wiedenmann [ID¹⁷⁶](#), M. Wielers [ID¹³⁷](#), R. Wierda [ID¹⁵⁰](#), C. Wiglesworth [ID⁴³](#), H.G. Wilkens [ID³⁷](#), J.J.H. Wilkinson [ID³³](#), D.M. Williams [ID⁴²](#), H.H. Williams¹³¹, S. Williams [ID³³](#), S. Willocq [ID¹⁰⁵](#), B.J. Wilson [ID¹⁰³](#), D.J. Wilson [ID¹⁰³](#), P.J. Windischhofer [ID⁴⁰](#), F.I. Winkel [ID³¹](#), F. Winklmeier [ID¹²⁶](#), B.T. Winter [ID⁵⁴](#), M. Wittgen¹⁴⁹, M. Wobisch [ID⁹⁹](#), T. Wojtkowski⁶⁰, Z. Wolffs [ID¹¹⁷](#), J. Wollrath³⁷, M.W. Wolter [ID⁸⁷](#), H. Wolters [ID^{133a,133c}](#), M.C. Wong¹³⁹, E.L. Woodward [ID⁴²](#), S.D. Worm [ID⁴⁸](#), B.K. Wosiek [ID⁸⁷](#), K.W. Woźniak [ID⁸⁷](#), S. Wozniewski [ID⁵⁵](#), K. Wraight [ID⁵⁹](#), C. Wu [ID¹⁶¹](#), C. Wu [ID²¹](#), J. Wu [ID¹⁵⁹](#), M. Wu [ID^{114b}](#), M. Wu [ID¹¹⁶](#), S.L. Wu [ID¹⁷⁶](#), S. Wu [ID¹⁴](#), X. Wu [ID⁶²](#), Y. Wu [ID⁶²](#), Z. Wu [ID⁴](#), Z. Wu [ID^{114a}](#), J. Wuerzinger [ID¹¹²](#), T.R. Wyatt [ID¹⁰³](#), B.M. Wynne [ID⁵²](#), S. Xella [ID⁴³](#), L. Xia [ID^{114a}](#), M. Xia [ID¹⁵](#), M. Xie [ID⁶²](#), A. Xiong [ID¹²⁶](#), J. Xiong [ID^{18a}](#), D. Xu [ID¹⁴](#), H. Xu [ID⁶²](#), L. Xu [ID⁶²](#), R. Xu [ID¹³¹](#), T. Xu [ID¹⁰⁸](#), Y. Xu [ID¹⁴²](#), Z. Xu [ID⁵²](#), R. Xue [ID¹³²](#), B. Yabsley [ID¹⁵³](#), S. Yacoob [ID^{34a}](#), Y. Yamaguchi [ID⁸⁴](#), E. Yamashita [ID¹⁵⁹](#), H. Yamauchi [ID¹⁶³](#), T. Yamazaki [ID^{18a}](#), Y. Yamazaki [ID⁸⁵](#), S. Yan [ID⁵⁹](#), Z. Yan [ID¹⁰⁵](#), H.J. Yang [ID^{144a,144b}](#), H.T. Yang [ID⁶²](#), S. Yang [ID⁶²](#), T. Yang [ID^{64c}](#), X. Yang [ID³⁷](#), X. Yang [ID¹⁴](#), Y. Yang [ID¹⁵⁹](#), Y. Yang⁶², W.-M. Yao [ID^{18a}](#), C.L. Yardley [ID¹⁵²](#), J. Ye [ID¹⁴](#), S. Ye [ID³⁰](#), X. Ye [ID⁶²](#), Y. Yeh [ID⁹⁸](#), I. Yeletskikh [ID³⁹](#), B. Yeo [ID^{18b}](#), M.R. Yexley [ID⁹⁸](#), T.P. Yildirim [ID¹²⁹](#), K. Yorita [ID¹⁷⁴](#), C.J.S. Young [ID³⁷](#), C. Young [ID¹⁴⁹](#), N.D. Young¹²⁶, Y. Yu [ID⁶²](#), J. Yuan [ID^{14,114c}](#), M. Yuan [ID¹⁰⁸](#), R. Yuan [ID^{144b,144a}](#), L. Yue [ID⁹⁸](#), M. Zaazoua [ID⁶²](#), B. Zabinski [ID⁸⁷](#), I. Zahir [ID^{36a}](#), A. Zaio^{57b,57a}, Z.K. Zak [ID⁸⁷](#), T. Zakareishvili [ID¹⁶⁹](#), S. Zambito [ID⁵⁶](#), J.A. Zamora Saa [ID^{140d}](#), J. Zang [ID¹⁵⁹](#), R. Zanzottera [ID^{71a,71b}](#), O. Zaplatilek [ID¹³⁵](#), C. Zeitnitz [ID¹⁷⁷](#), H. Zeng [ID¹⁴](#), J.C. Zeng [ID¹⁶⁸](#), D.T. Zenger Jr [ID²⁷](#), O. Zenin [ID³⁸](#), T. Ženiš [ID^{29a}](#), S. Zenz [ID⁹⁶](#), D. Zerwas [ID⁶⁶](#), M. Zhai [ID^{14,114c}](#), D.F. Zhang [ID¹⁴⁵](#), G. Zhang [ID¹⁴](#), J. Zhang [ID^{143a}](#), J. Zhang [ID⁶](#), K. Zhang [ID^{14,114c}](#), L. Zhang [ID⁶²](#), L. Zhang [ID^{114a}](#), P. Zhang [ID^{14,114c}](#), R. Zhang [ID^{114a}](#), S. Zhang [ID⁹¹](#), T. Zhang [ID¹⁵⁹](#), Y. Zhang [ID¹⁴²](#), Y. Zhang [ID⁹⁸](#), Y. Zhang [ID⁶²](#), Y. Zhang [ID^{114a}](#), Z. Zhang [ID^{143a}](#), Z. Zhang [ID⁶⁶](#), H. Zhao [ID¹⁴²](#), T. Zhao [ID^{143a}](#), Y. Zhao [ID³⁵](#), Z. Zhao [ID⁶²](#), Z. Zhao [ID⁶²](#), A. Zhemchugov [ID³⁹](#), J. Zheng [ID^{114a}](#), K. Zheng [ID¹⁶⁸](#), X. Zheng [ID⁶²](#), Z. Zheng [ID¹⁴⁹](#), D. Zhong [ID¹⁶⁸](#), B. Zhou [ID¹⁰⁸](#), H. Zhou [ID⁷](#), N. Zhou [ID^{144a}](#), Y. Zhou [ID¹⁵](#), Y. Zhou [ID^{114a}](#), Y. Zhou⁷, C.G. Zhu [ID^{143a}](#), J. Zhu [ID¹⁰⁸](#), X. Zhu^{144b}, Y. Zhu [ID^{144a}](#), Y. Zhu [ID⁶²](#), X. Zhuang [ID¹⁴](#), K. Zhukov [ID⁶⁸](#), N.I. Zimine [ID³⁹](#), J. Zinsser [ID^{63b}](#), M. Ziolkowski [ID¹⁴⁷](#), L. Živković [ID¹⁶](#), A. Zoccoli [ID^{24b,24a}](#), K. Zoch [ID⁶¹](#), A. Zografos [ID³⁷](#), T.G. Zorbas [ID¹⁴⁵](#), O. Zormpa [ID⁴⁶](#), L. Zwalski [ID³⁷](#).

¹Department of Physics, University of Adelaide, Adelaide; Australia.

²Department of Physics, University of Alberta, Edmonton AB; Canada.

^{3(a)}Department of Physics, Ankara University, Ankara; ^(b)Division of Physics, TOBB University of Economics and Technology, Ankara; Türkiye.

⁴LAPP, Université Savoie Mont Blanc, CNRS/IN2P3, Annecy; France.

⁵APC, Université Paris Cité, CNRS/IN2P3, Paris; France.

⁶High Energy Physics Division, Argonne National Laboratory, Argonne IL; United States of America.

⁷Department of Physics, University of Arizona, Tucson AZ; United States of America.

⁸Department of Physics, University of Texas at Arlington, Arlington TX; United States of America.

⁹Physics Department, National and Kapodistrian University of Athens, Athens; Greece.

¹⁰Physics Department, National Technical University of Athens, Zografou; Greece.

¹¹Department of Physics, University of Texas at Austin, Austin TX; United States of America.

¹²Institute of Physics, Azerbaijan Academy of Sciences, Baku; Azerbaijan.

¹³Institut de Física d'Altes Energies (IFAE), Barcelona Institute of Science and Technology, Barcelona; Spain.

¹⁴Institute of High Energy Physics, Chinese Academy of Sciences, Beijing; China.

¹⁵Physics Department, Tsinghua University, Beijing; China.

- ¹⁶Institute of Physics, University of Belgrade, Belgrade; Serbia.
- ¹⁷Department for Physics and Technology, University of Bergen, Bergen; Norway.
- ^{18(a)}Physics Division, Lawrence Berkeley National Laboratory, Berkeley CA; ^(b)University of California, Berkeley CA; United States of America.
- ¹⁹Institut für Physik, Humboldt Universität zu Berlin, Berlin; Germany.
- ²⁰Albert Einstein Center for Fundamental Physics and Laboratory for High Energy Physics, University of Bern, Bern; Switzerland.
- ²¹School of Physics and Astronomy, University of Birmingham, Birmingham; United Kingdom.
- ^{22(a)}Department of Physics, Bogazici University, Istanbul; ^(b)Department of Physics Engineering, Gaziantep University, Gaziantep; ^(c)Department of Physics, Istanbul University, Istanbul; Türkiye.
- ^{23(a)}Facultad de Ciencias y Centro de Investigaciones, Universidad Antonio Nariño, Bogotá; ^(b)Departamento de Física, Universidad Nacional de Colombia, Bogotá; Colombia.
- ^{24(a)}Dipartimento di Fisica e Astronomia A. Righi, Università di Bologna, Bologna; ^(b)INFN Sezione di Bologna; Italy.
- ²⁵Physikalisches Institut, Universität Bonn, Bonn; Germany.
- ²⁶Department of Physics, Boston University, Boston MA; United States of America.
- ²⁷Department of Physics, Brandeis University, Waltham MA; United States of America.
- ^{28(a)}Transilvania University of Brasov, Brasov; ^(b)Horia Hulubei National Institute of Physics and Nuclear Engineering, Bucharest; ^(c)Department of Physics, Alexandru Ioan Cuza University of Iasi, Iasi; ^(d)National Institute for Research and Development of Isotopic and Molecular Technologies, Physics Department, Cluj-Napoca; ^(e)National University of Science and Technology Politehnica, Bucharest; ^(f)West University in Timisoara, Timisoara; ^(g)Faculty of Physics, University of Bucharest, Bucharest; Romania.
- ^{29(a)}Faculty of Mathematics, Physics and Informatics, Comenius University, Bratislava; ^(b)Department of Subnuclear Physics, Institute of Experimental Physics of the Slovak Academy of Sciences, Kosice; Slovak Republic.
- ³⁰Physics Department, Brookhaven National Laboratory, Upton NY; United States of America.
- ³¹Universidad de Buenos Aires, Facultad de Ciencias Exactas y Naturales, Departamento de Física, y CONICET, Instituto de Física de Buenos Aires (IFIBA), Buenos Aires; Argentina.
- ³²California State University, CA; United States of America.
- ³³Cavendish Laboratory, University of Cambridge, Cambridge; United Kingdom.
- ^{34(a)}Department of Physics, University of Cape Town, Cape Town; ^(b)iThemba Labs, Western Cape; ^(c)Department of Mechanical Engineering Science, University of Johannesburg, Johannesburg; ^(d)National Institute of Physics, University of the Philippines Diliman (Philippines); ^(e)Department of Physics, Stellenbosch University, Matieland; ^(f)University of South Africa, Department of Physics, Pretoria; ^(g)University of Zululand, KwaDlangezwa; ^(h)School of Physics, University of the Witwatersrand, Johannesburg; South Africa.
- ³⁵Department of Physics, Carleton University, Ottawa ON; Canada.
- ^{36(a)}Faculté des Sciences Ain Chock, Université Hassan II de Casablanca; ^(b)Faculté des Sciences, Université Ibn-Tofail, Kénitra; ^(c)Faculté des Sciences Semlalia, Université Cadi Ayyad, LPHEA-Marrakech; ^(d)LPMR, Faculté des Sciences, Université Mohamed Premier, Oujda; ^(e)Faculté des sciences, Université Mohammed V, Rabat; ^(f)Institute of Applied Physics, Mohammed VI Polytechnic University, Ben Guerir; Morocco.
- ³⁷CERN, Geneva; Switzerland.
- ³⁸Affiliated with an institute formerly covered by a cooperation agreement with CERN.
- ³⁹Affiliated with an international laboratory covered by a cooperation agreement with CERN.
- ⁴⁰Enrico Fermi Institute, University of Chicago, Chicago IL; United States of America.
- ⁴¹LPC, Université Clermont Auvergne, CNRS/IN2P3, Clermont-Ferrand; France.

- ⁴²Nevis Laboratory, Columbia University, Irvington NY; United States of America.
- ⁴³Niels Bohr Institute, University of Copenhagen, Copenhagen; Denmark.
- ^{44(a)}Dipartimento di Fisica, Università della Calabria, Rende;^(b)INFN Gruppo Collegato di Cosenza, Laboratori Nazionali di Frascati; Italy.
- ⁴⁵Physics Department, Southern Methodist University, Dallas TX; United States of America.
- ⁴⁶National Centre for Scientific Research "Demokritos", Agia Paraskevi; Greece.
- ^{47(a)}Department of Physics, Stockholm University;^(b)Oskar Klein Centre, Stockholm; Sweden.
- ⁴⁸Deutsches Elektronen-Synchrotron DESY, Hamburg and Zeuthen; Germany.
- ⁴⁹Fakultät Physik , Technische Universität Dortmund, Dortmund; Germany.
- ⁵⁰Institut für Kern- und Teilchenphysik, Technische Universität Dresden, Dresden; Germany.
- ⁵¹Department of Physics, Duke University, Durham NC; United States of America.
- ⁵²SUPA - School of Physics and Astronomy, University of Edinburgh, Edinburgh; United Kingdom.
- ⁵³INFN e Laboratori Nazionali di Frascati, Frascati; Italy.
- ⁵⁴Physikalischs Institut, Albert-Ludwigs-Universität Freiburg, Freiburg; Germany.
- ⁵⁵II. Physikalischs Institut, Georg-August-Universität Göttingen, Göttingen; Germany.
- ⁵⁶Département de Physique Nucléaire et Corpusculaire, Université de Genève, Genève; Switzerland.
- ^{57(a)}Dipartimento di Fisica, Università di Genova, Genova;^(b)INFN Sezione di Genova; Italy.
- ⁵⁸II. Physikalischs Institut, Justus-Liebig-Universität Giessen, Giessen; Germany.
- ⁵⁹SUPA - School of Physics and Astronomy, University of Glasgow, Glasgow; United Kingdom.
- ⁶⁰LPSC, Université Grenoble Alpes, CNRS/IN2P3, Grenoble INP, Grenoble; France.
- ⁶¹Laboratory for Particle Physics and Cosmology, Harvard University, Cambridge MA; United States of America.
- ⁶²Department of Modern Physics and State Key Laboratory of Particle Detection and Electronics, University of Science and Technology of China, Hefei; China.
- ^{63(a)}Kirchhoff-Institut für Physik, Ruprecht-Karls-Universität Heidelberg, Heidelberg;^(b)Physikalischs Institut, Ruprecht-Karls-Universität Heidelberg, Heidelberg; Germany.
- ^{64(a)}Department of Physics, Chinese University of Hong Kong, Shatin, N.T., Hong Kong;^(b)Department of Physics, University of Hong Kong, Hong Kong;^(c)Department of Physics and Institute for Advanced Study, Hong Kong University of Science and Technology, Clear Water Bay, Kowloon, Hong Kong; China.
- ⁶⁵Department of Physics, National Tsing Hua University, Hsinchu; Taiwan.
- ⁶⁶IJCLab, Université Paris-Saclay, CNRS/IN2P3, 91405, Orsay; France.
- ⁶⁷Centro Nacional de Microelectrónica (IMB-CNM-CSIC), Barcelona; Spain.
- ⁶⁸Department of Physics, Indiana University, Bloomington IN; United States of America.
- ^{69(a)}INFN Gruppo Collegato di Udine, Sezione di Trieste, Udine;^(b)ICTP, Trieste;^(c)Dipartimento Politecnico di Ingegneria e Architettura, Università di Udine, Udine; Italy.
- ^{70(a)}INFN Sezione di Lecce;^(b)Dipartimento di Matematica e Fisica, Università del Salento, Lecce; Italy.
- ^{71(a)}INFN Sezione di Milano;^(b)Dipartimento di Fisica, Università di Milano, Milano; Italy.
- ^{72(a)}INFN Sezione di Napoli;^(b)Dipartimento di Fisica, Università di Napoli, Napoli; Italy.
- ^{73(a)}INFN Sezione di Pavia;^(b)Dipartimento di Fisica, Università di Pavia, Pavia; Italy.
- ^{74(a)}INFN Sezione di Pisa;^(b)Dipartimento di Fisica E. Fermi, Università di Pisa, Pisa; Italy.
- ^{75(a)}INFN Sezione di Roma;^(b)Dipartimento di Fisica, Sapienza Università di Roma, Roma; Italy.
- ^{76(a)}INFN Sezione di Roma Tor Vergata;^(b)Dipartimento di Fisica, Università di Roma Tor Vergata, Roma; Italy.
- ^{77(a)}INFN Sezione di Roma Tre;^(b)Dipartimento di Matematica e Fisica, Università Roma Tre, Roma; Italy.
- ^{78(a)}INFN-TIFPA;^(b)Università degli Studi di Trento, Trento; Italy.
- ⁷⁹Universität Innsbruck, Department of Astro and Particle Physics, Innsbruck; Austria.

- ⁸⁰University of Iowa, Iowa City IA; United States of America.
- ⁸¹Department of Physics and Astronomy, Iowa State University, Ames IA; United States of America.
- ⁸²Istinye University, Sarıyer, İstanbul; Türkiye.
- ⁸³^(a)Departamento de Engenharia Elétrica, Universidade Federal de Juiz de Fora (UFJF), Juiz de Fora; ^(b)Universidade Federal do Rio De Janeiro COPPE/EE/IF, Rio de Janeiro; ^(c)Instituto de Física, Universidade de São Paulo, São Paulo; ^(d)Rio de Janeiro State University, Rio de Janeiro; ^(e)Federal University of Bahia, Bahia; Brazil.
- ⁸⁴KEK, High Energy Accelerator Research Organization, Tsukuba; Japan.
- ⁸⁵Graduate School of Science, Kobe University, Kobe; Japan.
- ⁸⁶^(a)AGH University of Krakow, Faculty of Physics and Applied Computer Science, Krakow; ^(b)Marian Smoluchowski Institute of Physics, Jagiellonian University, Krakow; Poland.
- ⁸⁷Institute of Nuclear Physics Polish Academy of Sciences, Krakow; Poland.
- ⁸⁸^(a)Khalifa University of Science and Technology, Abu Dhabi; ^(b)University of Sharjah, Sharjah; United Arab Emirates.
- ⁸⁹Faculty of Science, Kyoto University, Kyoto; Japan.
- ⁹⁰Research Center for Advanced Particle Physics and Department of Physics, Kyushu University, Fukuoka ; Japan.
- ⁹¹L2IT, Université de Toulouse, CNRS/IN2P3, UPS, Toulouse; France.
- ⁹²Instituto de Física La Plata, Universidad Nacional de La Plata and CONICET, La Plata; Argentina.
- ⁹³Physics Department, Lancaster University, Lancaster; United Kingdom.
- ⁹⁴Oliver Lodge Laboratory, University of Liverpool, Liverpool; United Kingdom.
- ⁹⁵Department of Experimental Particle Physics, Jožef Stefan Institute and Department of Physics, University of Ljubljana, Ljubljana; Slovenia.
- ⁹⁶Department of Physics and Astronomy, Queen Mary University of London, London; United Kingdom.
- ⁹⁷Department of Physics, Royal Holloway University of London, Egham; United Kingdom.
- ⁹⁸Department of Physics and Astronomy, University College London, London; United Kingdom.
- ⁹⁹Louisiana Tech University, Ruston LA; United States of America.
- ¹⁰⁰Fysiska institutionen, Lunds universitet, Lund; Sweden.
- ¹⁰¹Departamento de Física Teórica C-15 and CIAFF, Universidad Autónoma de Madrid, Madrid; Spain.
- ¹⁰²Institut für Physik, Universität Mainz, Mainz; Germany.
- ¹⁰³School of Physics and Astronomy, University of Manchester, Manchester; United Kingdom.
- ¹⁰⁴CPPM, Aix-Marseille Université, CNRS/IN2P3, Marseille; France.
- ¹⁰⁵Department of Physics, University of Massachusetts, Amherst MA; United States of America.
- ¹⁰⁶Department of Physics, McGill University, Montreal QC; Canada.
- ¹⁰⁷School of Physics, University of Melbourne, Victoria; Australia.
- ¹⁰⁸Department of Physics, University of Michigan, Ann Arbor MI; United States of America.
- ¹⁰⁹Department of Physics and Astronomy, Michigan State University, East Lansing MI; United States of America.
- ¹¹⁰Group of Particle Physics, University of Montreal, Montreal QC; Canada.
- ¹¹¹Fakultät für Physik, Ludwig-Maximilians-Universität München, München; Germany.
- ¹¹²Max-Planck-Institut für Physik (Werner-Heisenberg-Institut), München; Germany.
- ¹¹³Graduate School of Science and Kobayashi-Maskawa Institute, Nagoya University, Nagoya; Japan.
- ¹¹⁴^(a)Department of Physics, Nanjing University, Nanjing; ^(b)School of Science, Shenzhen Campus of Sun Yat-sen University; ^(c)University of Chinese Academy of Science (UCAS), Beijing; China.
- ¹¹⁵Department of Physics and Astronomy, University of New Mexico, Albuquerque NM; United States of America.
- ¹¹⁶Institute for Mathematics, Astrophysics and Particle Physics, Radboud University/Nikhef, Nijmegen;

Netherlands.

¹¹⁷Nikhef National Institute for Subatomic Physics and University of Amsterdam, Amsterdam; Netherlands.

¹¹⁸Department of Physics, Northern Illinois University, DeKalb IL; United States of America.

^{119(a)}New York University Abu Dhabi, Abu Dhabi; ^(b)United Arab Emirates University, Al Ain; United Arab Emirates.

¹²⁰Department of Physics, New York University, New York NY; United States of America.

¹²¹Ochanomizu University, Otsuka, Bunkyo-ku, Tokyo; Japan.

¹²²Ohio State University, Columbus OH; United States of America.

¹²³Homer L. Dodge Department of Physics and Astronomy, University of Oklahoma, Norman OK; United States of America.

¹²⁴Department of Physics, Oklahoma State University, Stillwater OK; United States of America.

¹²⁵Palacký University, Joint Laboratory of Optics, Olomouc; Czech Republic.

¹²⁶Institute for Fundamental Science, University of Oregon, Eugene, OR; United States of America.

¹²⁷Graduate School of Science, University of Osaka, Osaka; Japan.

¹²⁸Department of Physics, University of Oslo, Oslo; Norway.

¹²⁹Department of Physics, Oxford University, Oxford; United Kingdom.

¹³⁰LPNHE, Sorbonne Université, Université Paris Cité, CNRS/IN2P3, Paris; France.

¹³¹Department of Physics, University of Pennsylvania, Philadelphia PA; United States of America.

¹³²Department of Physics and Astronomy, University of Pittsburgh, Pittsburgh PA; United States of America.

^{133(a)}Laboratório de Instrumentação e Física Experimental de Partículas - LIP, Lisboa; ^(b)Departamento de Física, Faculdade de Ciências, Universidade de Lisboa, Lisboa; ^(c)Departamento de Física, Universidade de Coimbra, Coimbra; ^(d)Centro de Física Nuclear da Universidade de Lisboa, Lisboa; ^(e)Departamento de Física, Escola de Ciências, Universidade do Minho, Braga; ^(f)Departamento de Física Teórica y del Cosmos, Universidad de Granada, Granada (Spain); ^(g)Departamento de Física, Instituto Superior Técnico, Universidade de Lisboa, Lisboa; Portugal.

¹³⁴Institute of Physics of the Czech Academy of Sciences, Prague; Czech Republic.

¹³⁵Czech Technical University in Prague, Prague; Czech Republic.

¹³⁶Charles University, Faculty of Mathematics and Physics, Prague; Czech Republic.

¹³⁷Particle Physics Department, Rutherford Appleton Laboratory, Didcot; United Kingdom.

¹³⁸IRFU, CEA, Université Paris-Saclay, Gif-sur-Yvette; France.

¹³⁹Santa Cruz Institute for Particle Physics, University of California Santa Cruz, Santa Cruz CA; United States of America.

^{140(a)}Departamento de Física, Pontificia Universidad Católica de Chile, Santiago; ^(b)Millennium Institute for Subatomic physics at high energy frontier (SAPHIR), Santiago; ^(c)Instituto de Investigación Multidisciplinario en Ciencia y Tecnología, y Departamento de Física, Universidad de La Serena; ^(d)Universidad Andres Bello, Department of Physics, Santiago; ^(e)Universidad San Sebastian, Recoleta; ^(f)Instituto de Alta Investigación, Universidad de Tarapacá, Arica; ^(g)Departamento de Física, Universidad Técnica Federico Santa María, Valparaíso; Chile.

¹⁴¹Department of Physics, Institute of Science, Tokyo; Japan.

¹⁴²Department of Physics, University of Washington, Seattle WA; United States of America.

^{143(a)}Institute of Frontier and Interdisciplinary Science and Key Laboratory of Particle Physics and Particle Irradiation (MOE), Shandong University, Qingdao; ^(b)School of Physics, Zhengzhou University; China.

^{144(a)}State Key Laboratory of Dark Matter Physics, School of Physics and Astronomy, Shanghai Jiao Tong University, Key Laboratory for Particle Astrophysics and Cosmology (MOE), SKLPPC, Shanghai; ^(b)State Key Laboratory of Dark Matter Physics, Tsung-Dao Lee Institute, Shanghai Jiao Tong University,

Shanghai; China.

¹⁴⁵Department of Physics and Astronomy, University of Sheffield, Sheffield; United Kingdom.

¹⁴⁶Department of Physics, Shinshu University, Nagano; Japan.

¹⁴⁷Department Physik, Universität Siegen, Siegen; Germany.

¹⁴⁸Department of Physics, Simon Fraser University, Burnaby BC; Canada.

¹⁴⁹SLAC National Accelerator Laboratory, Stanford CA; United States of America.

¹⁵⁰Department of Physics, Royal Institute of Technology, Stockholm; Sweden.

¹⁵¹Departments of Physics and Astronomy, Stony Brook University, Stony Brook NY; United States of America.

¹⁵²Department of Physics and Astronomy, University of Sussex, Brighton; United Kingdom.

¹⁵³School of Physics, University of Sydney, Sydney; Australia.

¹⁵⁴Institute of Physics, Academia Sinica, Taipei; Taiwan.

^{155(a)}E. Andronikashvili Institute of Physics, Iv. Javakhishvili Tbilisi State University, Tbilisi; ^(b)High Energy Physics Institute, Tbilisi State University, Tbilisi; ^(c)University of Georgia, Tbilisi; Georgia.

¹⁵⁶Department of Physics, Technion, Israel Institute of Technology, Haifa; Israel.

¹⁵⁷Raymond and Beverly Sackler School of Physics and Astronomy, Tel Aviv University, Tel Aviv; Israel.

¹⁵⁸Department of Physics, Aristotle University of Thessaloniki, Thessaloniki; Greece.

¹⁵⁹International Center for Elementary Particle Physics and Department of Physics, University of Tokyo, Tokyo; Japan.

¹⁶⁰Graduate School of Science and Technology, Tokyo Metropolitan University, Tokyo; Japan.

¹⁶¹Department of Physics, University of Toronto, Toronto ON; Canada.

^{162(a)}TRIUMF, Vancouver BC; ^(b)Department of Physics and Astronomy, York University, Toronto ON; Canada.

¹⁶³Division of Physics and Tomonaga Center for the History of the Universe, Faculty of Pure and Applied Sciences, University of Tsukuba, Tsukuba; Japan.

¹⁶⁴Department of Physics and Astronomy, Tufts University, Medford MA; United States of America.

¹⁶⁵Department of Physics and Astronomy, University of California Irvine, Irvine CA; United States of America.

¹⁶⁶University of West Attica, Athens; Greece.

¹⁶⁷Department of Physics and Astronomy, University of Uppsala, Uppsala; Sweden.

¹⁶⁸Department of Physics, University of Illinois, Urbana IL; United States of America.

¹⁶⁹Instituto de Física Corpuscular (IFIC), Centro Mixto Universidad de Valencia - CSIC, Valencia; Spain.

¹⁷⁰Department of Physics, University of British Columbia, Vancouver BC; Canada.

¹⁷¹Department of Physics and Astronomy, University of Victoria, Victoria BC; Canada.

¹⁷²Fakultät für Physik und Astronomie, Julius-Maximilians-Universität Würzburg, Würzburg; Germany.

¹⁷³Department of Physics, University of Warwick, Coventry; United Kingdom.

¹⁷⁴Waseda University, Tokyo; Japan.

¹⁷⁵Department of Particle Physics and Astrophysics, Weizmann Institute of Science, Rehovot; Israel.

¹⁷⁶Department of Physics, University of Wisconsin, Madison WI; United States of America.

¹⁷⁷Fakultät für Mathematik und Naturwissenschaften, Fachgruppe Physik, Bergische Universität Wuppertal, Wuppertal; Germany.

¹⁷⁸Department of Physics, Yale University, New Haven CT; United States of America.

¹⁷⁹Yerevan Physics Institute, Yerevan; Armenia.

^a Also at Affiliated with an institute formerly covered by a cooperation agreement with CERN.

^b Also at An-Najah National University, Nablus; Palestine.

^c Also at Borough of Manhattan Community College, City University of New York, New York NY; United States of America.

^d Also at Center for Interdisciplinary Research and Innovation (CIRI-AUTH), Thessaloniki; Greece.

^e Also at Centre of Physics of the Universities of Minho and Porto (CF-UM-UP); Portugal.

^f Also at CERN, Geneva; Switzerland.

^g Also at Département de Physique Nucléaire et Corpusculaire, Université de Genève, Genève; Switzerland.

^h Also at Departament de Fisica de la Universitat Autonoma de Barcelona, Barcelona; Spain.

ⁱ Also at Department of Financial and Management Engineering, University of the Aegean, Chios; Greece.

^j Also at Department of Mathematical Sciences, University of South Africa, Johannesburg; South Africa.

^k Also at Department of Modern Physics and State Key Laboratory of Particle Detection and Electronics, University of Science and Technology of China, Hefei; China.

^l Also at Department of Physics, Bolu Abant Izzet Baysal University, Bolu; Türkiye.

^m Also at Department of Physics, King's College London, London; United Kingdom.

ⁿ Also at Department of Physics, Stanford University, Stanford CA; United States of America.

^o Also at Department of Physics, Stellenbosch University; South Africa.

^p Also at Department of Physics, University of Fribourg, Fribourg; Switzerland.

^q Also at Department of Physics, University of Thessaly; Greece.

^r Also at Department of Physics, Westmont College, Santa Barbara; United States of America.

^s Also at Faculty of Physics, Sofia University, 'St. Kliment Ohridski', Sofia; Bulgaria.

^t Also at Faculty of Physics, University of Bucharest ; Romania.

^u Also at Hellenic Open University, Patras; Greece.

^v Also at Henan University; China.

^w Also at Imam Mohammad Ibn Saud Islamic University; Saudi Arabia.

^x Also at Institutio Catalana de Recerca i Estudis Avancats, ICREA, Barcelona; Spain.

^y Also at Institut für Experimentalphysik, Universität Hamburg, Hamburg; Germany.

^z Also at Institute for Nuclear Research and Nuclear Energy (INRNE) of the Bulgarian Academy of Sciences, Sofia; Bulgaria.

^{aa} Also at Institute of Applied Physics, Mohammed VI Polytechnic University, Ben Guerir; Morocco.

^{ab} Also at Institute of Particle Physics (IPP); Canada.

^{ac} Also at Institute of Physics and Technology, Mongolian Academy of Sciences, Ulaanbaatar; Mongolia.

^{ad} Also at Institute of Physics, Azerbaijan Academy of Sciences, Baku; Azerbaijan.

^{ae} Also at Institute of Theoretical Physics, Ilia State University, Tbilisi; Georgia.

^{af} Also at National Institute of Physics, University of the Philippines Diliman (Philippines); Philippines.

^{ag} Also at The Collaborative Innovation Center of Quantum Matter (CICQM), Beijing; China.

^{ah} Also at TRIUMF, Vancouver BC; Canada.

^{ai} Also at Università di Napoli Parthenope, Napoli; Italy.

^{aj} Also at University of Colorado Boulder, Department of Physics, Colorado; United States of America.

^{ak} Also at University of Sienna; Italy.

^{al} Also at Washington College, Chestertown, MD; United States of America.

^{am} Also at Yeditepe University, Physics Department, Istanbul; Türkiye.

* Deceased